Evolution of Molecular Cloud Cores Formed in Strongly Magnetized Molecular Filaments

Yoshiaki Misugi (Kyushu Sangyo University)

Collaborator

Shu-ichiro Inutsuka (Nagoya Univ.), Doris Arzoumanian (Kyushu Univ.) ,

Yusuke Tsukamoto, Haruka Fukihara (Kagoshima Univ) ,

Silvia Spezzano, Sigurd S. Jensen, Tommaso Grassi, Jaime E. Pineda, Paola Caselli (MPE)

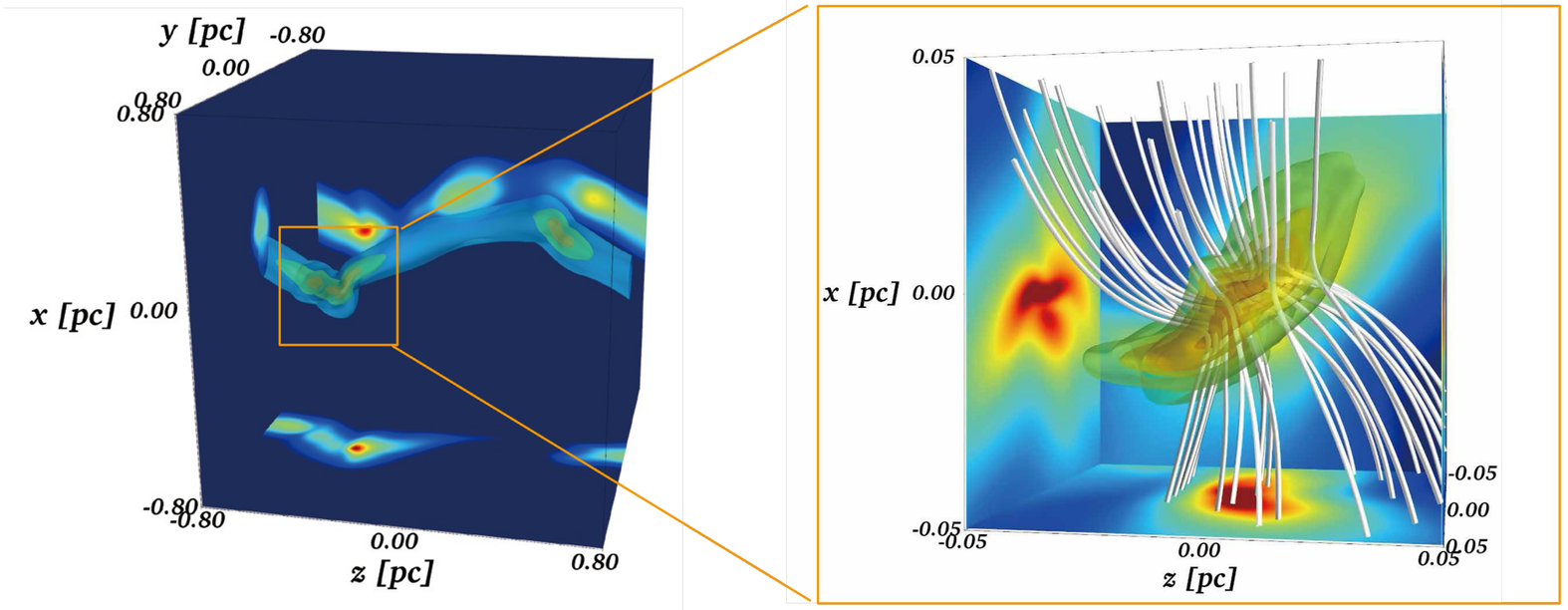

Universal Filamentary Structure

Star formation process

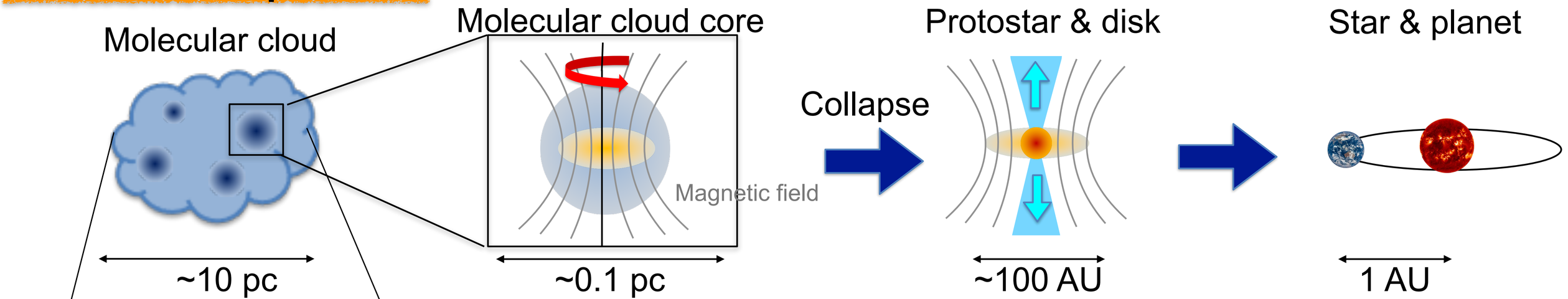

Dust continuum observations by Herschel space telescope

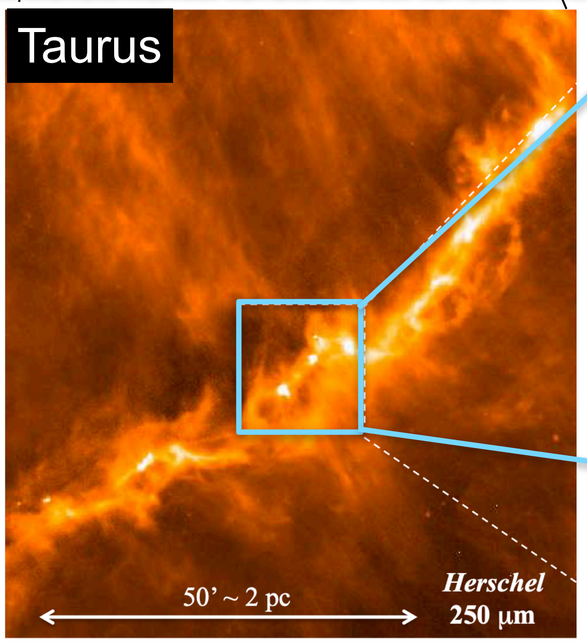

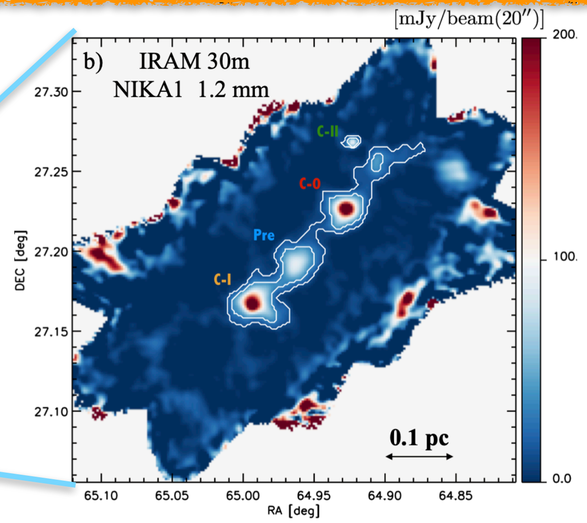

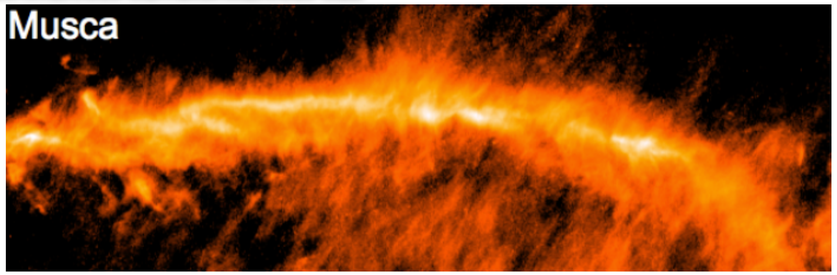

- Many dense elongated structures (filamentary structures) are observed in molecular clouds.
- Filamentary structure is ubiquitous in molecular clouds.
- Cores are along the crests of filaments.

Studying the properties of cores formed from filament fragmentation is important.

Role of Angular Momentum of Core

Molecular cloud core

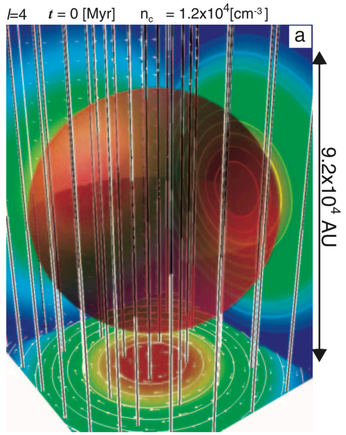

Machida et al. (2008)

Driving outflow and jet

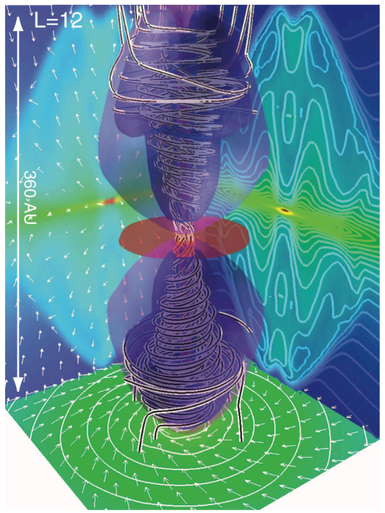

Initial angular velocity of core (normalized by free fall time)

Formation of multiple system

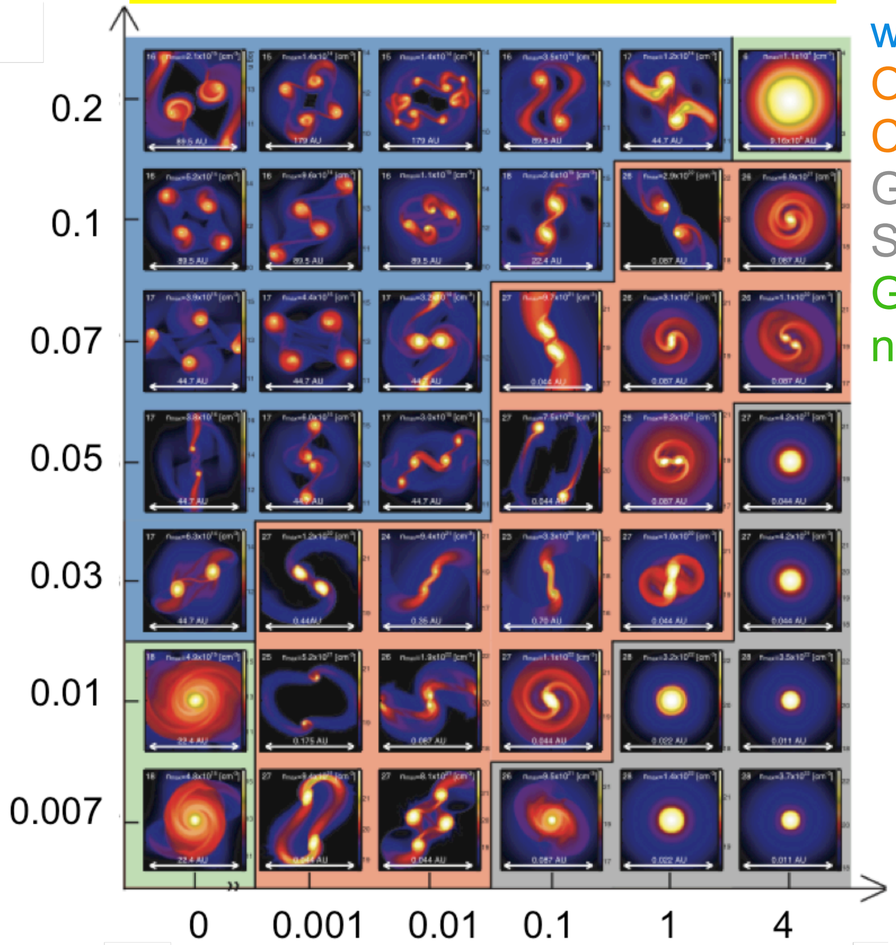

Blue: wide binary
Orange: Close binary
Grey: Single
Green: not collapsed

Machida et al. (2008)

Formation of Protoplanetary disk

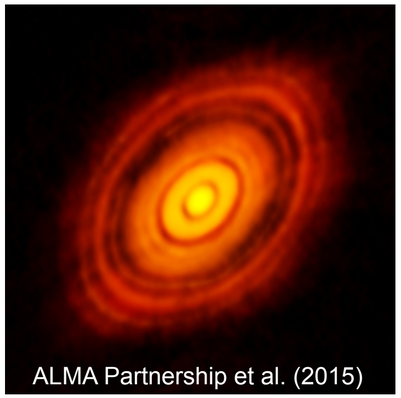

Birth place of planets

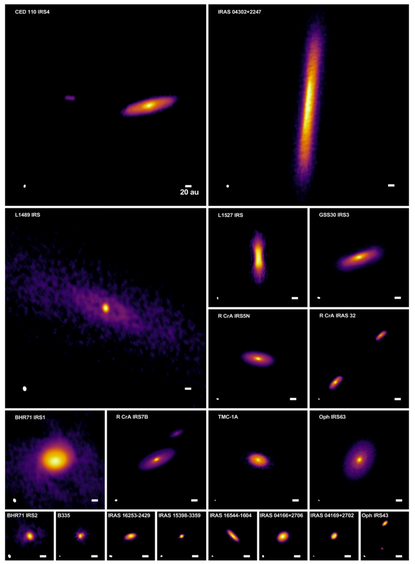

Ohashi et al. (2023)

Angular momentum (AM) of cores plays an essential role in star formation process.

Importance of Magnetic Field

Observations of magnetic fields

B-fields are perpendicular to the filament axis.

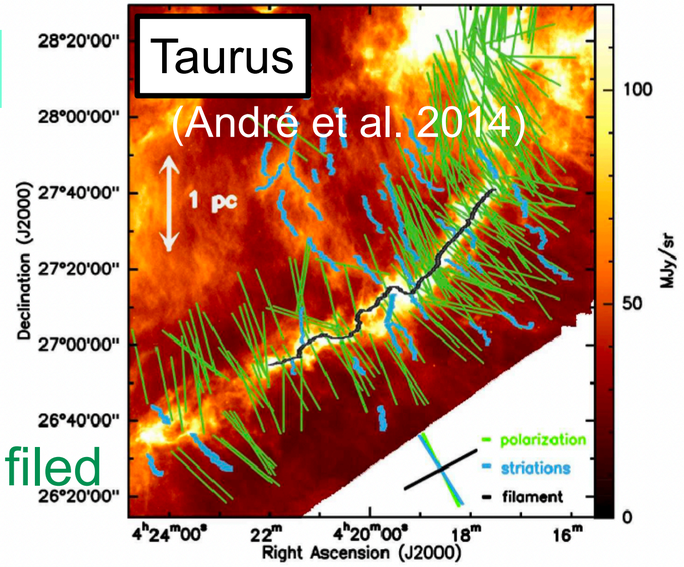

Magnetic filed

Magnetic braking

Magnetic field

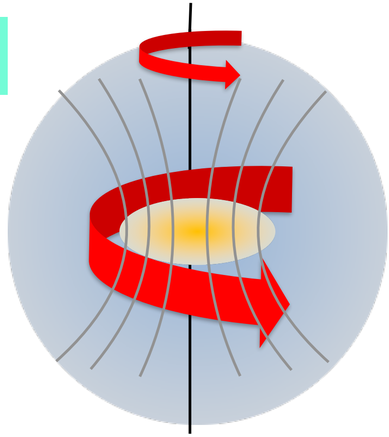

Magnetic field can extract the AM from inner region to outer envelope.

Magnetic braking from core to disk scale

Magnetic Field

Weak ⟷ Strong

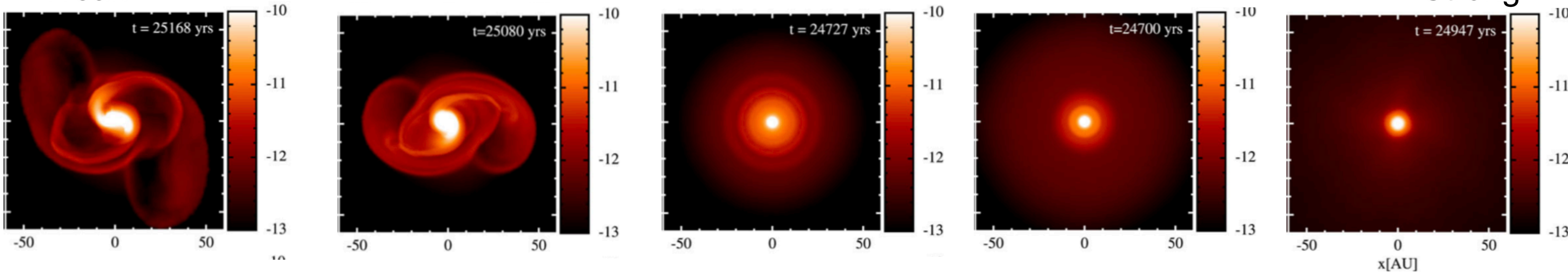

Magntic field plays a key role in the AM transfer.

Previous Works for AM of Cores

From the molecular cloud scale to the core scale

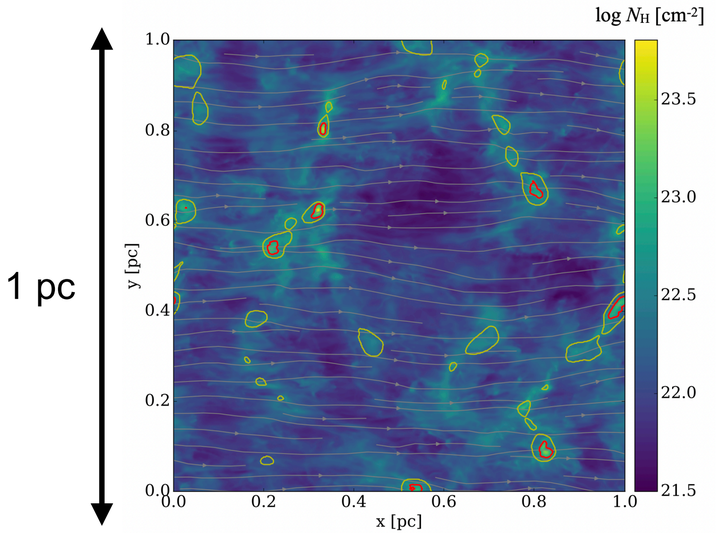

Chen & Ostriker (2014)

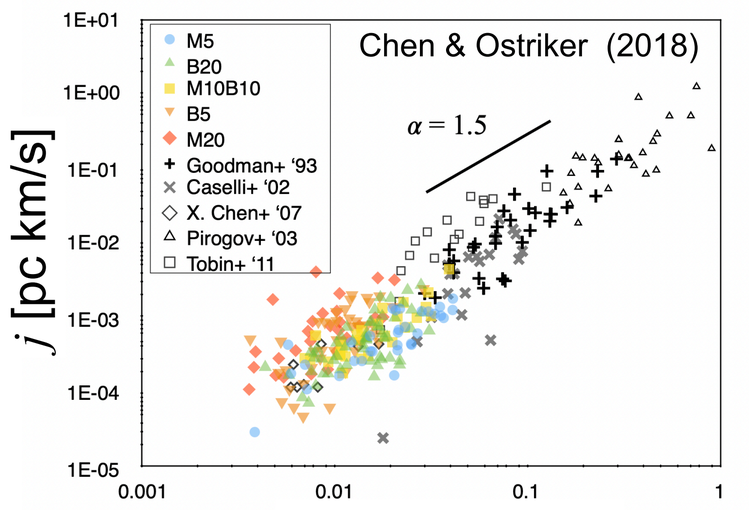

The observed AM of core can be explained by the turbulent velocity field (See also Burkert & Bodenheimer 2000).

$$j \sim R\sigma \propto R^{1.5}$$

$$\sigma^2 \sim \int P(k)k^2dk \propto k^{-n+3}$$

$$P(k)d^3k \propto k^{-n}d^3k$$

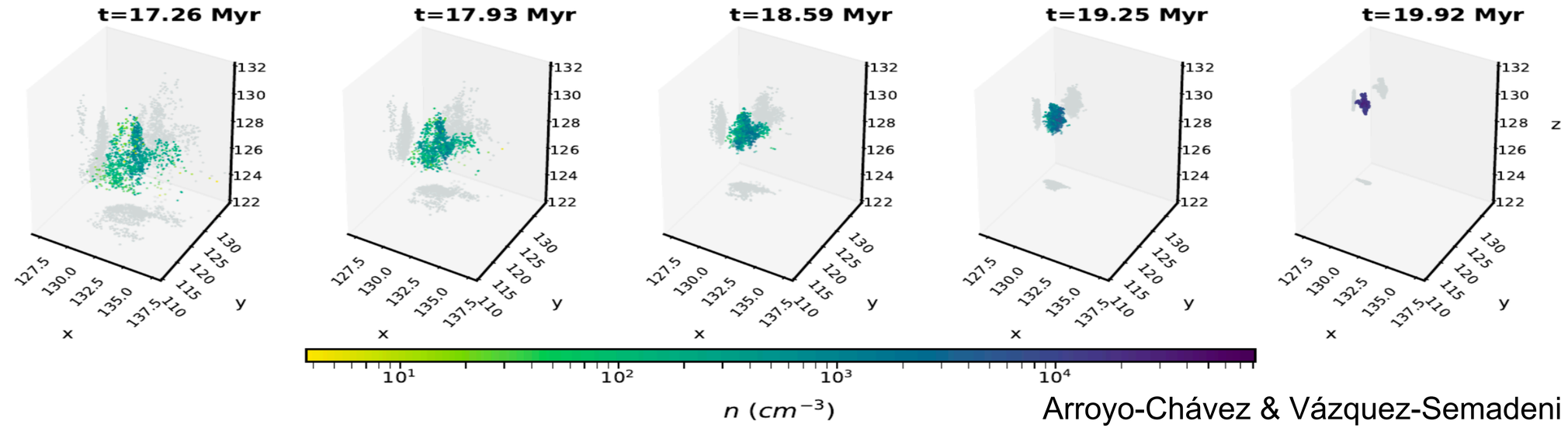

Arroyo-Chávez & Vázquez-Semadeni (2022)

Previous Works for AM of Cores

From the molecular cloud scale to the core scale

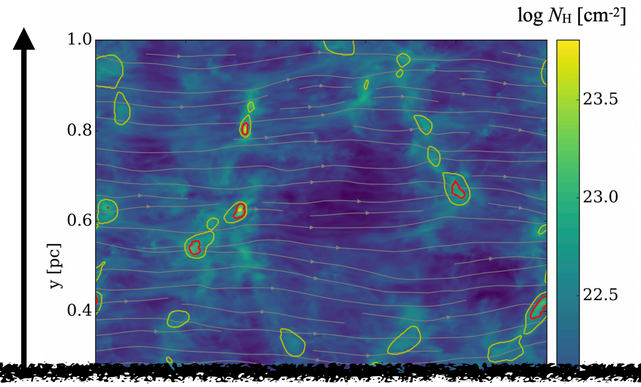

1 pc

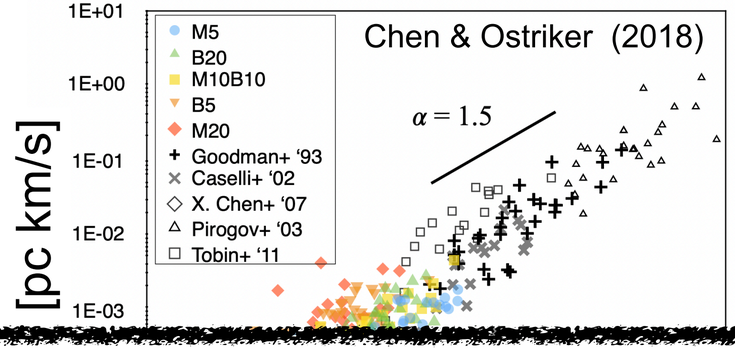

The observed AM of core can be explained by the turbulent velocity field (See also Burkert & Bodenheimer 2000).

$$j \sim R\sigma \propto R^{1.5}$$

$$\sigma^2 \sim \int P(k)k^2 dk \propto k^{-n+3}$$

Evolution of core AM in magnetized filamentary molecular clouds has not yet been understood in detail.

AM transfer due to the magnetic field during filament fragmentation should be investigated.

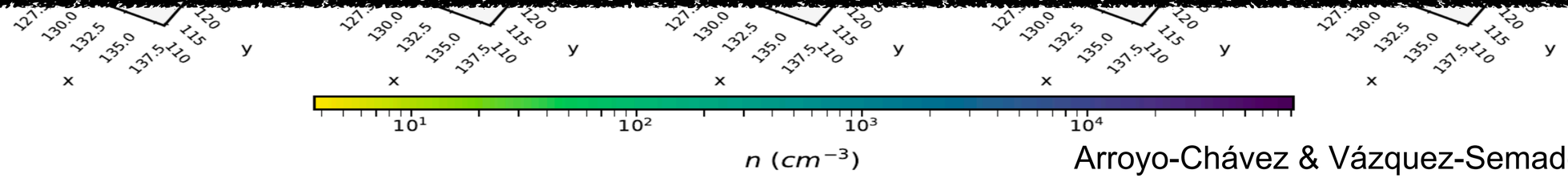

Arroyo-Chávez & Vázquez-Semadeni (2022)

Observed Magnetic Field Strength

L1495/B213 (Taurus)

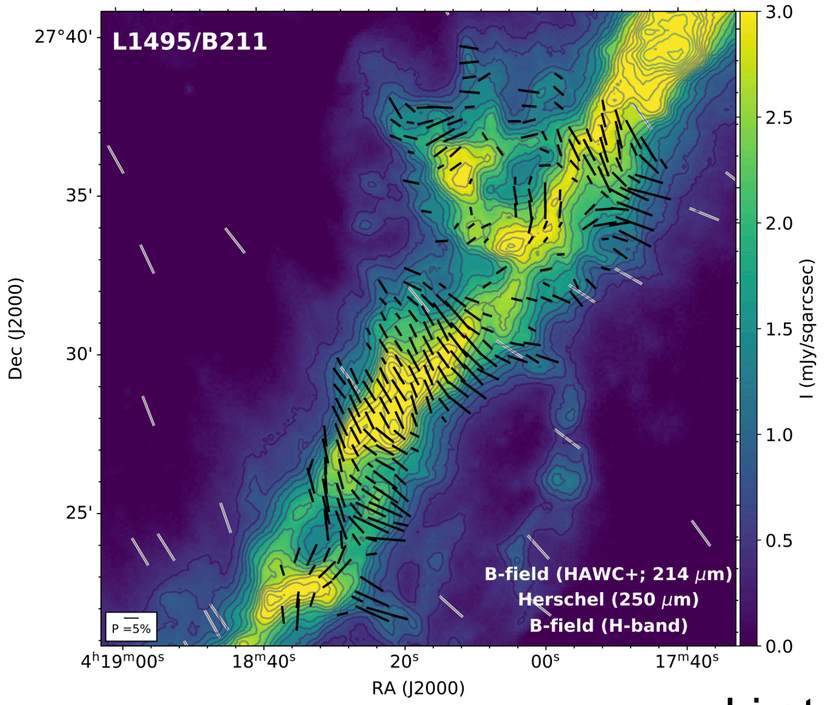

Li et al. (2022)

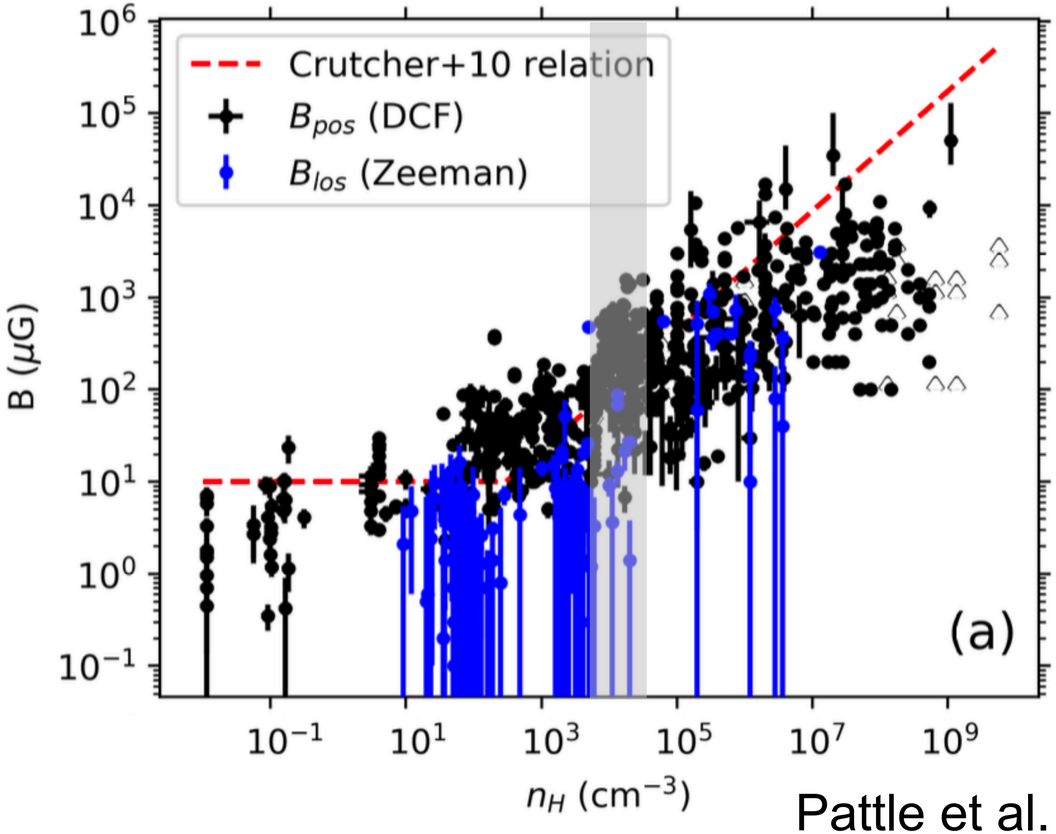

Pattle et al. (2022)

From the Davis-Chandrasekhar-Fermi (DCF) method,
$B_0 = 10 - 80\mu\mathrm{G}$

$B_0 \simeq 10 - 100\mu\mathrm{G}$ at
the filament ridge.

Observed Magnetic Field Strength

Misugi+2024

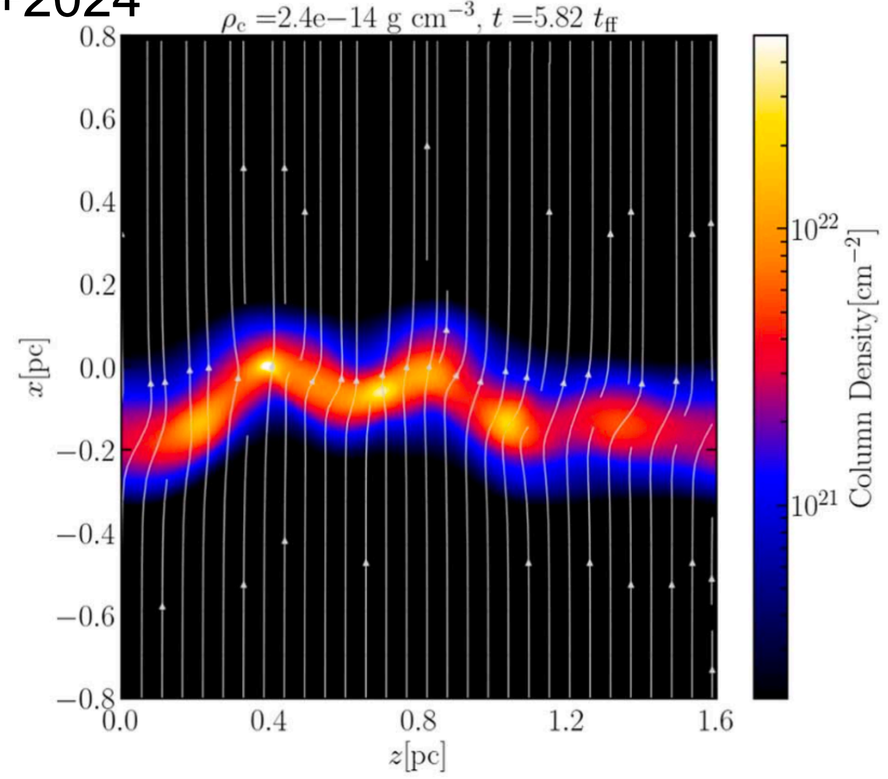

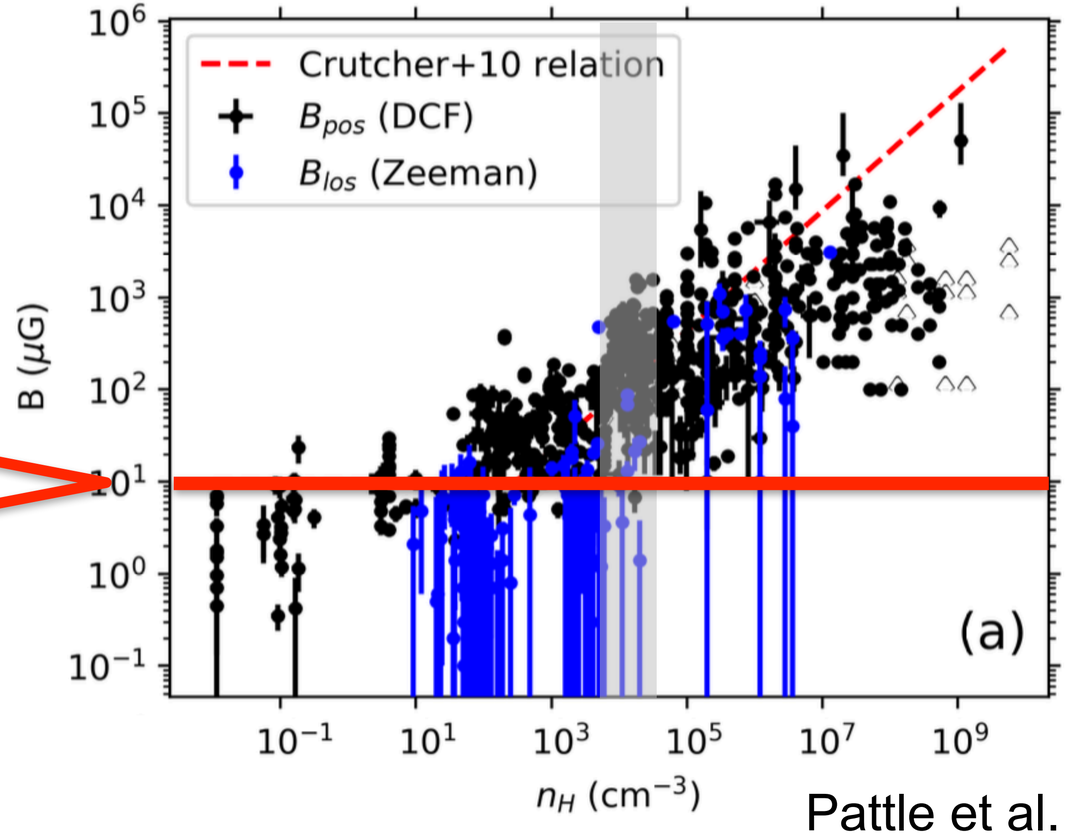

Pattle et al. (2022)

We need to investigate the AM evolution of cores formed in filaments in the **strong magnetic field enviroment.**

In today's talk,

1. Moderately strong magnetic field ($B_0 = 20\ \mu\mathrm{G}$)
2. Strong magnetic field ($B_0 = 50\ \mu\mathrm{G}$)

Method and Setup of Simulations

Basic equations (Ideal MHD)

Equation of motion: $$\frac{d\boldsymbol{v}}{dt} = -\frac{1}{\rho}\left\{\nabla\left(P + \frac{1}{2}|\boldsymbol{B}|^2\right) - \boldsymbol{B}\cdot\nabla\boldsymbol{B}\right\} - \nabla\Phi$$

Gas + Magnetic Pressure | Magnetic tension | Gravity

Induction equation: $$\frac{\mathrm{d}}{\mathrm{d}t}\left(\frac{\boldsymbol{B}}{\rho}\right) = \left(\frac{\boldsymbol{B}}{\rho}\cdot\nabla\right)\boldsymbol{v}$$

Equation of state: Isothermal

Solved by Godunov Smoothed Particle Magnetohydrodynamics (GSPM) (Iwasaki & Inutsuka 2011; 2013; in perp)

Setup

- Number of particle: 1,890,144
- Line mass: Critical line mass $M_{\rm line} = 18 \mathrm{M}_\odot \mathrm{pc}^{-1}$
- Turbulent velocity field: Kolmogorov turbulence

  $P(k)dk = Ak^{-5/3}dk$

  $\sigma_{\rm 3D} = 2c_{\rm s}$ (Hacar & Tafalla 2011)
- Density profile: $$\rho(r) = \rho_{\rm c}\left[1 + \left(\frac{r}{H_0}\right)^2\right]^{-2} \quad H_0 = 0.05\mathrm{pc}$$ (Arzoumanian et al. 2011; 2019)
- Magnetic fields

Hydro

$B_0 = 10\mu\mathrm{G}$

$B_0 = 20\mu\mathrm{G}$

$$B_0 = 20\mu\mathrm{G}$$

Perpendicular to the filament axis (x-axis)
(e.g., Planck Collaboration XXXV 2016)

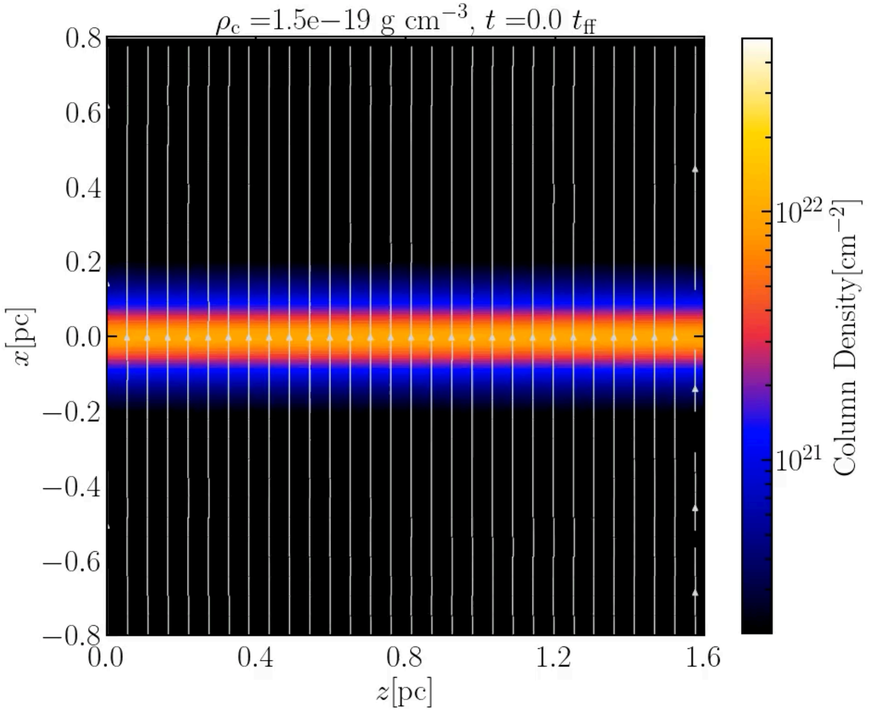

Evolution of Angular Momentum

We stop the simulation when the maximum density reaches $n_{\rm max} = 10^9\ {\rm cm}^{-3}$ (before the protostar formation)

Final State

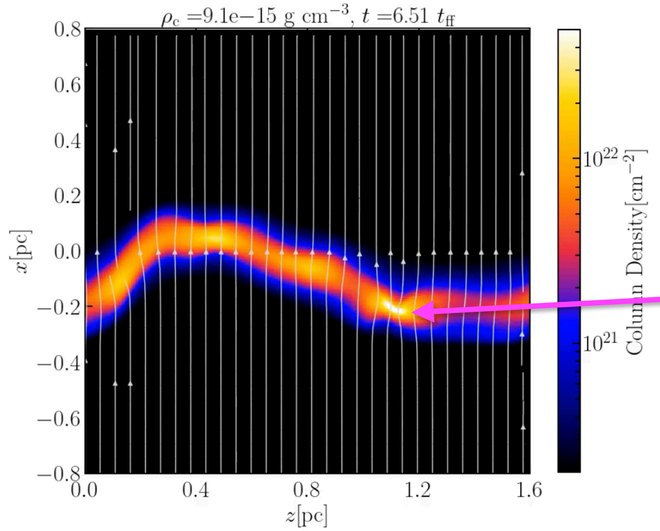

We define a core using density contour threshold.

Final State

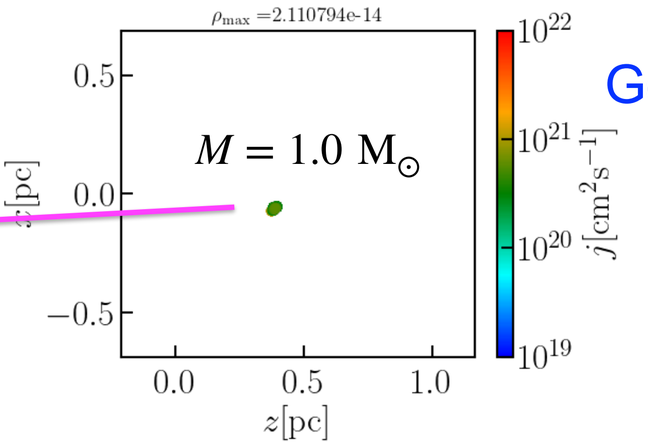

Go back in time

Initial State

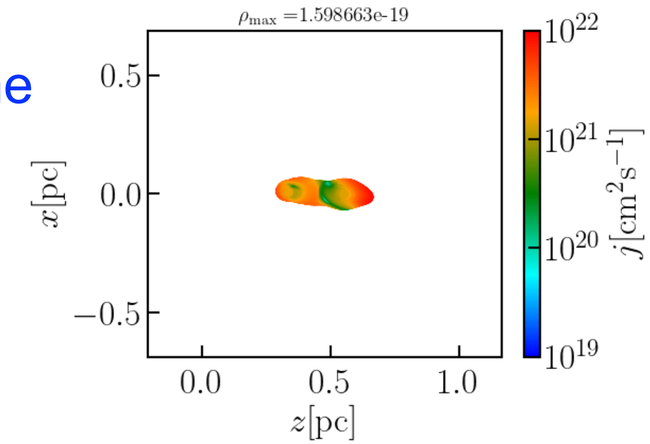

Examples of the trajectory of the gas particles

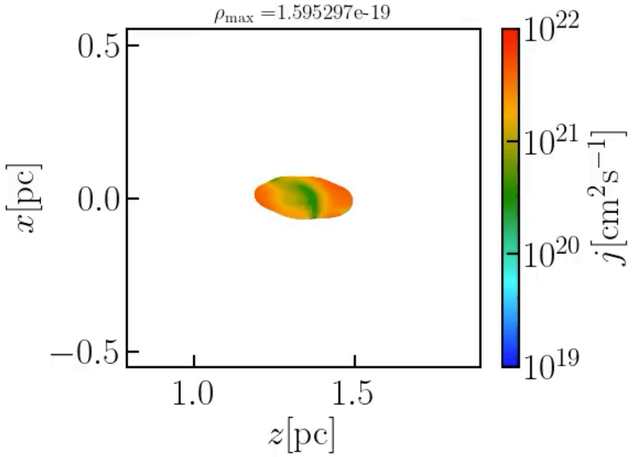

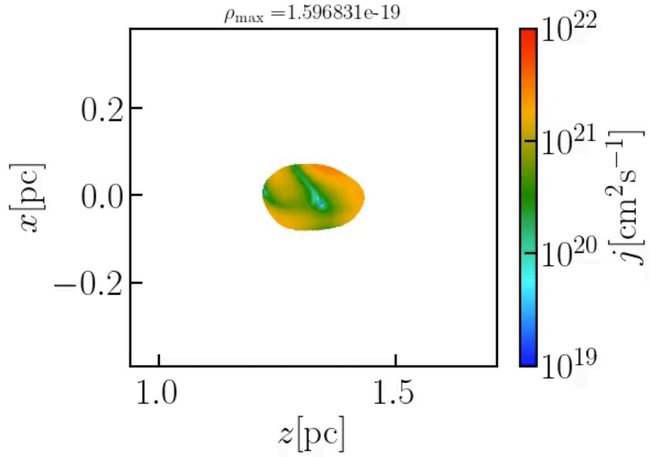

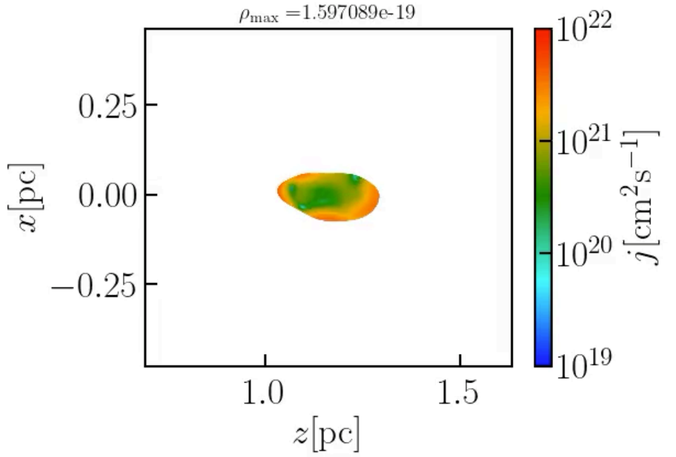

Filament longitudinal axis direction

Evolution of Angular Momentum

We stop the simulation when the maximum density reaches $n_{\rm max} = 10^9\ {\rm cm}^{-3}$ (before the protostar formation)

Final State

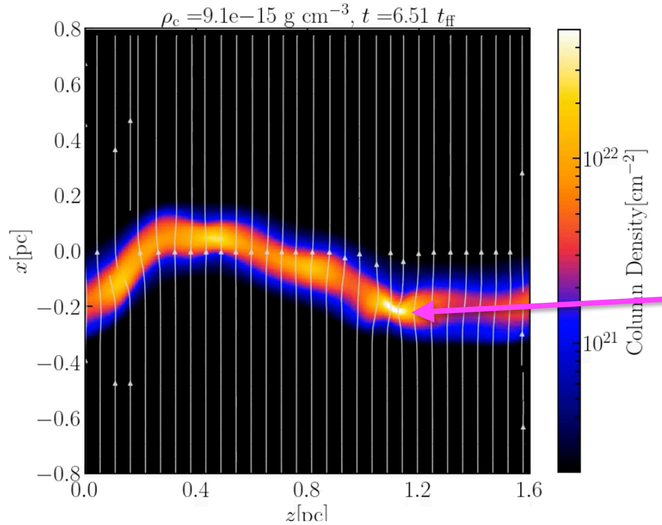

We define a core using density contour threshold.

Final State

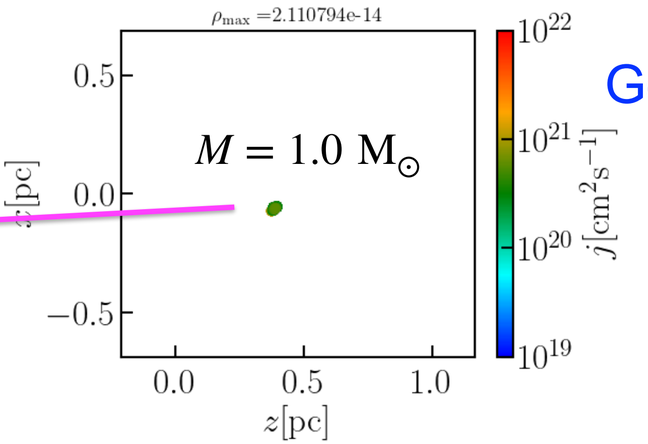

Go back in time

Initial State

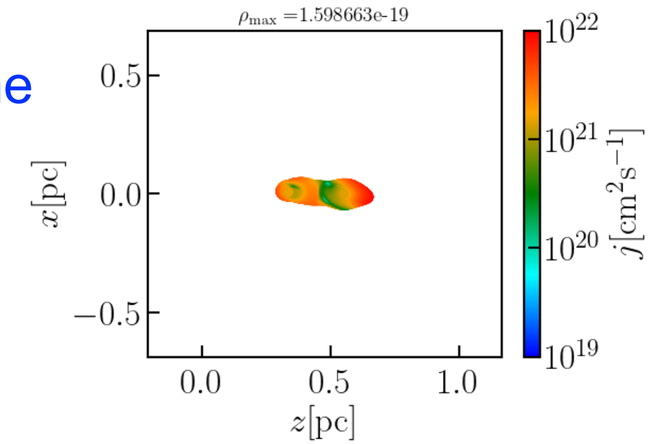

Dependence of AM transfer on core mass

$|\boldsymbol{J}_{\rm fin} - \boldsymbol{J}_{\rm ini}| \,/\, |\boldsymbol{J}_{\rm ini}|$

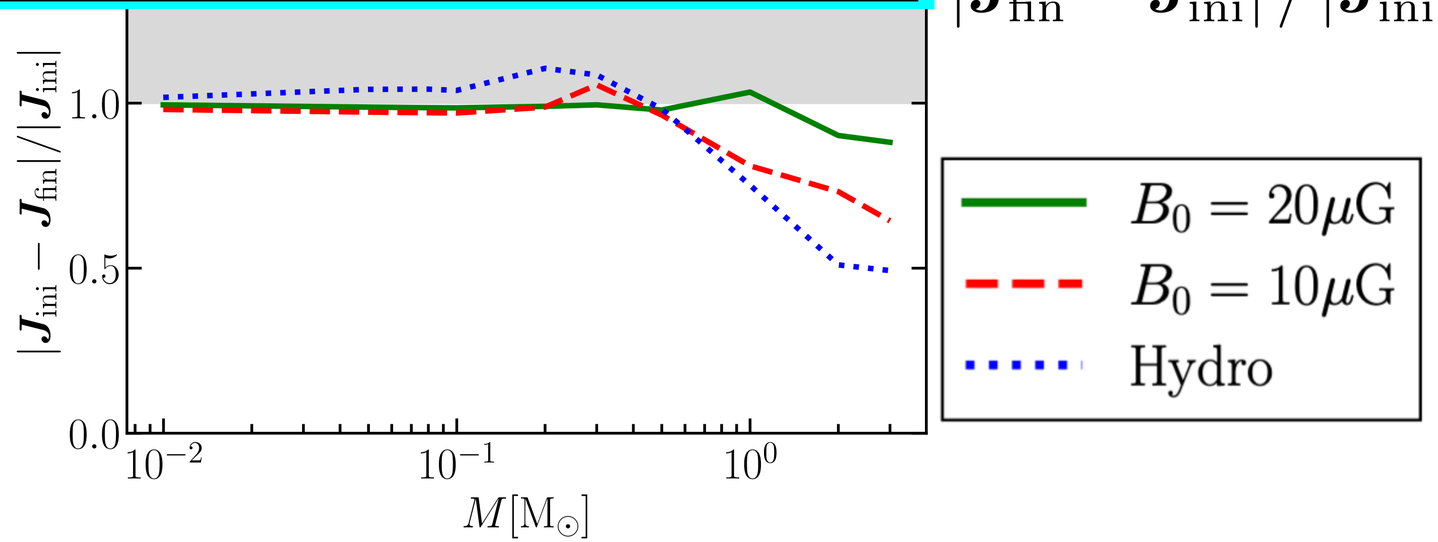

$J_{\rm fin}$: AM at the final state

$J_{\rm ini}$: AM at the initial state

In the case of 20μG, most of the cores with $\rm M_{core} \lesssim 1.0\ M_\odot$ lose their initial AM during the filament fragmentation phase.

Misalignment between AM and Magnetic Field

Observations suggest that the direction of the magnetic field is random with respect to the direction of the velocity gradient.

Outflow vs B-field

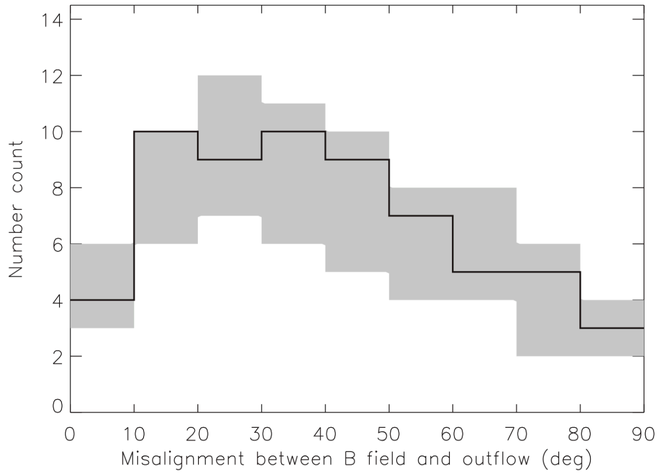

dust polarized emission at 850μm JCMT BISTRO survey

Yen et al. (2021)

Velocity gradient vs B-field

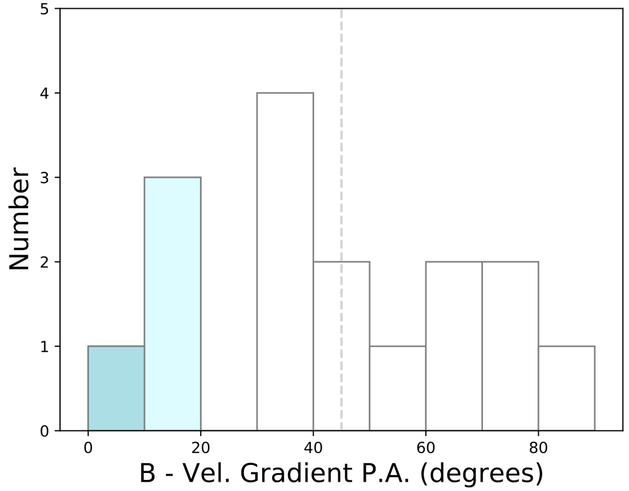

dust polarized emission at 0.87 mm, N_2H^+ (SMA)

Galametz et al. (2020)

(See also Hull 2013, Gupta 2022, Huang 2024)

Previous works shows that the component of AM perpendicular to B-filed is more efficiently removed compared with the parallel component.

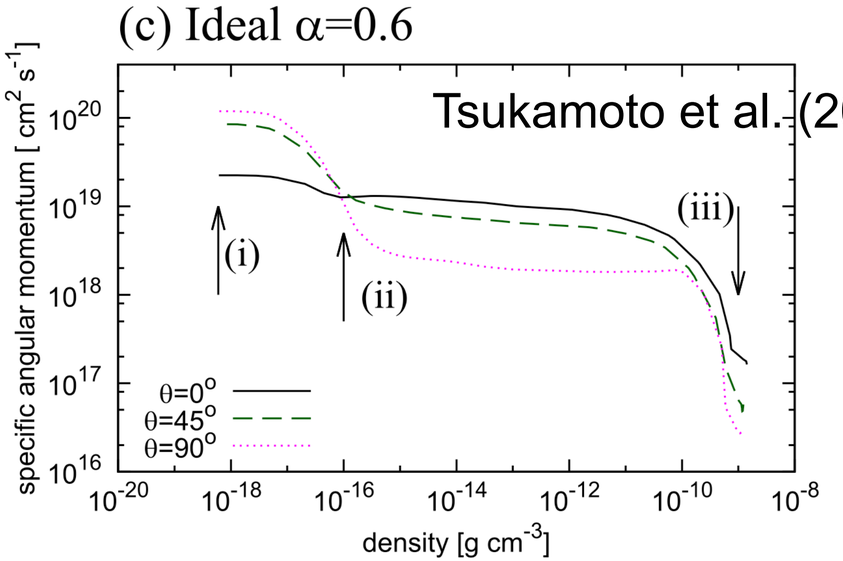

AM vector should be aligned with B-field?

Misalignment between AM and Magnetic Field

Observations suggest that the direction of the magnetic field is random with respect to the direction of the velocity gradient.

Outflow vs B-field

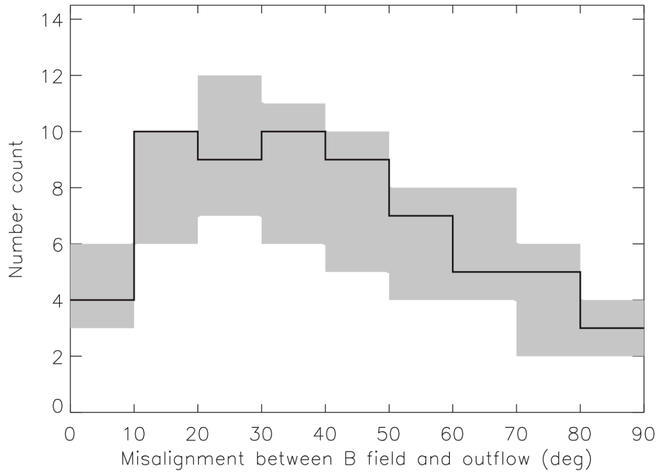

dust polarized emission at 850μm JCMT BISTRO survey

Yen et al. (2021)

Velocity gradient vs B-field

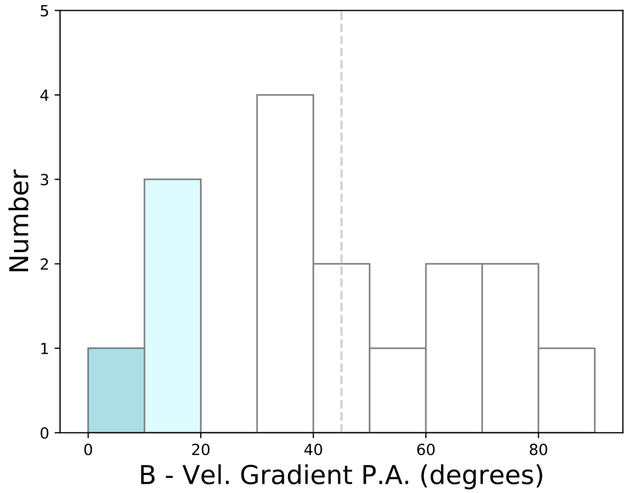

dust polarized emission at 0.87 mm, N_2H^+ (SMA)

Galametz et al. (2020)

(See also Hull 2013, Gupta 2022, Huang 2024)

$B_0 = 20\mu\mathrm{G}$ $1.0\ \mathrm{M}_\odot$

$\theta_{j,B}$: Angle between local magnetic field and AM

Final state

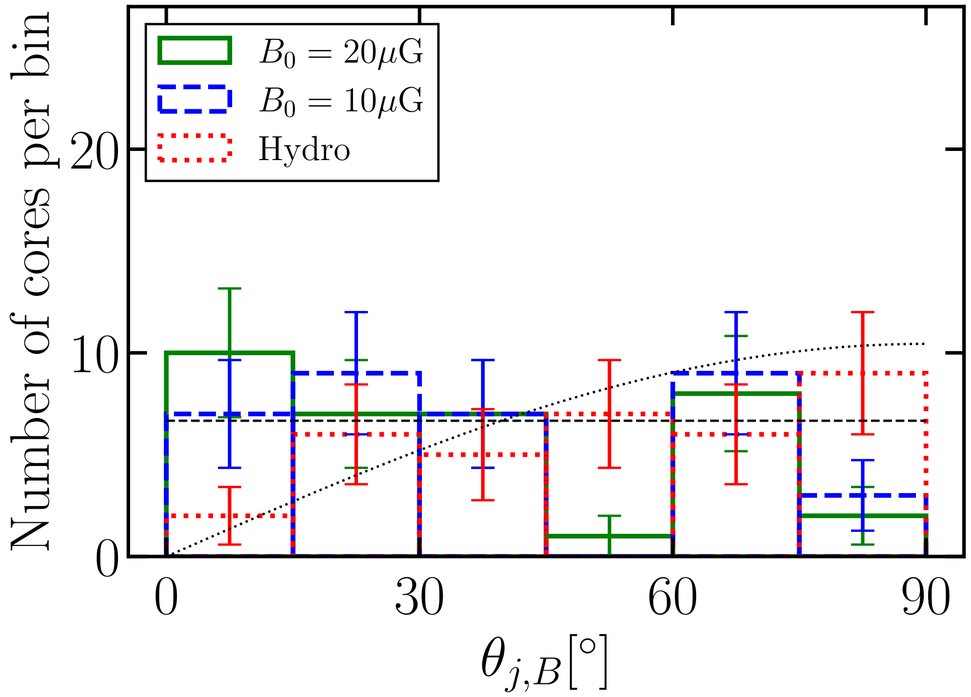

Our results also show that the direction of the magnetic field is random at the final state of simulation, but why?

Misalignment between AM and Magnetic Field

Angle between local magnetic field direction and AM

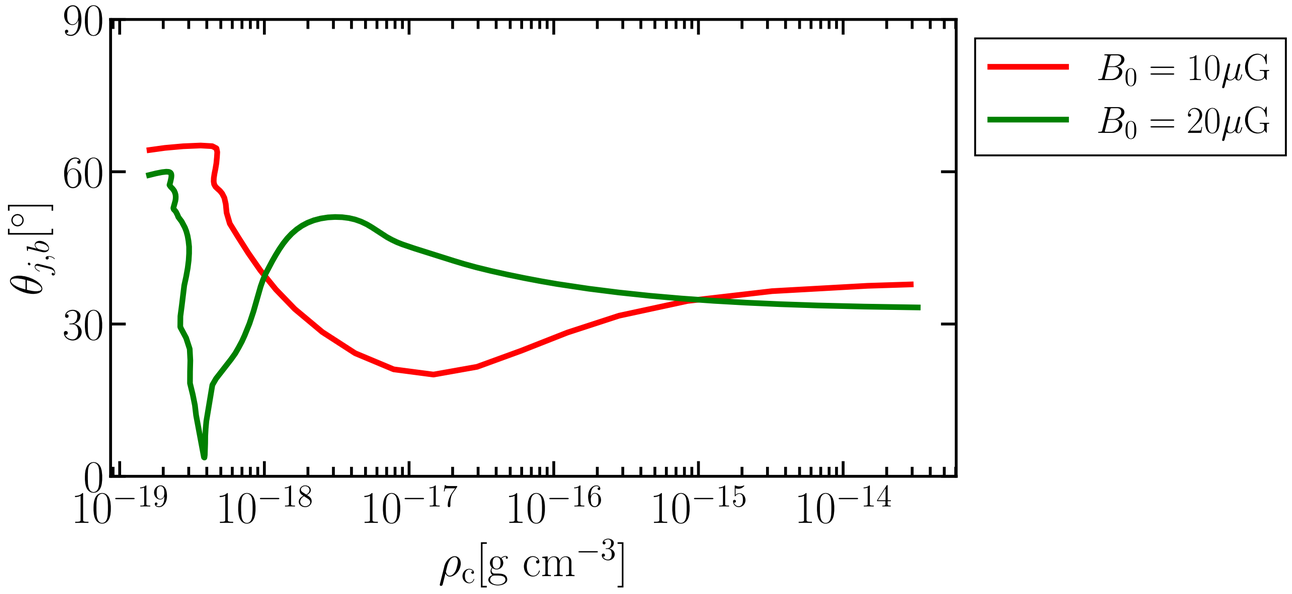

The minimum of $\theta_{j,B}$ during their evolution

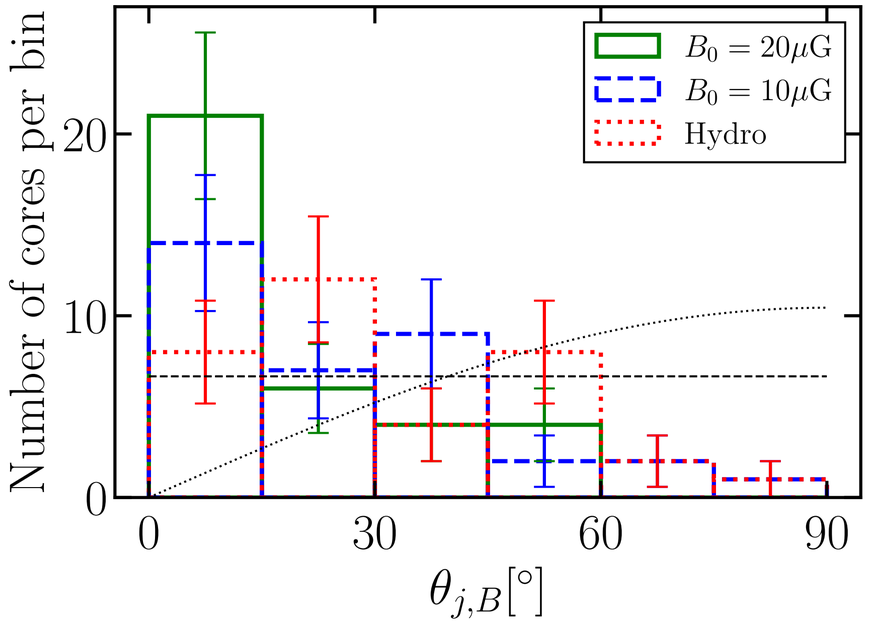

In the case of $20\mu\mathrm{G}$, most of the cores experience the alignment with the magnetic field, but the AM vector continue to oscillate.

The oscillation hides the alignment when we measure the angle at the final state of simulations.

AM profile

$B_0 = 20\mu\mathrm{G}$

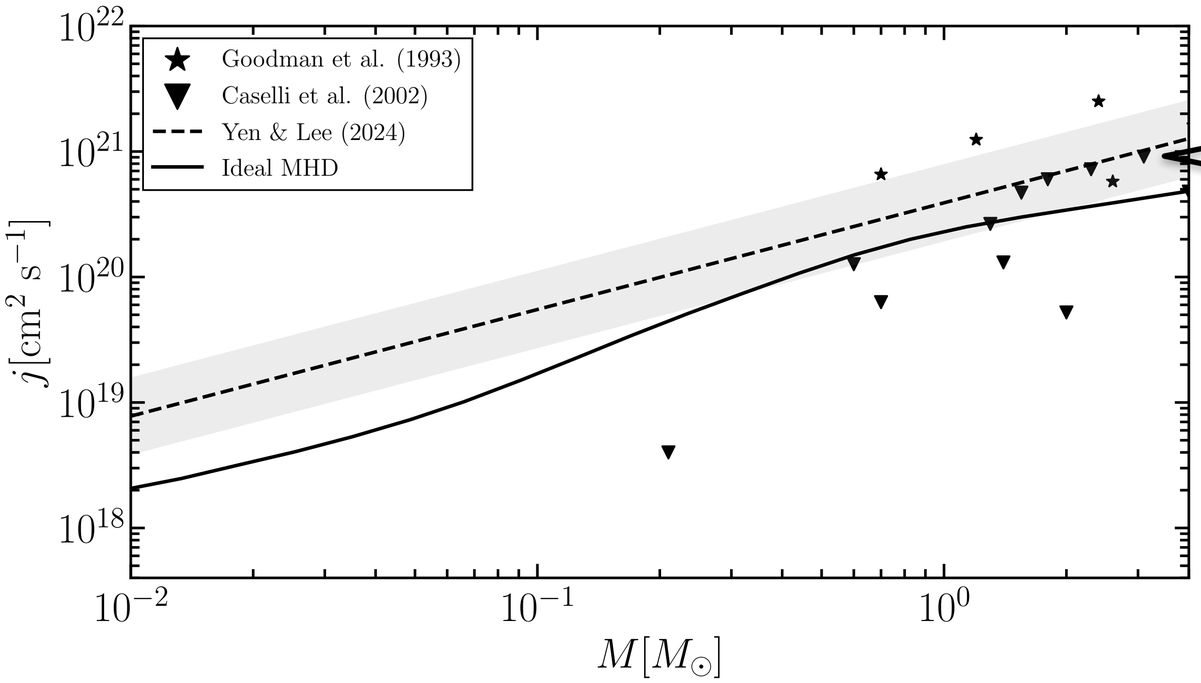

It is expected that the AM transfer become more effective in the strong magnetic field environment.

Observed disk radius (Yen and Lee 2024)

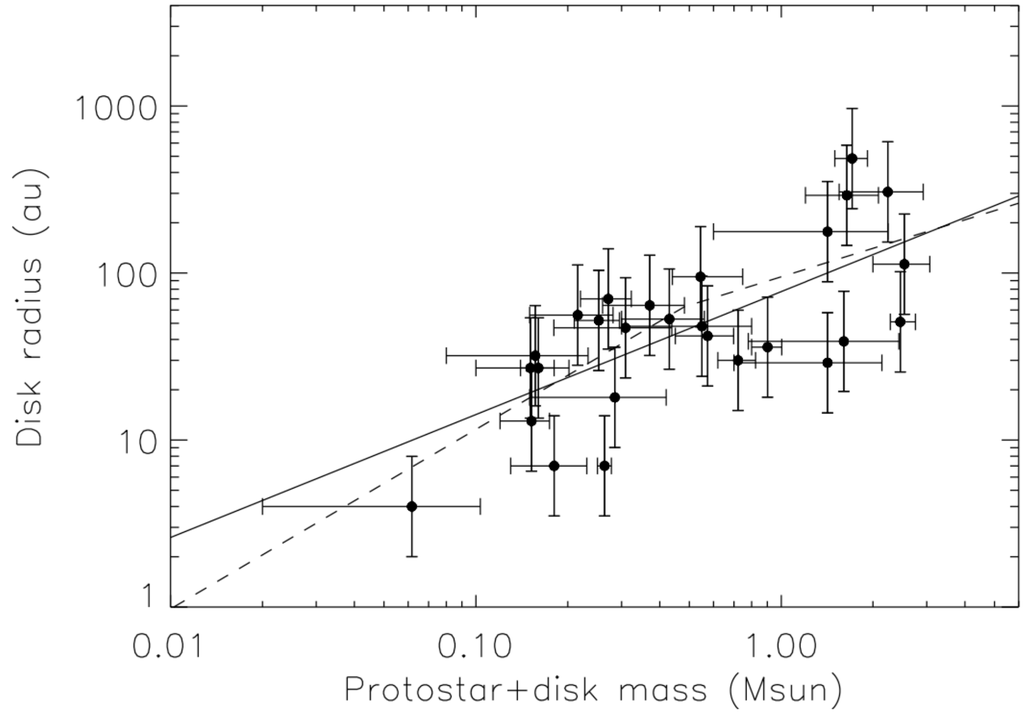

$$j = \sqrt{G(M_{\mathrm{star}} + M_{\mathrm{disk}})R_{\mathrm{disk}}}$$

Can disks form in the strong magnetized filaments?

Ambipolar Diffusion

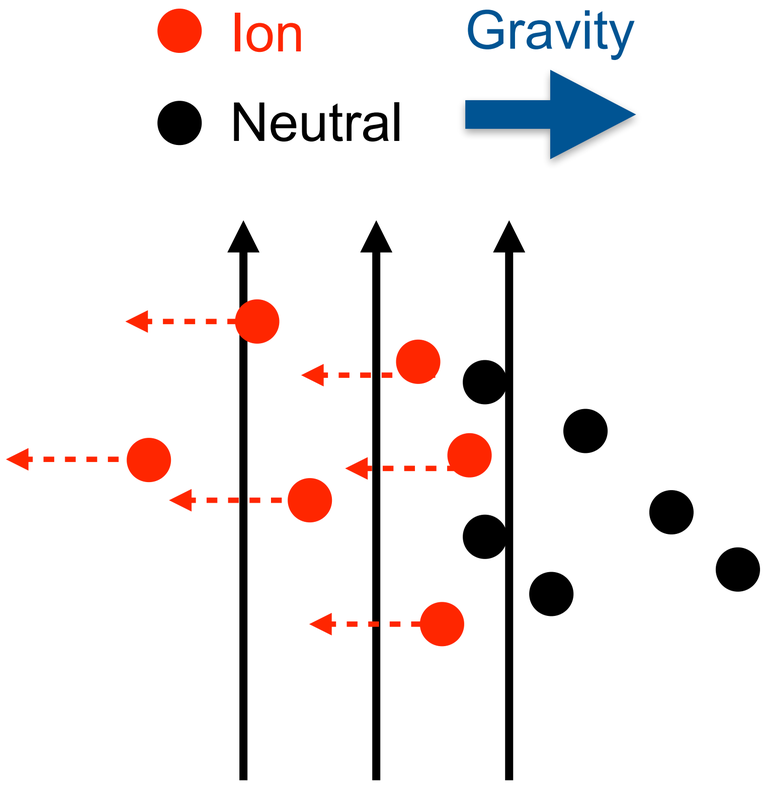

Neutrals and ions has different velocity if the ambipolar diffusion is efficient

Observation: Neutral pNH2D(1-1) - ion N2D+(2-1) velocity shift

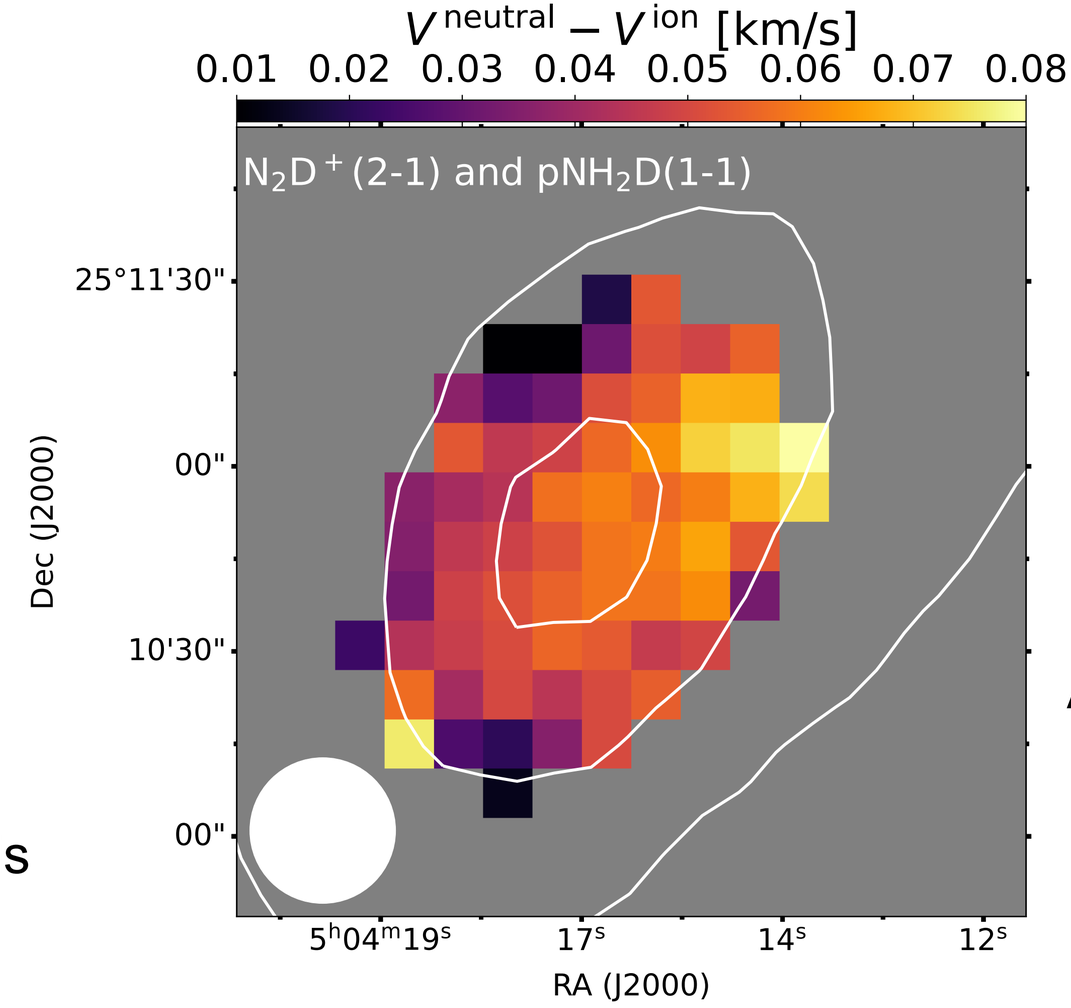

Observed velocity difference between ion and neutral reaches **~0.05 km/s**.

Arzoumanian et al. in prep

Ambipolar diffusion should be taken into account if the magnetic field is strong.

Importance of Dust Grain

$$\frac{\partial \mathbf{B}}{\partial t} = \nabla \times (\mathbf{v} \times \mathbf{B}) - \nabla \times \left\{ \eta_A \frac{\mathbf{B}}{B} \times \left[(\nabla \times \mathbf{B}) \times \frac{\mathbf{B}}{B} \right] \right\}$$

$$\frac{dn_d}{da_d} = A a_d^{-q} \left(a_{min} < a_d < a_{max} \right)$$

$$a_{min} = 5 \text{ nm}, \; q = 3.5$$

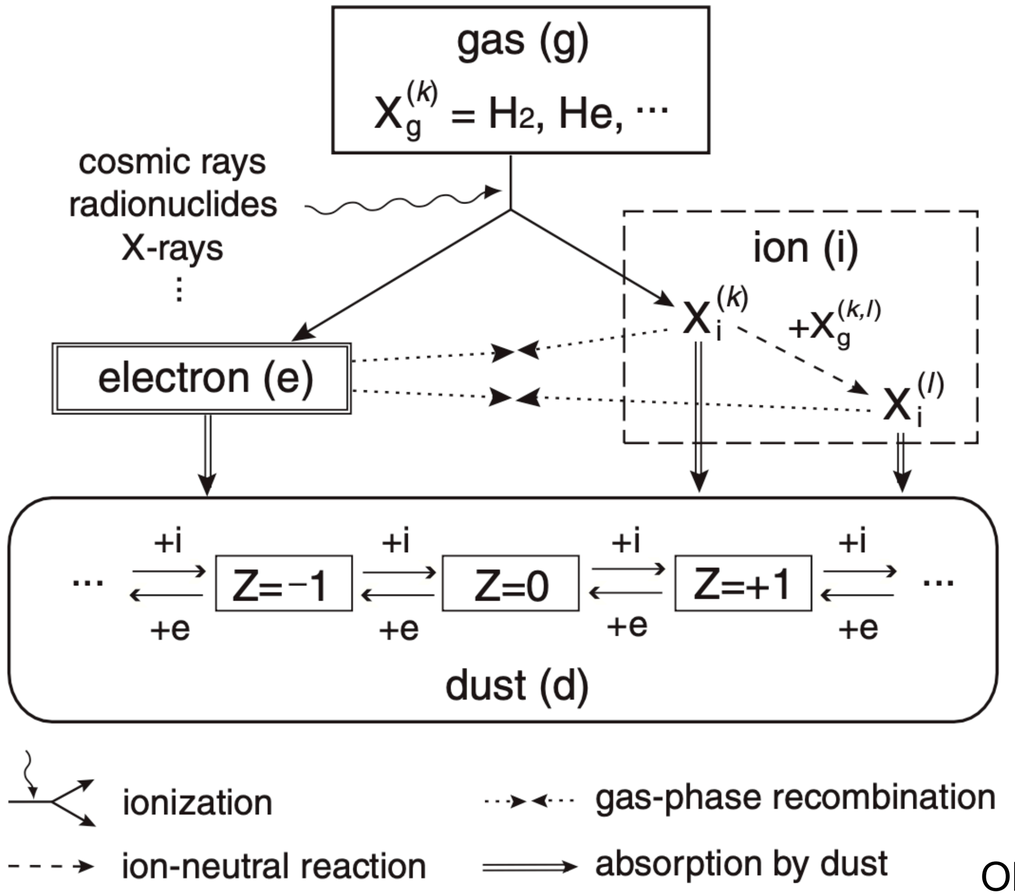

Okuzumi (2009)

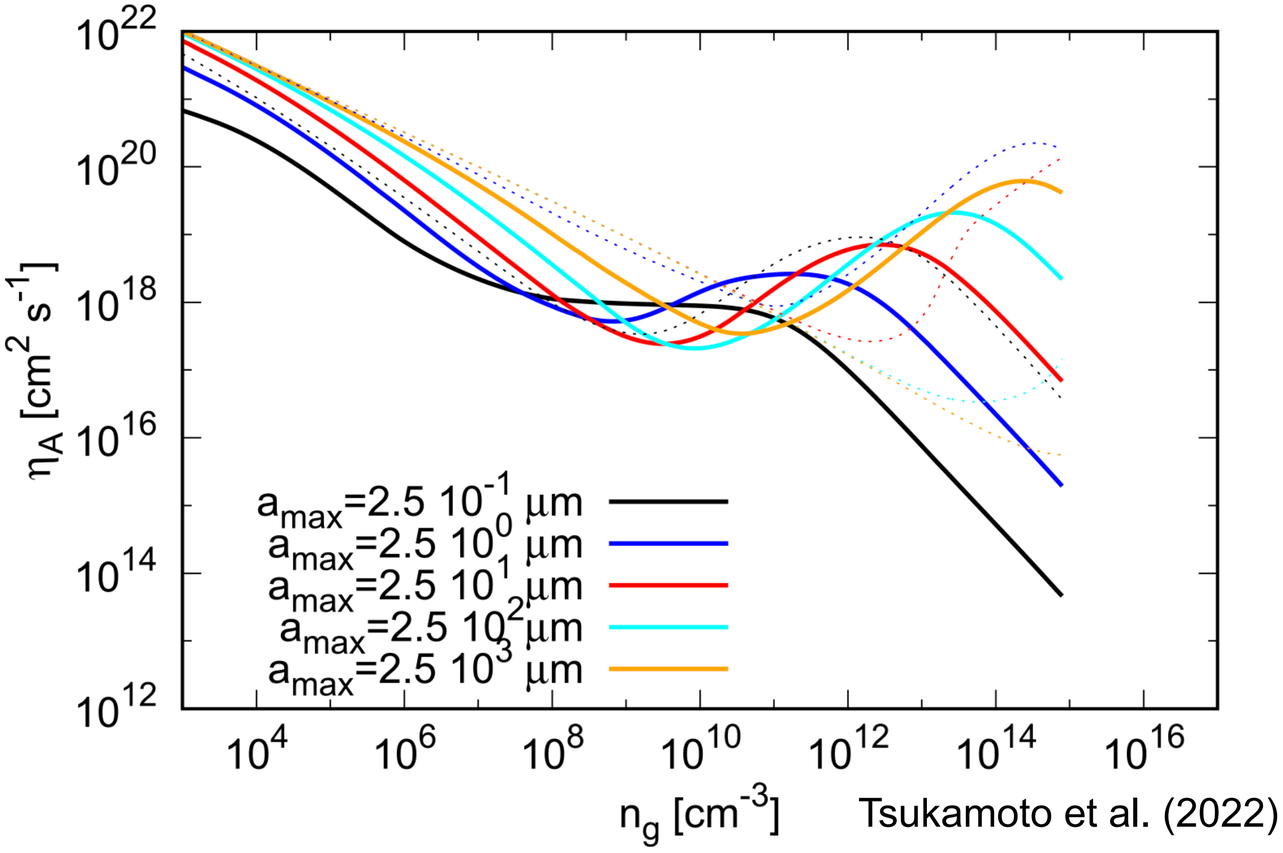

Tsukamoto et al. (2022)

The dust and its size distribution play an important role to determine the ionization state and resistivity of the molecular clouds.

Method and Setup

Basic equations (non-Ideal MHD)

Solved by Godunov Smoothed Particle Magnetohydrodynamics (GSPM) (Iwasaki & Inutsuka 2011; 2013; in perp)

Equation of motion: $$\frac{d\boldsymbol{v}}{dt} = -\frac{1}{\rho}\left\{\nabla\left(P+\frac{1}{2}B^2\right) - \nabla\cdot(\boldsymbol{BB})\right\} - \nabla\Phi$$

Gas + Magnetic Pressure | Magnetic tension | Gravity

Induction equation: $$\frac{d}{dt}\left(\frac{\boldsymbol{B}}{\rho}\right) = \left(\frac{\boldsymbol{B}}{\rho}\cdot\nabla\right)\boldsymbol{v} - \frac{1}{\rho}\nabla\times\left\{\eta_{\rm A}(\nabla\times\boldsymbol{B})\times\hat{\boldsymbol{B}}\times\hat{\boldsymbol{B}}\right\}$$

Ambipolar diffusion

Equation of state: Isothermal

Setup

- Number of particle: 14,824,000
- Line mass: Critical line mass $M_{\rm line} = 18{\rm M}_\odot{\rm pc}^{-1}$
- Turbulent velocity field: Kolmogorov turbulence

$$P(k)dk = Ak^{-5/3}dk$$

$$\sigma_{\rm 3D} = 2c_{\rm s}$$ (Hacar & Tafalla 2011)

- Density profile: $$\rho(r) = \rho_{\rm c}\left[1+\left(\frac{r}{H_0}\right)^2\right]^{-2} \quad H_0 = 0.05{\rm pc}$$ (Arzoumanian et al. 2011; 2019)
- Magnetic fields

Perpendicular to the filament axis (x-axis) (e.g., Planck Collaboration XXXV 2016)

$B_0 = 50\mu{\rm G}$

Resistivity

Tsukamoto & Okuzumi (2022)

$$\frac{dn_{\rm d}}{da_{\rm d}} = Aa_{\rm d}^{-q}\left(a_{\rm min} < a_{\rm d} < a_{\rm max}\right)$$

$$a_{\rm min} = 5\ {\rm nm}, a_{\rm max} = 0.25\ \mu{\rm m}, q = 3.5$$

$$a_{\rm max} = 0.25\ \mu{\rm m}, q = 2.5$$

$$a_{\rm max} = 2.5\ \mu{\rm m}, q = 2.5$$

Mass-to-flux ratio

The molecular cloud core is sub critical when

$$B_0 > 62\mu{\rm G}$$

Marginally super critical

Result: Ideal MHD

$B_0 = 50\mu$G, Ideal MHD

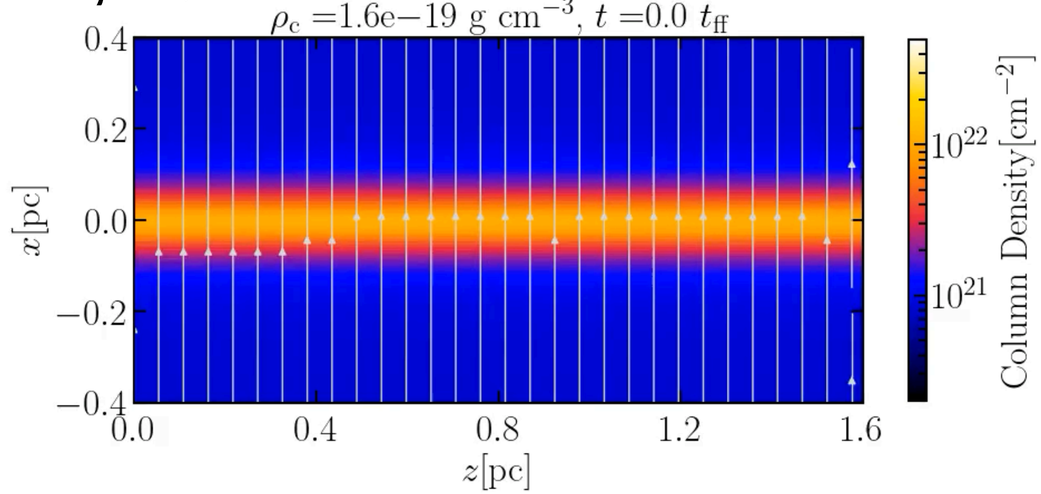

AM profile in the core

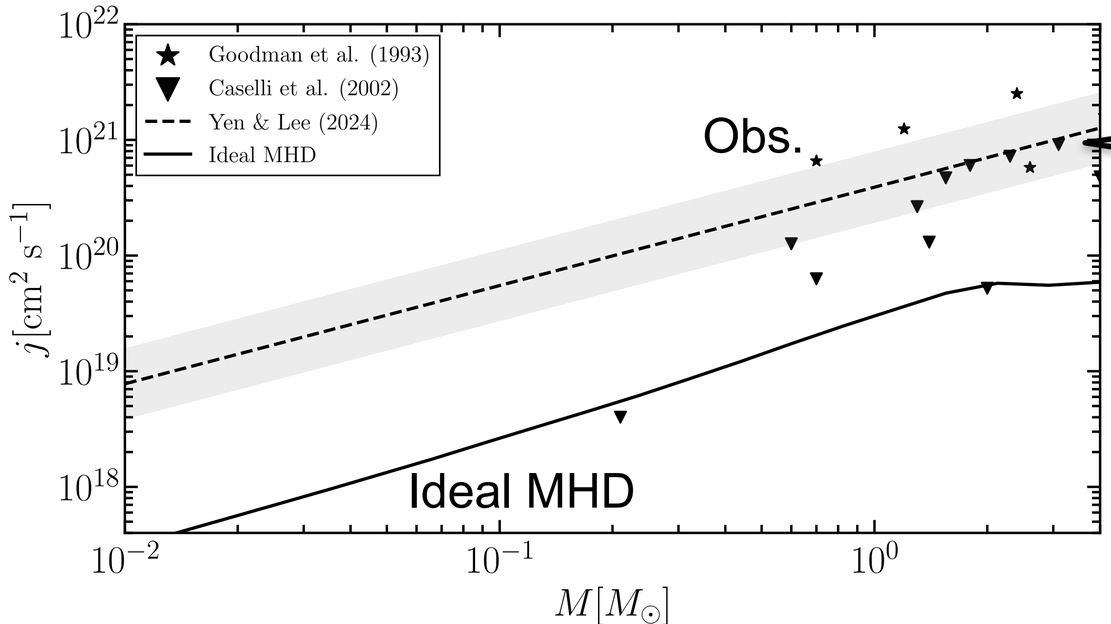

Observed disk radius (Yen and Lee 2024)

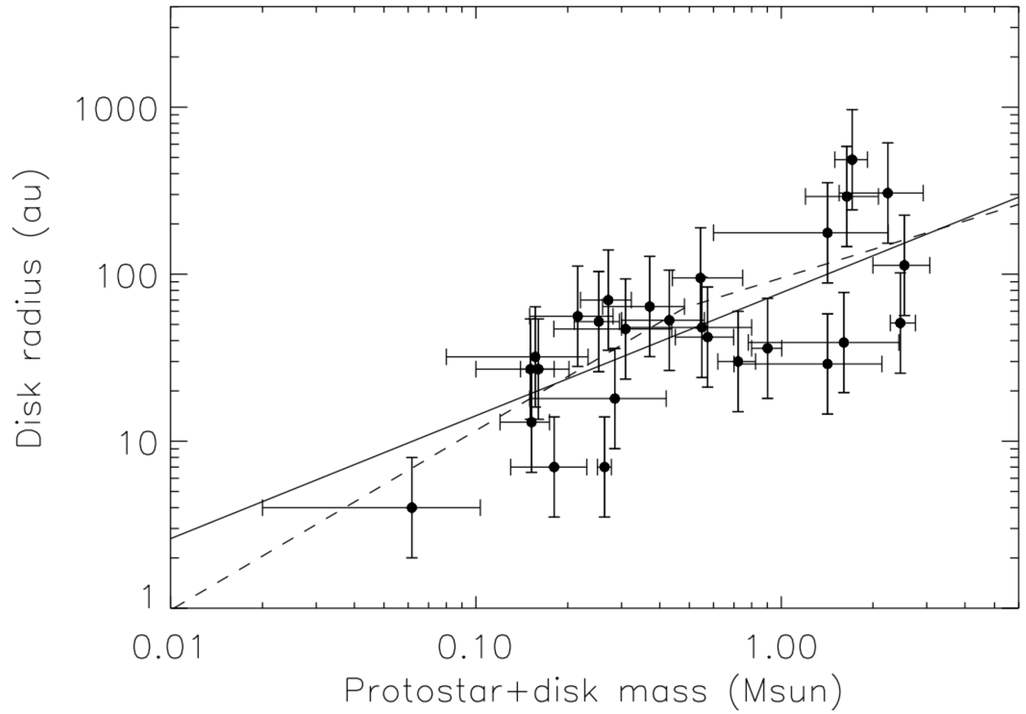

$$j = \sqrt{G(M_{\rm star} + M_{\rm disk})R_{\rm disk}}$$

In the ideal MHD case, AM is too small compared with observations.

AM profile

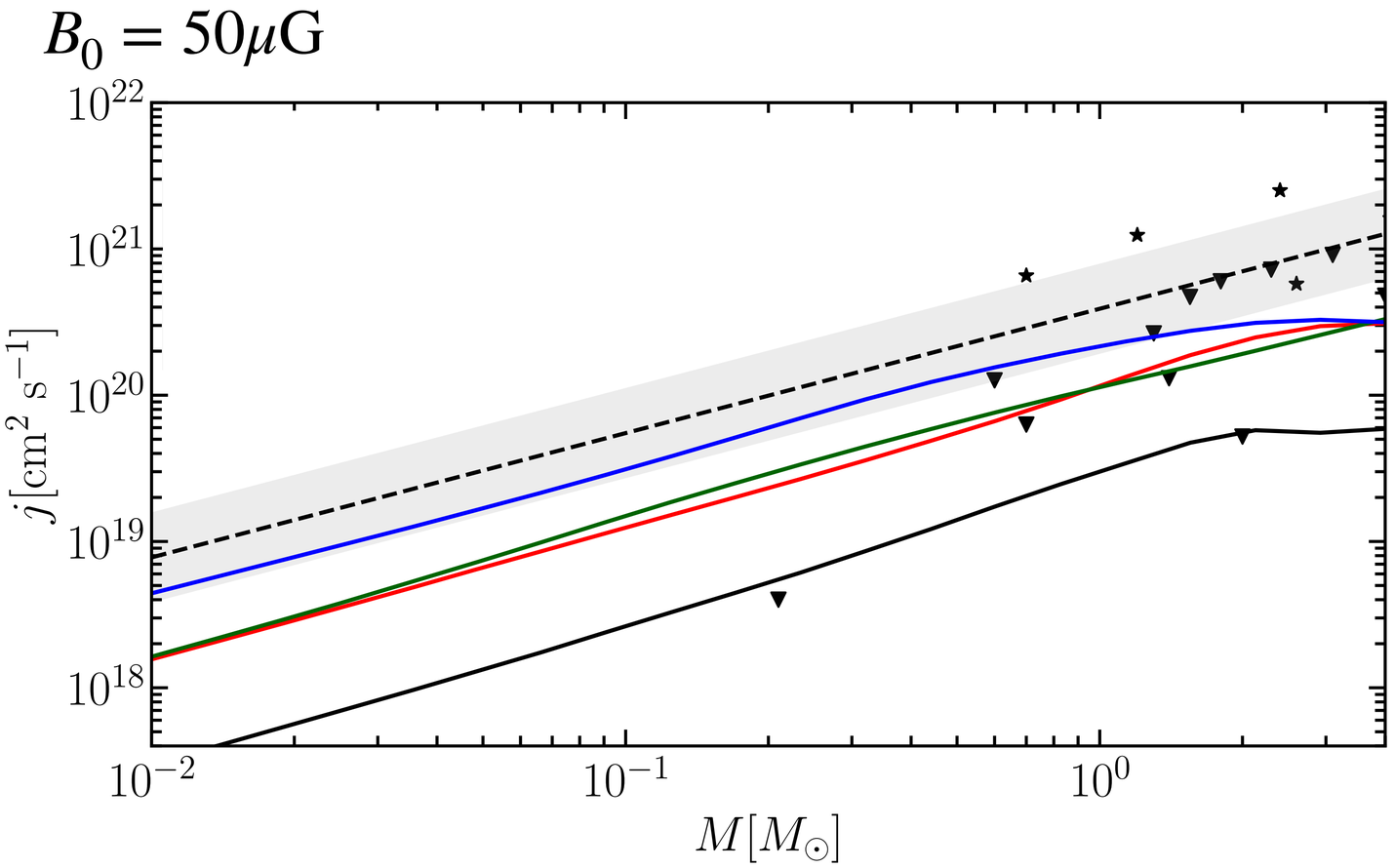

$$\frac{dn_\mathrm{d}}{da_\mathrm{d}} = A a_\mathrm{d}^{-q} \left(a_\mathrm{min} < a_\mathrm{d} < a_\mathrm{max}\right)$$

$$a_\mathrm{min} = 5\ \mathrm{nm}$$

- Goodman et al. (1993)
- Caselli et al. (2002)
- Yen & Lee (2024)
- Ideal MHD
- $q = 3.5,\ a_\mathrm{max} = 0.25\ \mu\mathrm{m}$ (MRN)
- $q = 3.5,\ a_\mathrm{max} = 2.5\ \mu\mathrm{m}$
- $q = 2.5,\ a_\mathrm{max} = 2.5\ \mu\mathrm{m}$

AM profile

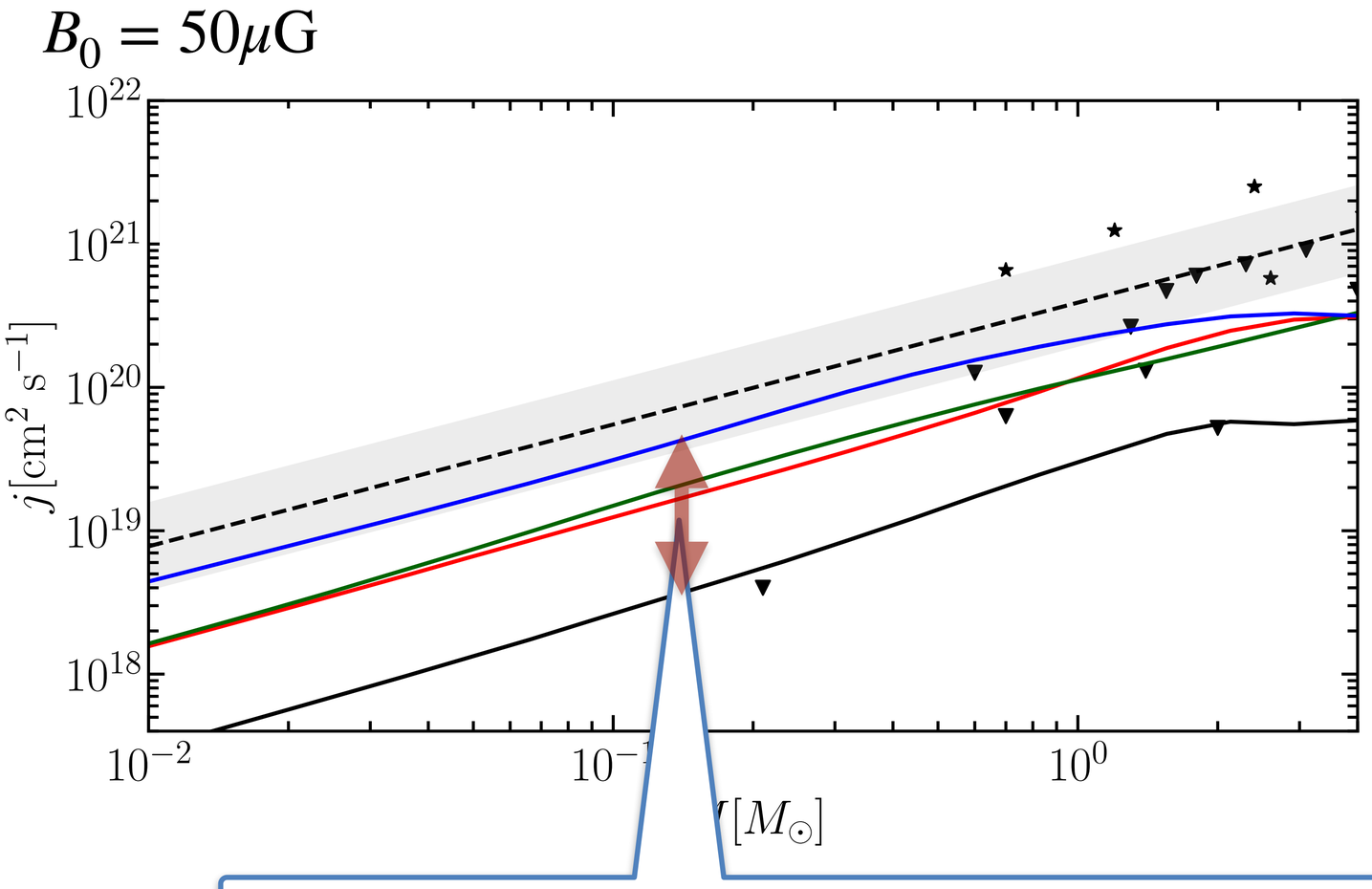

$$\frac{dn_\mathrm{d}}{da_\mathrm{d}} = A a_\mathrm{d}^{-q} \left(a_\mathrm{min} < a_\mathrm{d} < a_\mathrm{max}\right)$$
$$a_\mathrm{min} = 5\ \mathrm{nm}$$

- Goodman et al. (1993)
- Caselli et al. (2002)
- Yen & Lee (2024)
- Ideal MHD
- $q = 3.5,\ a_\mathrm{max} = 0.25\ \mu\mathrm{m}$ (MRN)
- $q = 3.5,\ a_\mathrm{max} = 2.5\ \mu\mathrm{m}$
- $q = 2.5,\ a_\mathrm{max} = 2.5\ \mu\mathrm{m}$

Ambipolar diffusion weakens the AM transfer compared with ideal MHD case by an order of magnitude.

AM profile

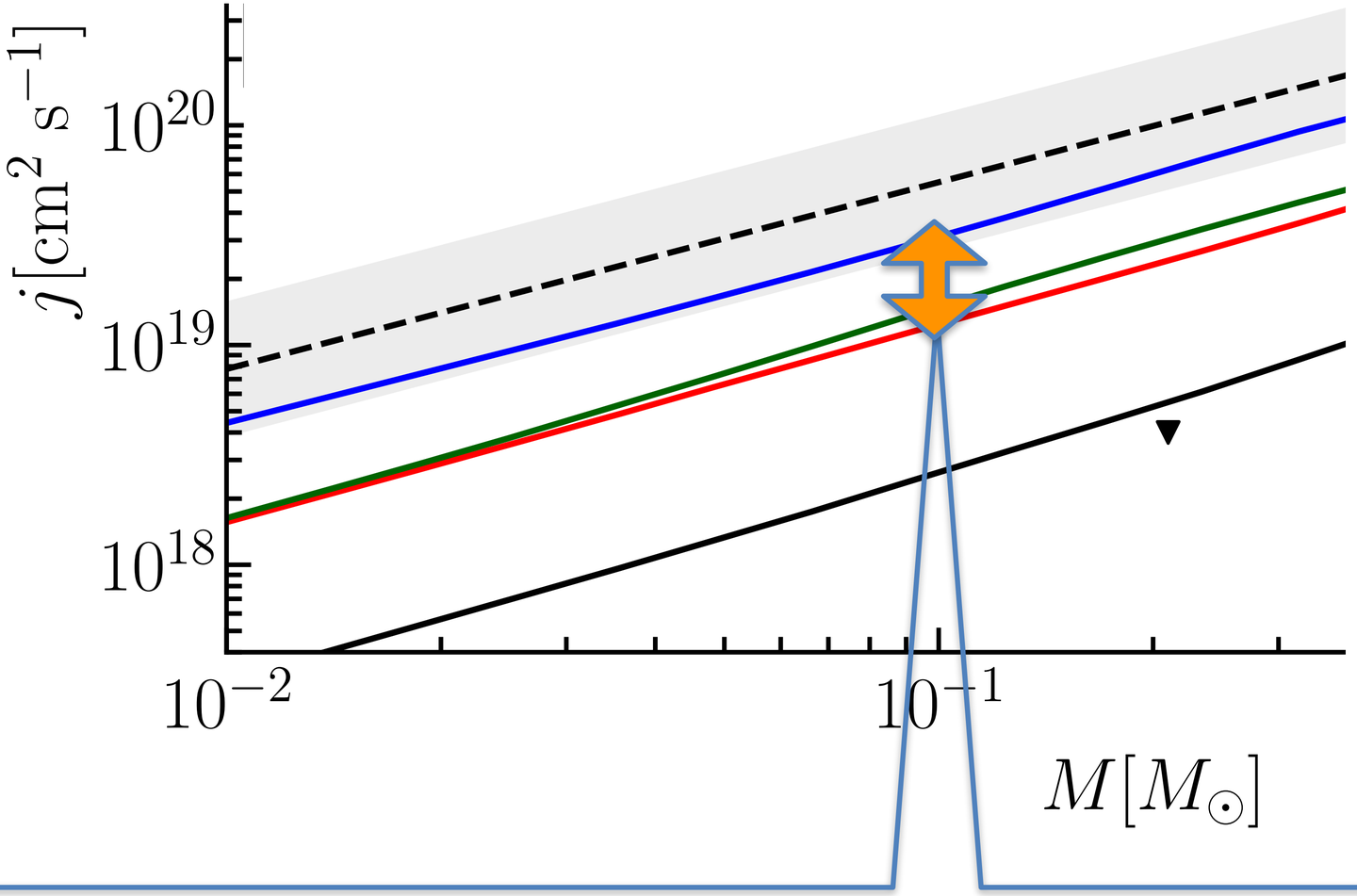

$$\frac{dn_\mathrm{d}}{da_\mathrm{d}} = A a_\mathrm{d}^{-q} \left(a_\mathrm{min} < a_\mathrm{d} < a_\mathrm{max}\right)$$
$$a_\mathrm{min} = 5\ \mathrm{nm}$$

- ★ Goodman et al. (1993)
- ▼ Caselli et al. (2002)
- Yen & Lee (2024)
- Ideal MHD
- $q = 3.5,\ a_\mathrm{max} = 0.25\ \mu\mathrm{m}$ (MRN)
- $q = 3.5,\ a_\mathrm{max} = 2.5\ \mu\mathrm{m}$
- $q = 2.5,\ a_\mathrm{max} = 2.5\ \mu\mathrm{m}$

If the dust growth is efficient, resultant AM become large compared with MRN distribution (red line) by a factor of 2.

Summary

❖We investigate the evolution of the angular momentum of molecular cloud cores in strongly magnetized filamentary molecular clouds.

❖In the case of $B_0 = 20\ \mu G$, the most of the cores experience the alignment with the magnetic field, but it is difficult to observe the alignment because of the oscillation of the AM vector.

❖Ambipolar diffusion weakens the AM transfer compared with ideal MHD case by an order of magnitude.

❖If the dust growth is efficient, resultant AM become large compared with MRN distribution by a factor of 2.

Future work

- Effect of the dust size evolution
- Synthetic observation using radiative transfer code

Appendix

Dust Growth in Molecular Clouds

Core shine (e.g., Pagani et al. 2010)

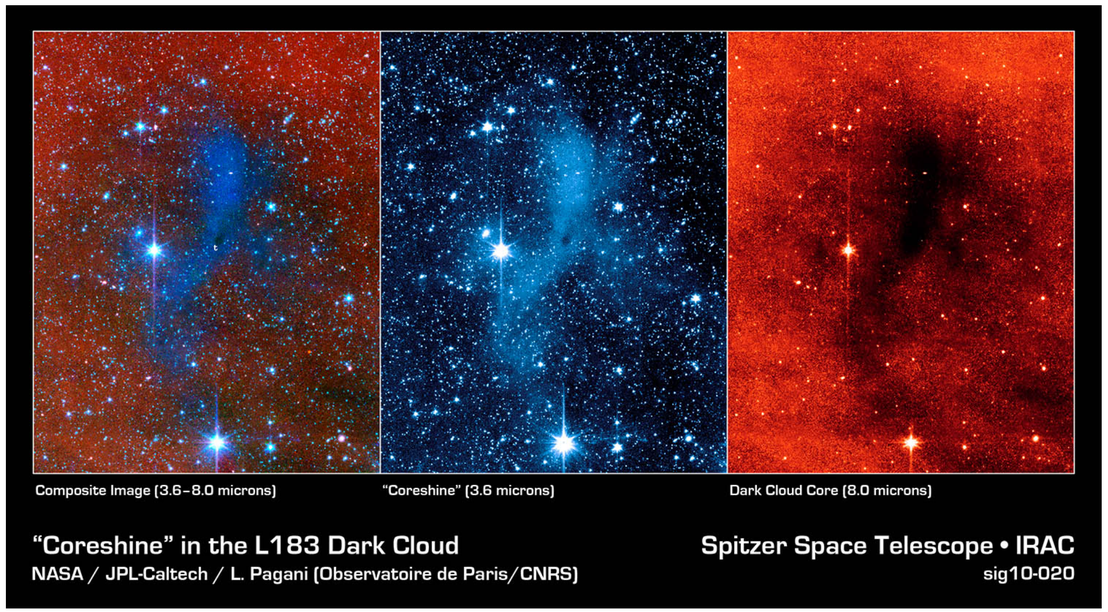

Dust opacity (Roy et al. 2013)

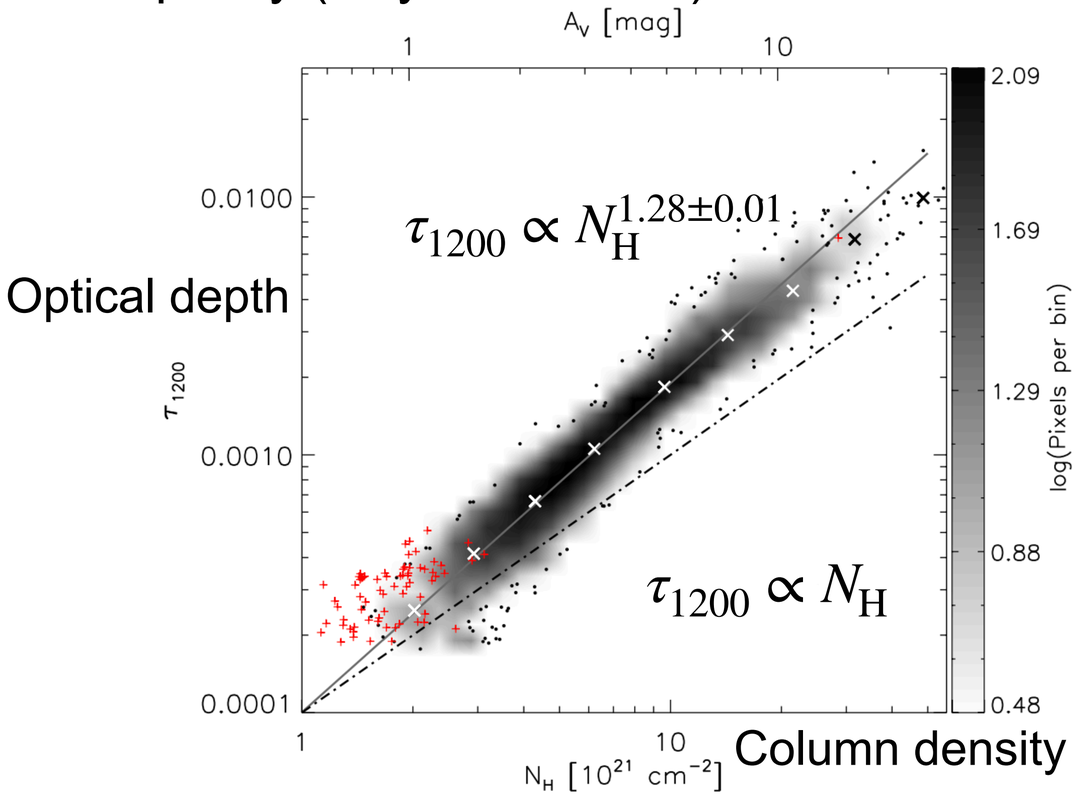

Observations suggest that the dust grains grow in the high density region.

Purpose of this study

To investigate the effect of the ambipolar diffusion on filament fragmentation by changing the initial dust size distribution.

Direction of the Angular Momentum

$$\cos\theta_{\mathrm{fil},J} = J_z/J$$

Angle between angular momentum direction and filament axis

$1.0\ \mathrm{M}_\odot$

Initial state

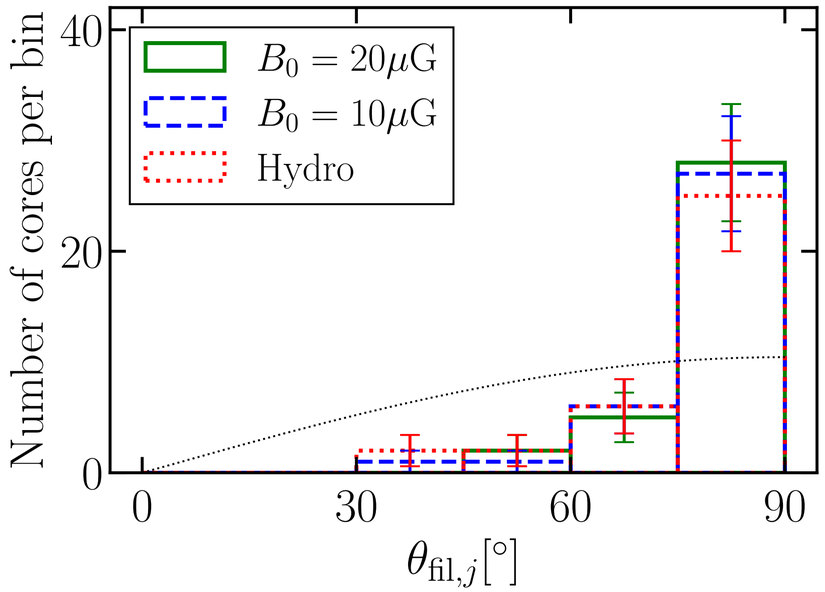

Final state

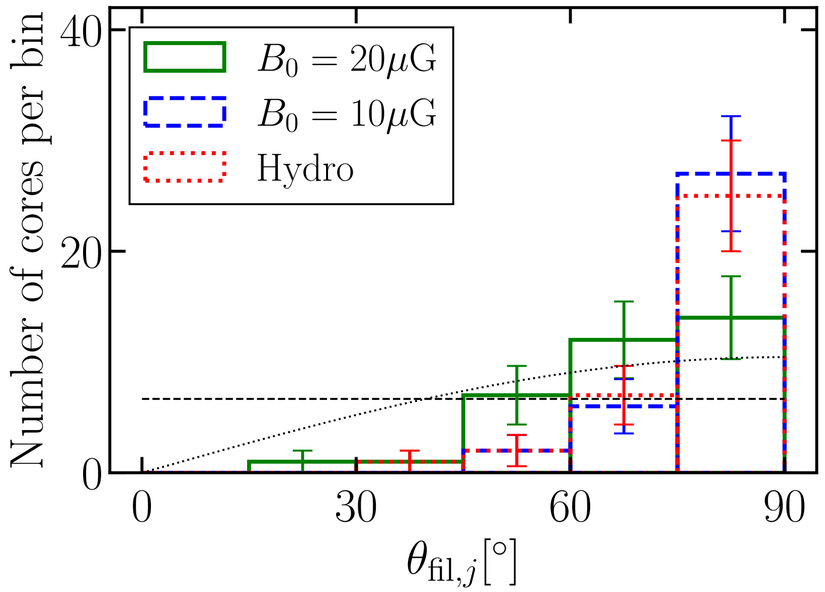

At the initial state, most cores rotate perpendicular to the filament axis.

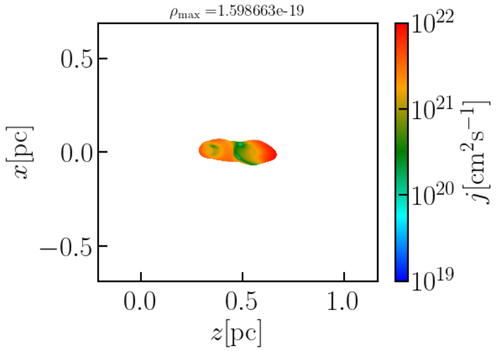

In the case of $20\mu\mathrm{G}$, the distribution follows random distribution in 3D rather than perpendicular distribution at the final state.

Drift Velocity on Synthetic Observation Map

Fiducial model $\frac{dn_{\rm d}}{da_{\rm d}} = A a_{\rm d}^{-q} \left(a_{\rm min} < a_{\rm d} < a_{\rm max}\right)$

$a_{\rm min} = 5\ {\rm nm}, a_{\rm max} = 0.25\ \mu{\rm m},\ q = 3.5$ (MRN)

$$\boldsymbol{v}_{\rm drift} \equiv \eta_A \frac{(\nabla \times \boldsymbol{B}) \times \boldsymbol{B}}{|\boldsymbol{B}|^2}$$

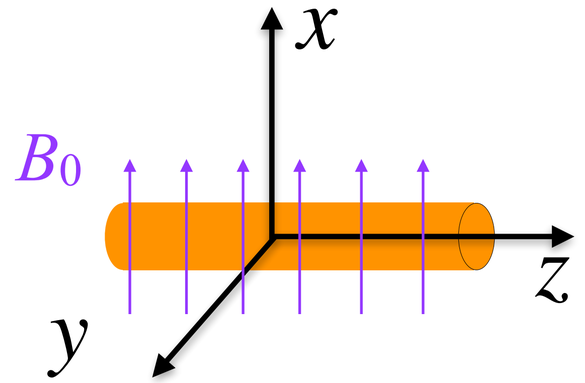

To mimic the observation, we integrate the density and velocity along the y-axis

Slice on the x-y place

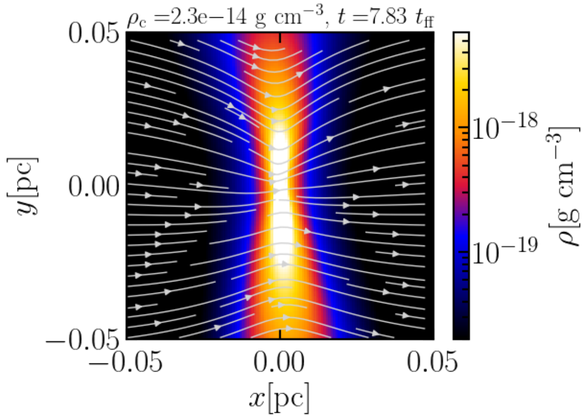

Line-of-sight

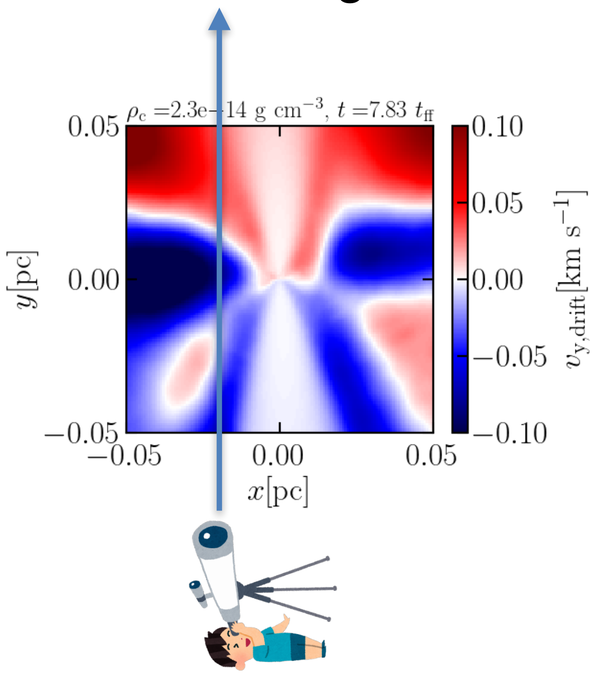

Projection map

$$\int_{n_{\rm H_2}(\boldsymbol{x}) > n_{\rm crit}} \rho v_{\rm y,drift} dy \qquad n_{\rm crit} = 10^3\ {\rm cm}^{-3}$$

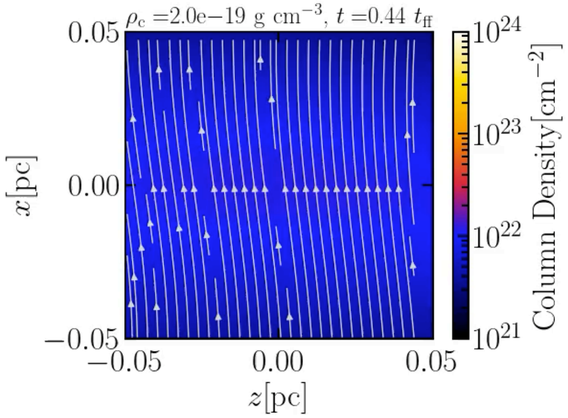

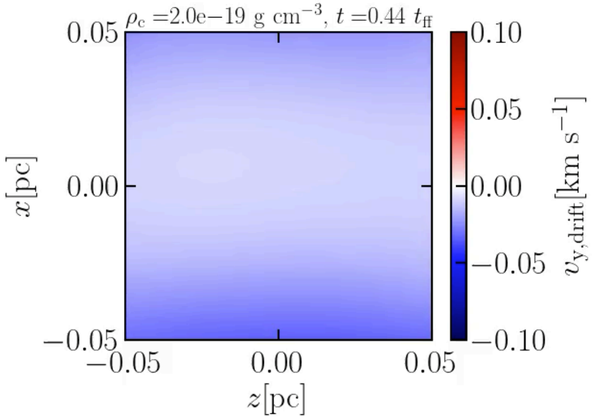

The drift velocity is mostly cancelled out due to the line-of-sight integration.

Drift Velocity on Synthetic Observation Map

Dependence of the drift velocity on the maximum dust size

$$\frac{dn_{\rm d}}{da_{\rm d}} = A a_{\rm d}^{-q} \left(a_{\rm min} < a_{\rm d} < a_{\rm max}\right)$$

$a_{\rm min} = 5$ nm, $a_{\rm max} = 0.25$ μm, $q = 3.5$ (MRN)

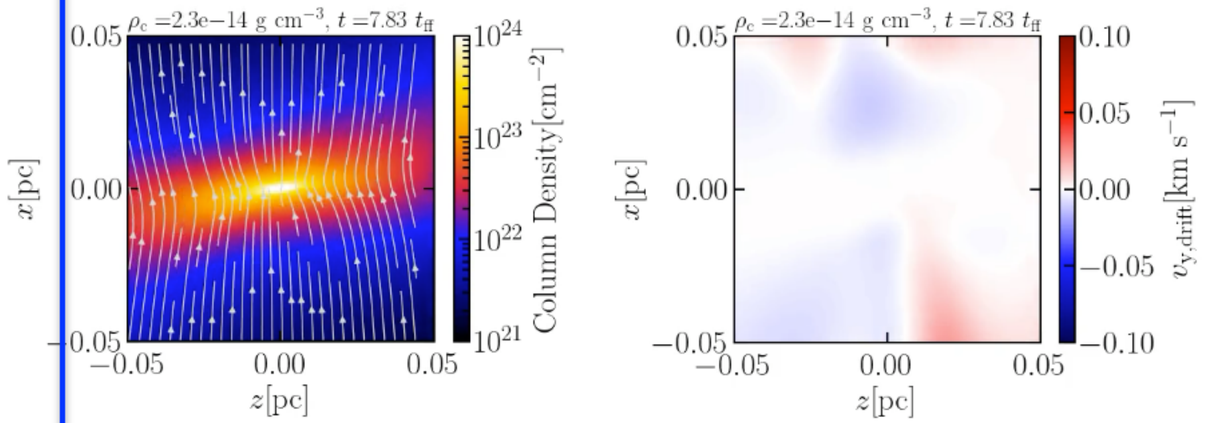

Too small to detect in the observations.

$a_{\rm min} = 5$ nm, $a_{\rm max} = 2.5$ μm, $q = 2.5$

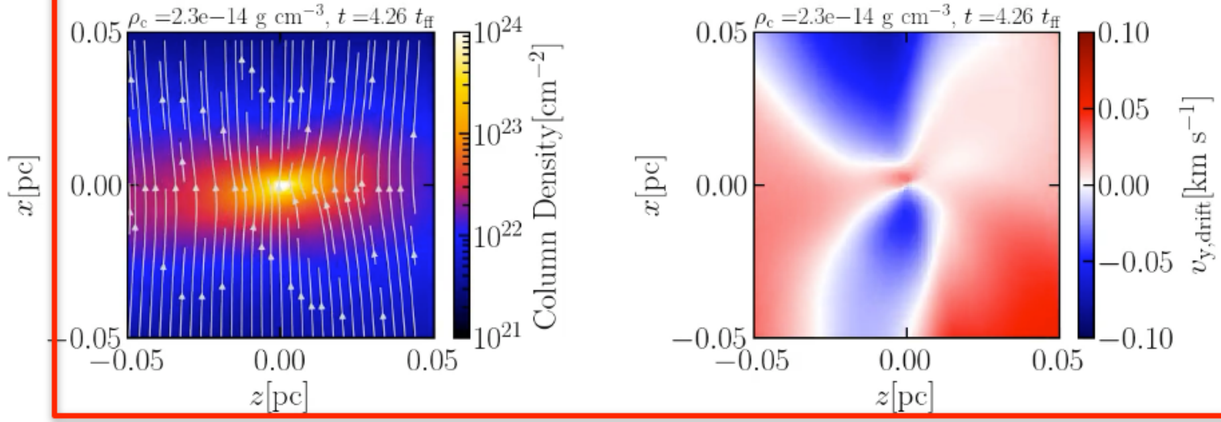

Drift velocity reaches ~ 0.05km/s.

Dust growth is needed to explain the observation.

Drift Velocity on Synthetic Observation Map

Dependence of the drift velocity on the maximum dust size

$$\frac{dn_{\rm d}}{da_{\rm d}} = A a_{\rm d}^{-q} \left(a_{\rm min} < a_{\rm d} < a_{\rm max}\right)$$

Projection map

$a_{\rm min} = 5\ {\rm nm}, a_{\rm max} = 0.25\ \mu{\rm m},\ q = 3.5$

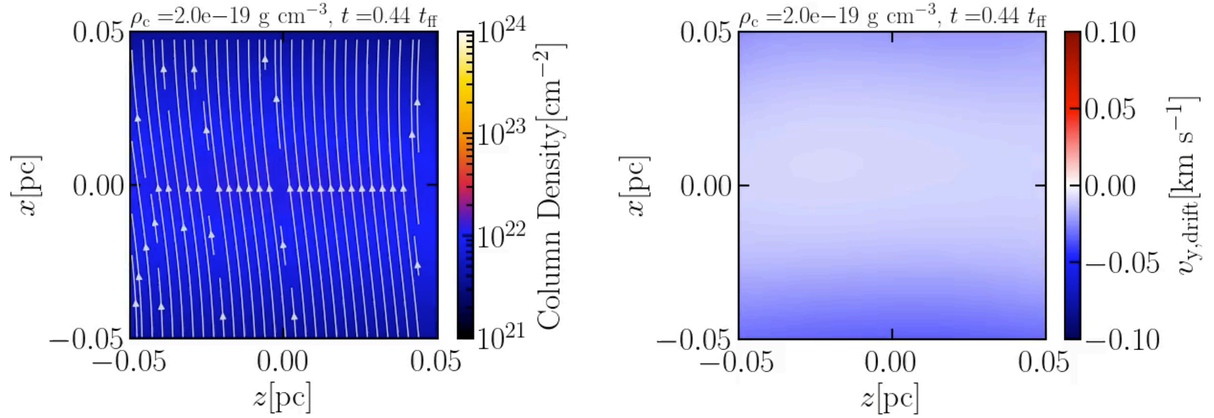

$a_{\rm min} = 5\ {\rm nm}, a_{\rm max} = 2.5\ \mu{\rm m},\ q = 3.5$

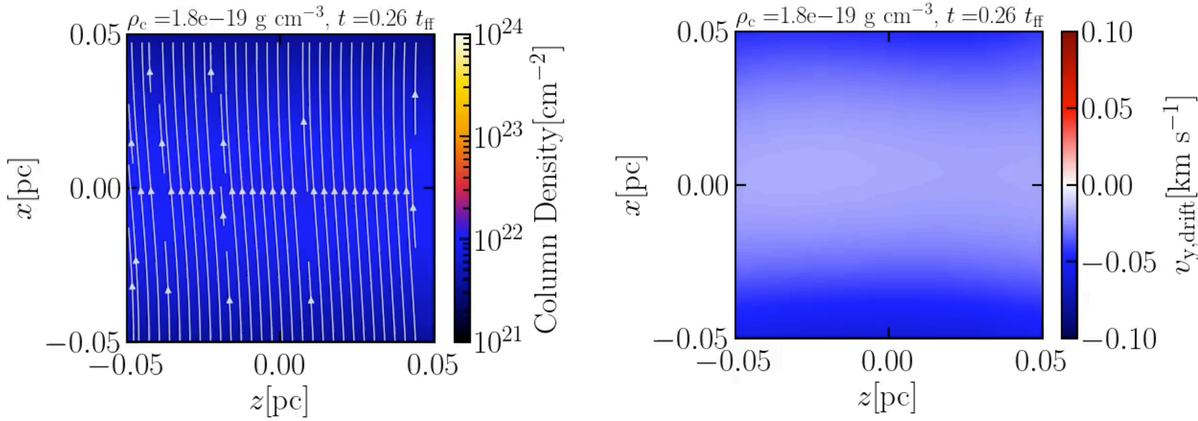

$a_{\rm min} = 5\ {\rm nm}, a_{\rm max} = 2.5\ \mu{\rm m},\ q = 2.5$

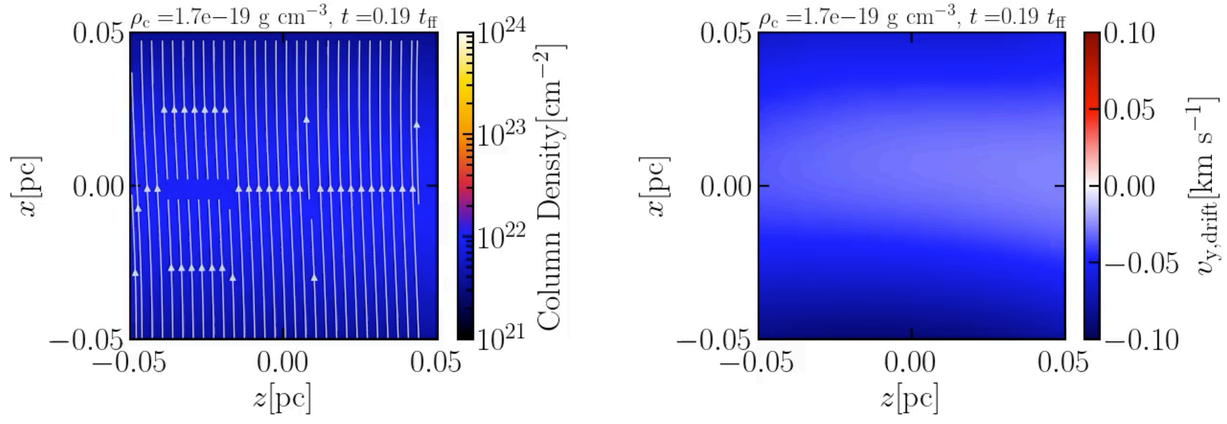

Drift Velocity on Synthetic Observation Map

Dependence of the drift velocity on the maximum dust size

$$\frac{dn_{\rm d}}{da_{\rm d}} = A a_{\rm d}^{-q} \left(a_{\rm min} < a_{\rm d} < a_{\rm max}\right)$$

$$a_{\rm min} = 5\ {\rm nm}, a_{\rm max} = 0.25\ \mu{\rm m},\ q = 3.5$$

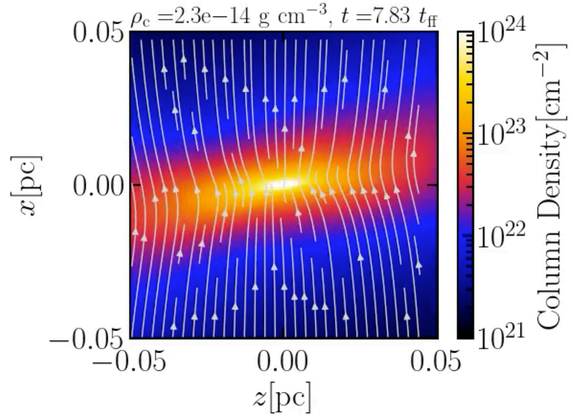

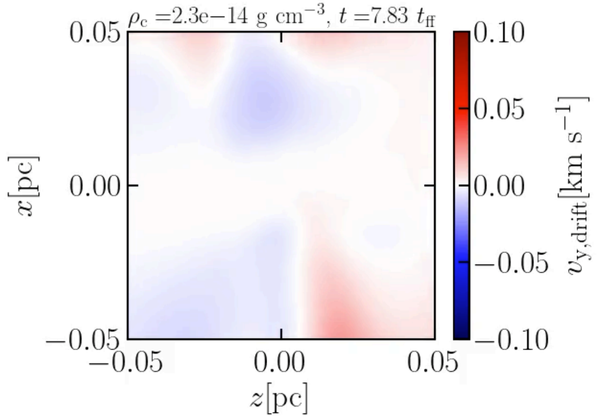

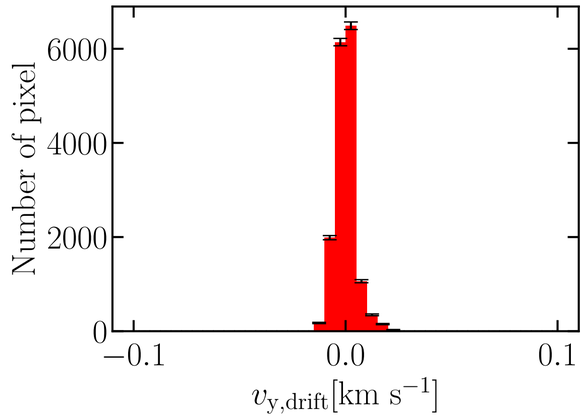

$$a_{\rm min} = 5\ {\rm nm}, a_{\rm max} = 2.5\ \mu{\rm m},\ q = 2.5$$

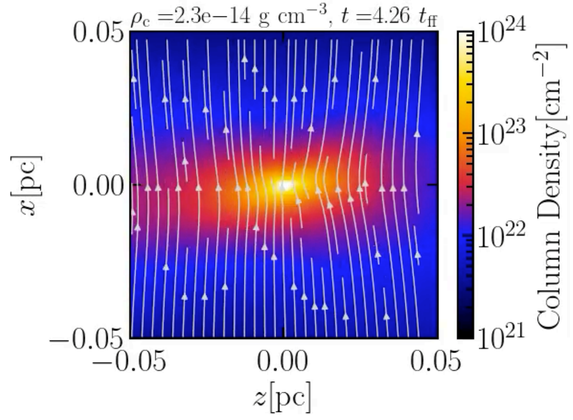

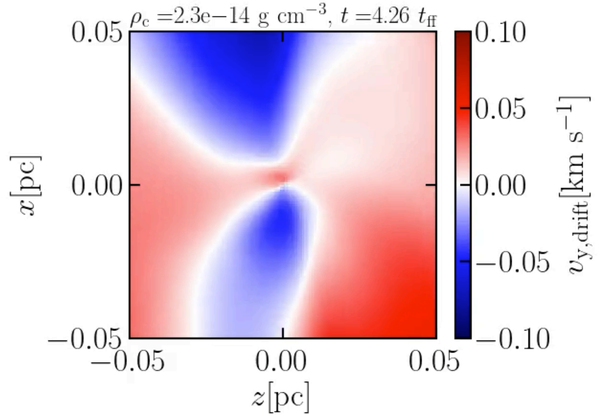

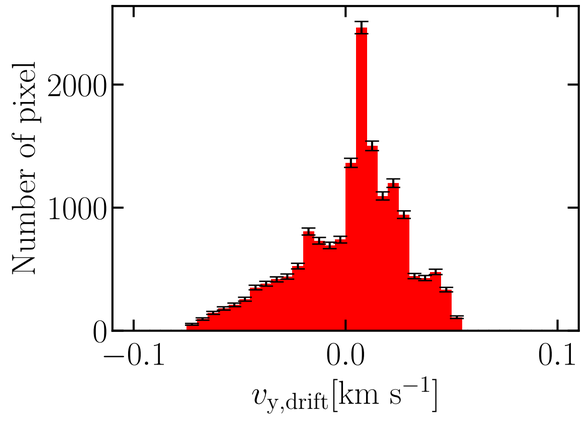

Evolution of AM

Core mass: $1\ \mathrm{M}_\odot$

Evolution of the angle between the rotation and B-field

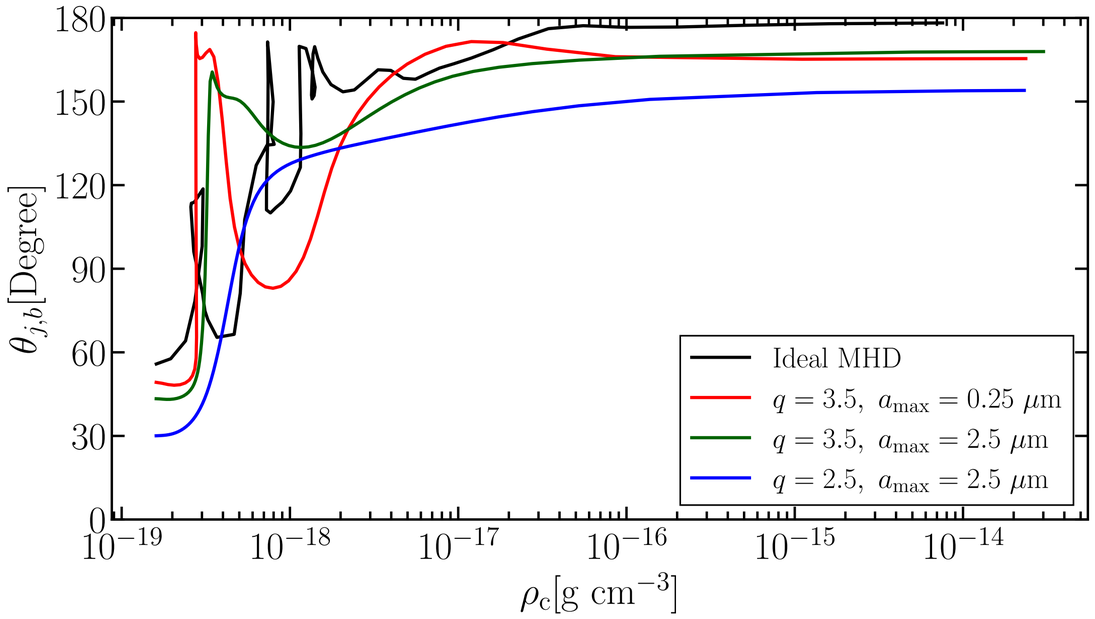

$$\frac{dn_d}{da_d} = A a_d^{-q} \left(a_{min} < a_d < a_{max}\right)$$

Observations

Outflow vs B-field

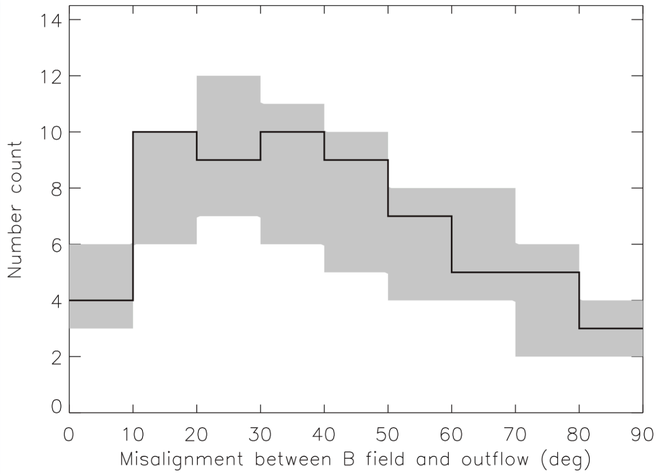

dust polarized emission at 850μm JCMT BISTRO survey

Yen et al. (2021)

Velocity gradient vs B-field

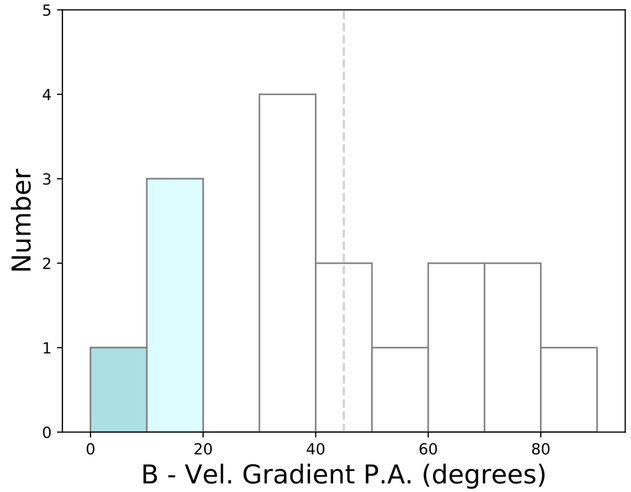

dust polarized emission at 0.87 mm, N_2H^+ (SMA)

Galametz et al. (2020)

(See also Hull 2013, Gupta 2022, Huang 2024)

The effect of the ambipolar diffusion is needed to explain the observations.

Evolution of B-field

$B_0 = 50\mu\mathrm{G}$, Ideal MHD

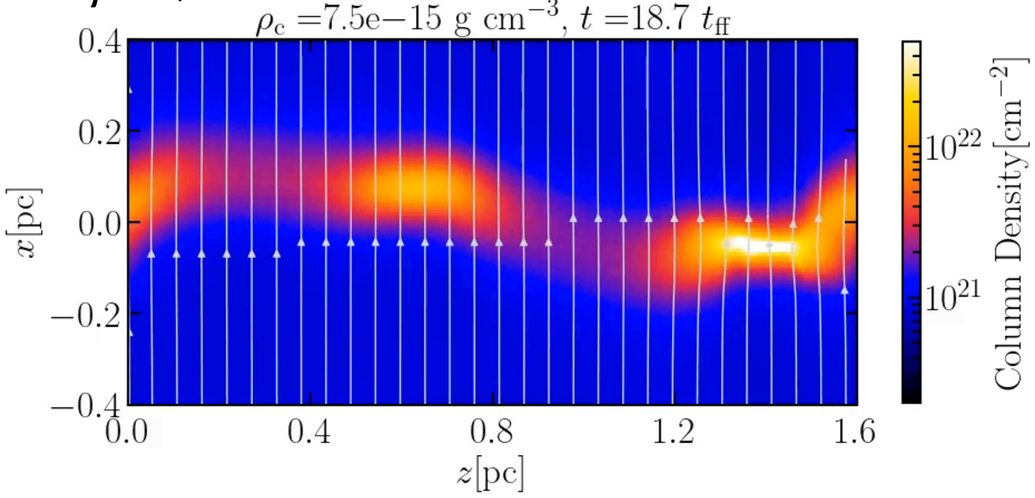

$$\frac{dn_d}{da_d} = Aa_d^{-q} \left(a_{min} < a_d < a_{max}\right)$$

$a_{min} = 5$ nm, $a_{max} = 0.25$ μm, $q = 3.5$ (fiducial model)

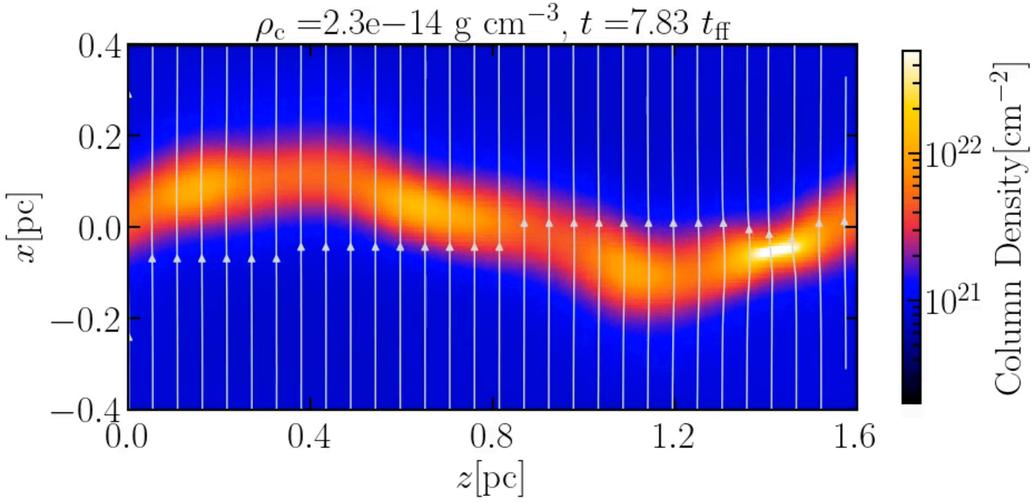

Evolution of the maximum B-field

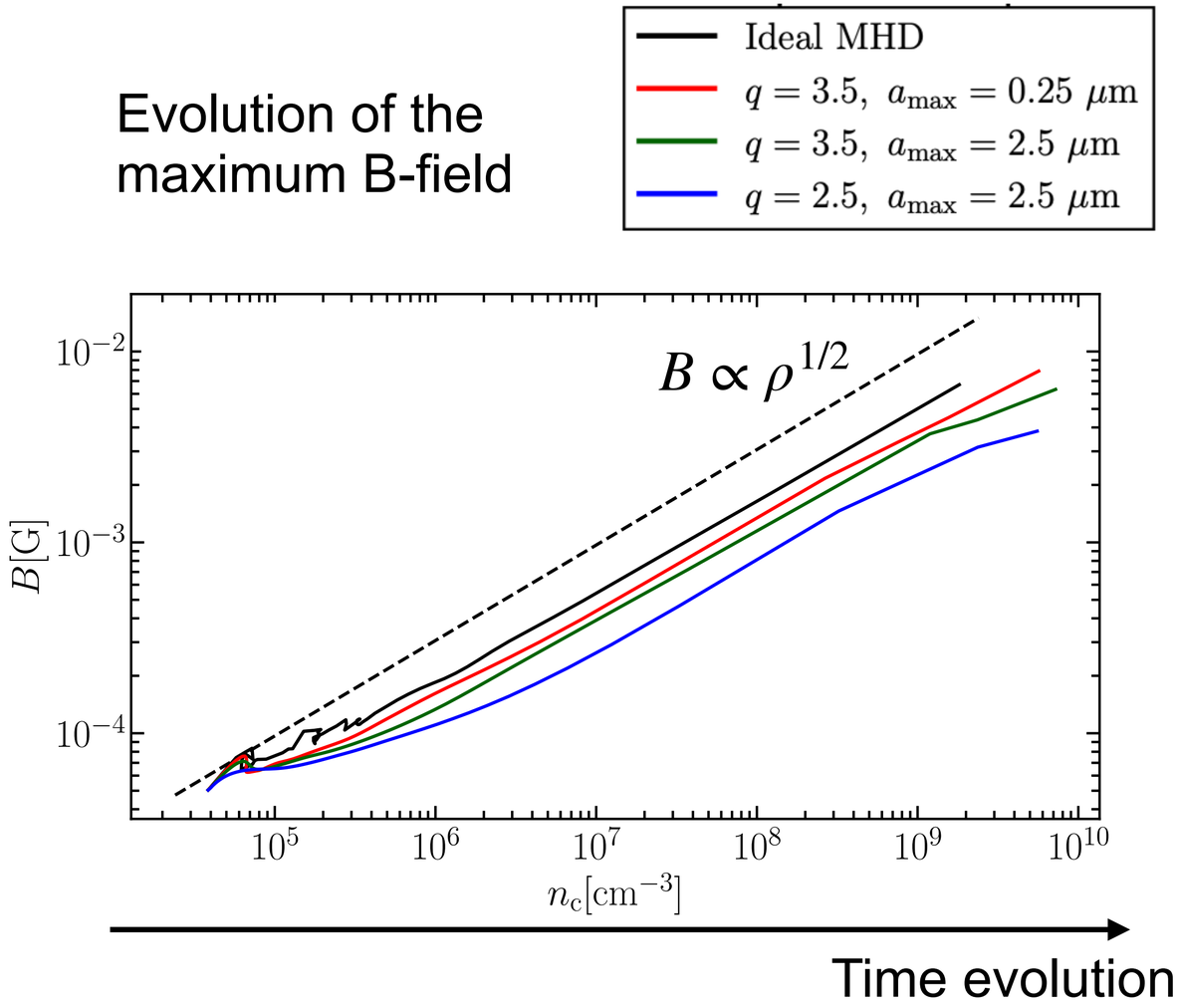

Observed Drift Velocity

Neutral pNH2D(1-1) - ion N2D+(2-1) velocity shift

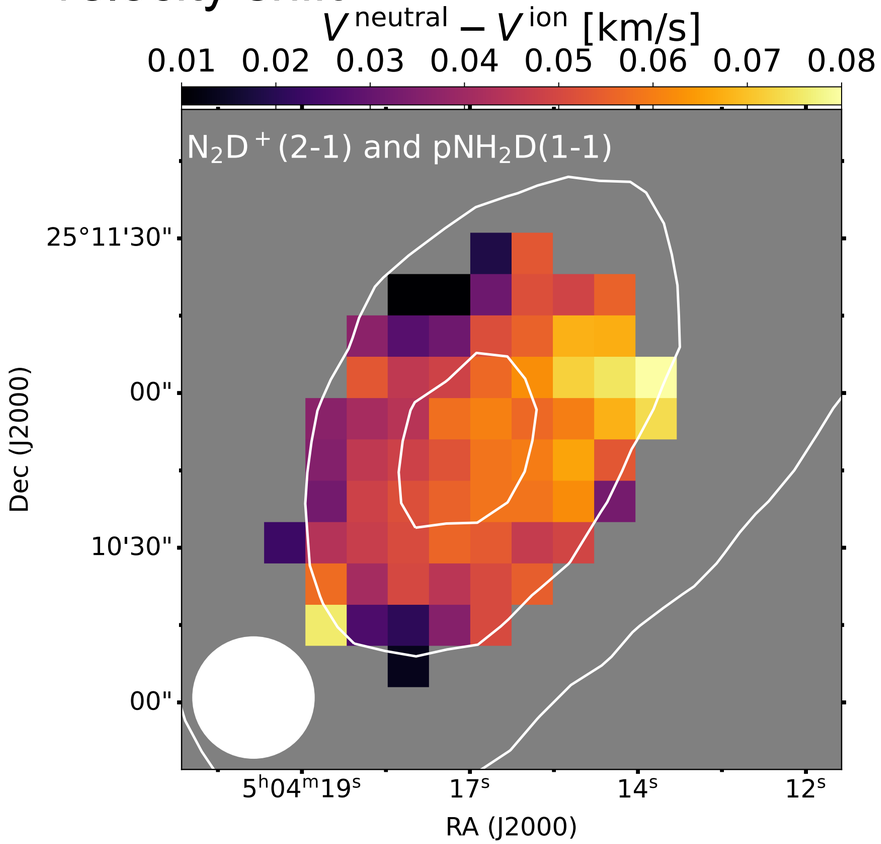

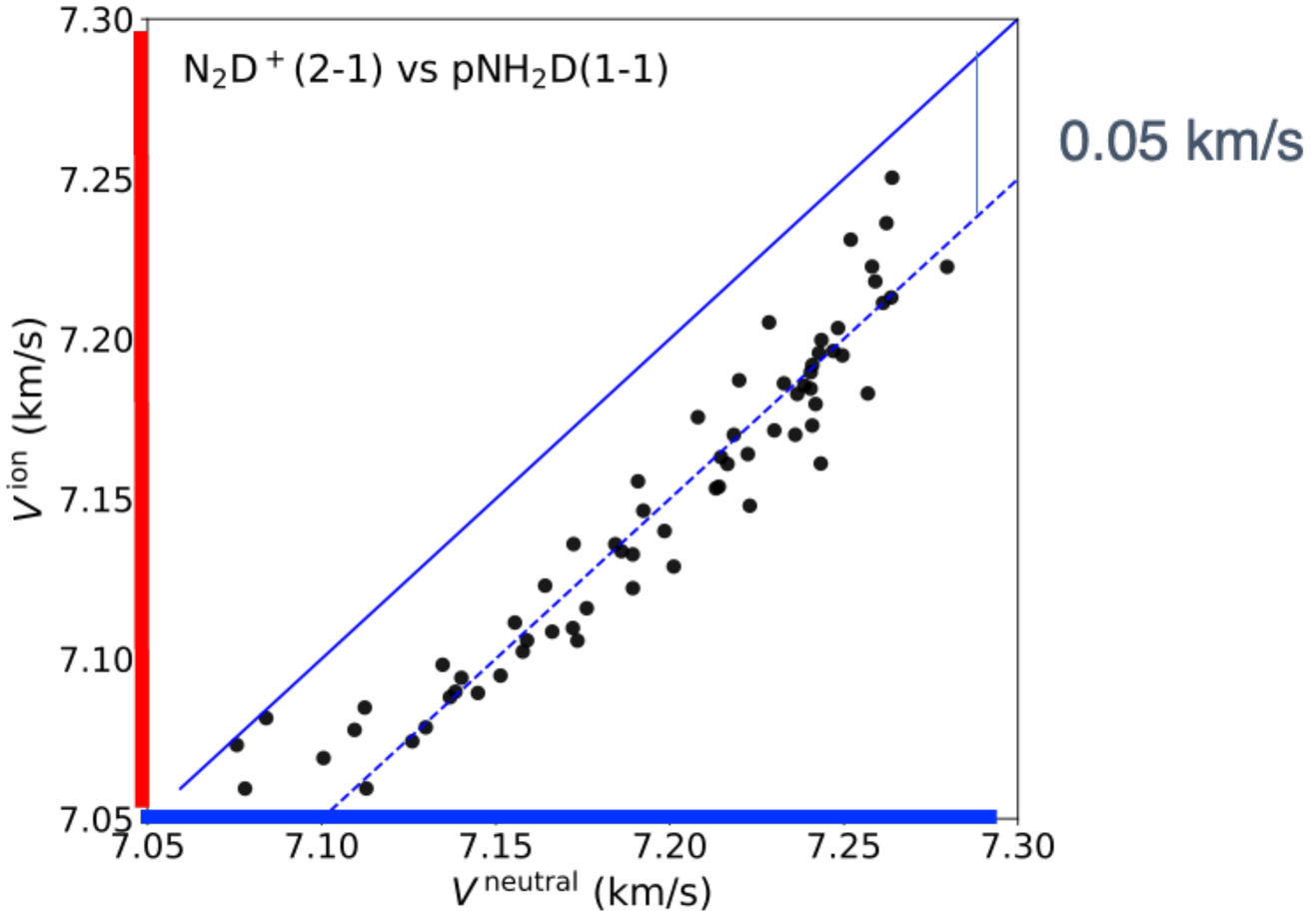

Arzoumanian et al. in prep

Observed drift velocity reaches ~0.05 km/s.

Drift Velocity in Weak B-field Case

Dependence of the drift velocity on the maximum dust size

$$\frac{dn_{\rm d}}{da_{\rm d}} = A a_{\rm d}^{-q} \left(a_{\rm min} < a_{\rm d} < a_{\rm max}\right)$$

$$a_{\rm min} = 5\ {\rm nm}, a_{\rm max} = 0.25\ \mu{\rm m},\ q = 3.5$$

Projection map

$B_0 = 50\ \mu{\rm G}$

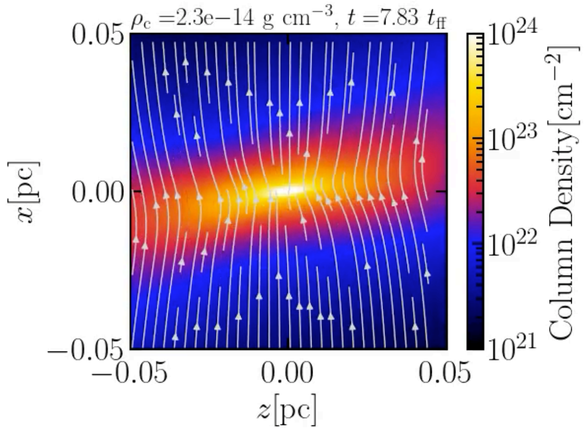

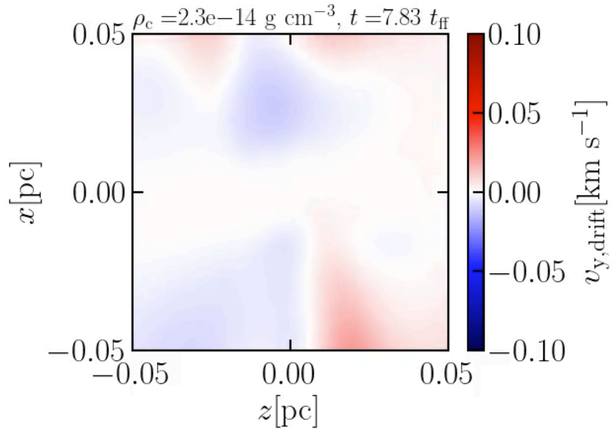

$B_0 = 20\ \mu{\rm G}$

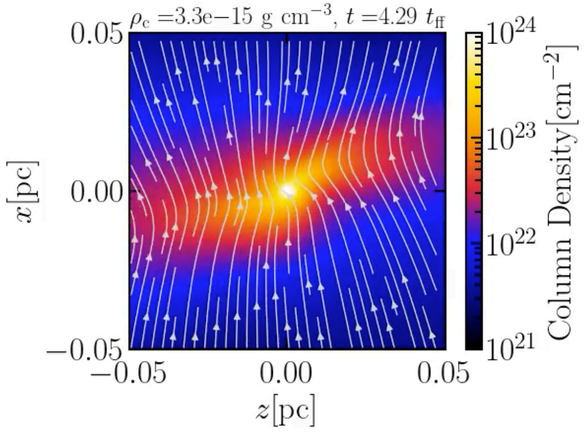

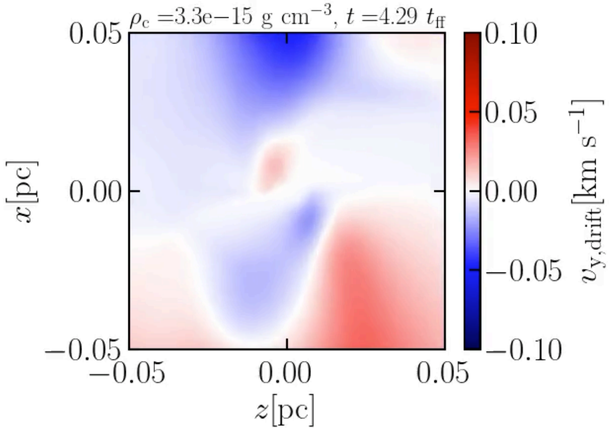

Drift Velocity measured in $B_0 = 20\ \mu{\rm G}$ is comparable with $B_0 = 50\ \mu{\rm G}$

Column density vs Drift velocity

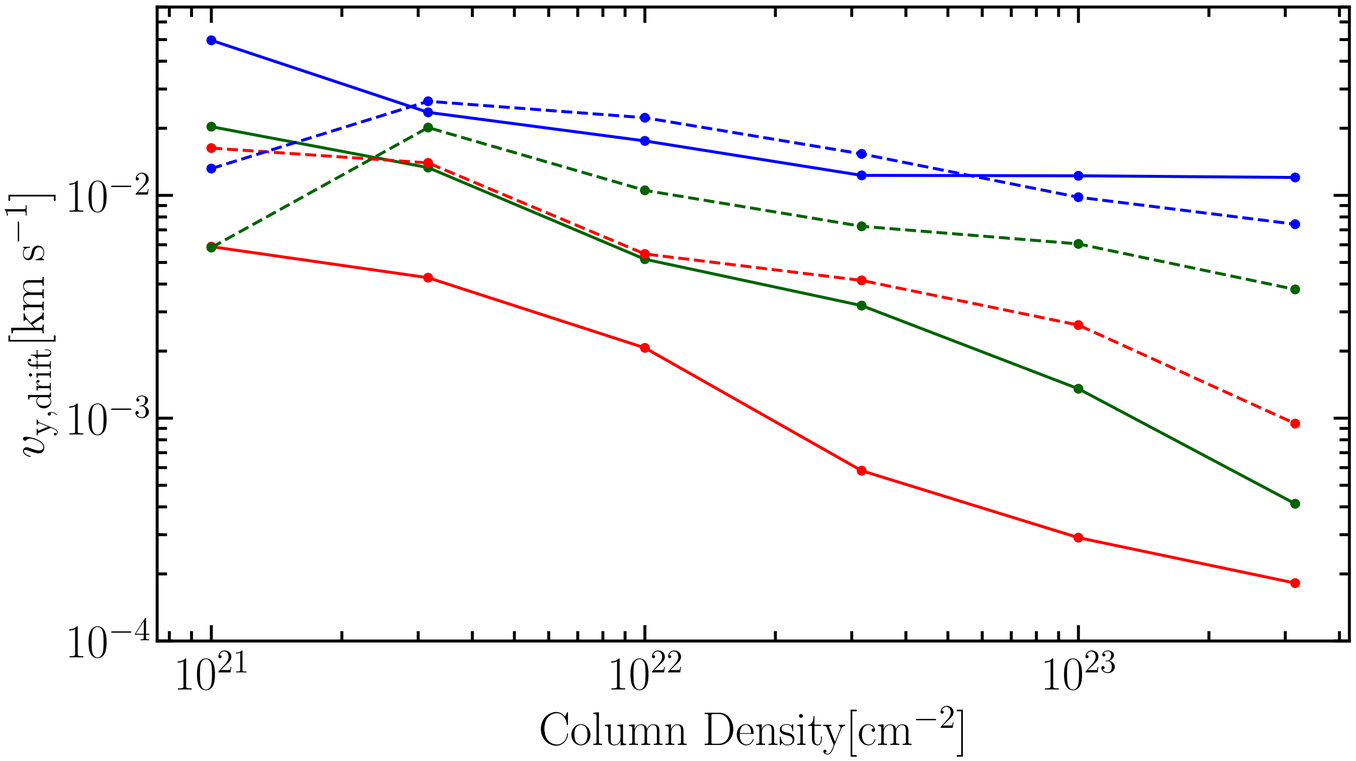

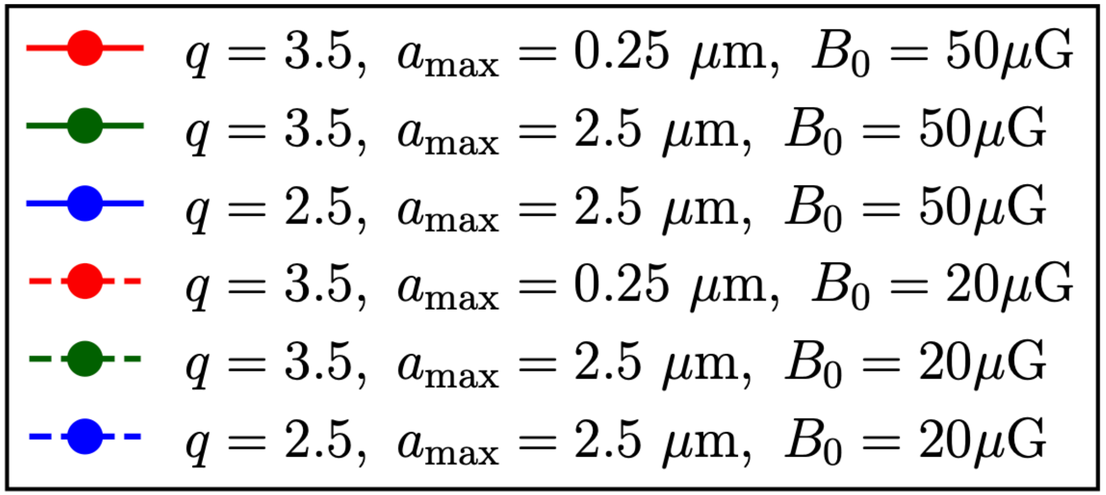

Drift velocity measured in the projection map in the case of 20uG is larger than that of 50uG.

Column density vs Drift velocity

Slice map on the x-y plane

$B_0 = 50\ \mu\mathrm{G}$

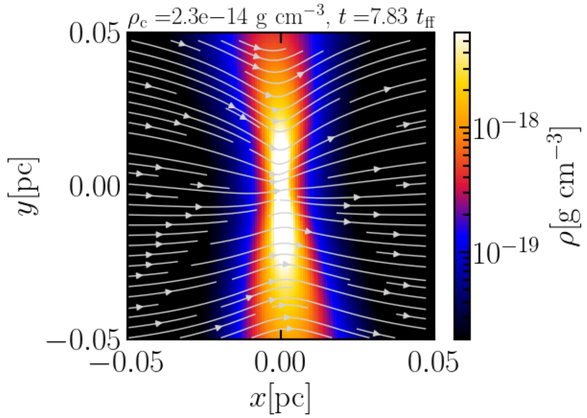

Line-of-sight

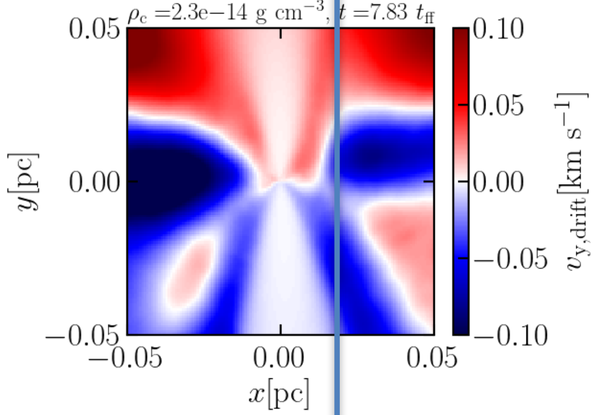

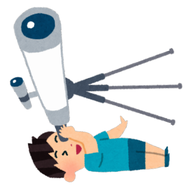

$B_0 = 20\ \mu\mathrm{G}$

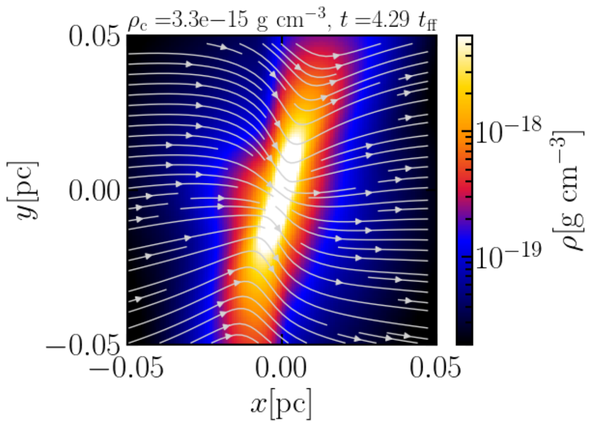

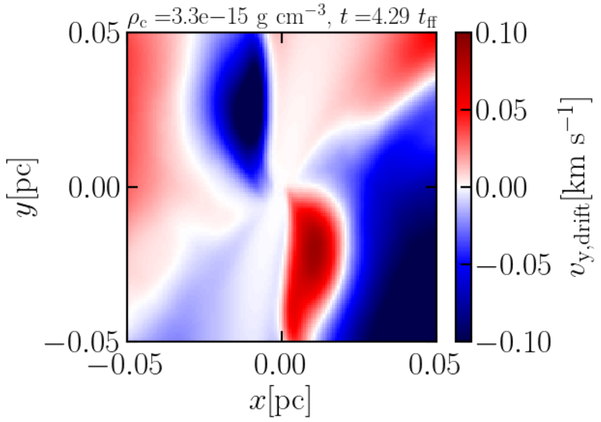

When the magnetic field is weak, the magnetic field and resultant drift velocity has more complex non-axis symmetric structure.

This effect makes the drift velocity larger in the case of 20uG.

AM profile

$B_0 = 20\ \mu\mathrm{G}$

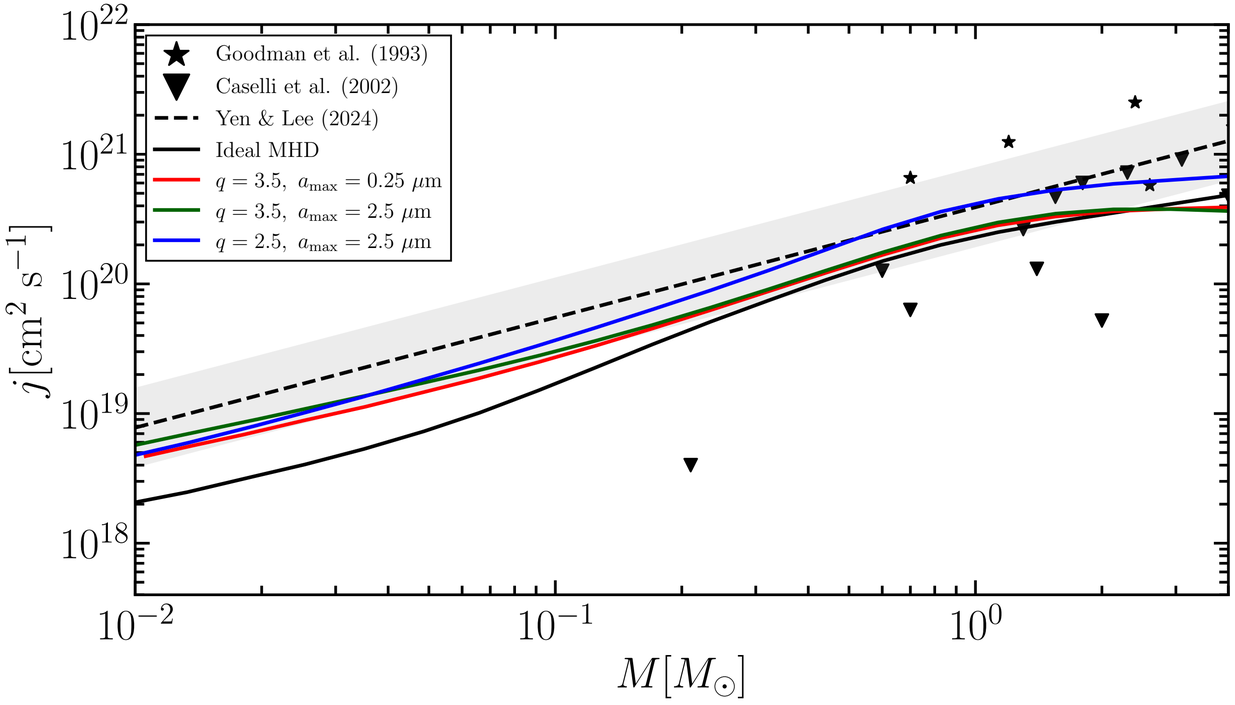

$$\frac{dn_\mathrm{d}}{da_\mathrm{d}} = A a_\mathrm{d}^{-q} \left(a_\mathrm{min} < a_\mathrm{d} < a_\mathrm{max}\right)$$

$$a_\mathrm{min} = 5\ \mathrm{nm}$$

Goodman et al. (1993)

Caselli et al. (2002)

Yen & Lee (2024)

Ideal MHD

$q = 3.5,\ a_{\max} = 0.25\ \mu$m

$q = 3.5,\ a_{\max} = 2.5\ \mu$m

$q = 2.5,\ a_{\max} = 2.5\ \mu$m

Number density vs Drift velocity

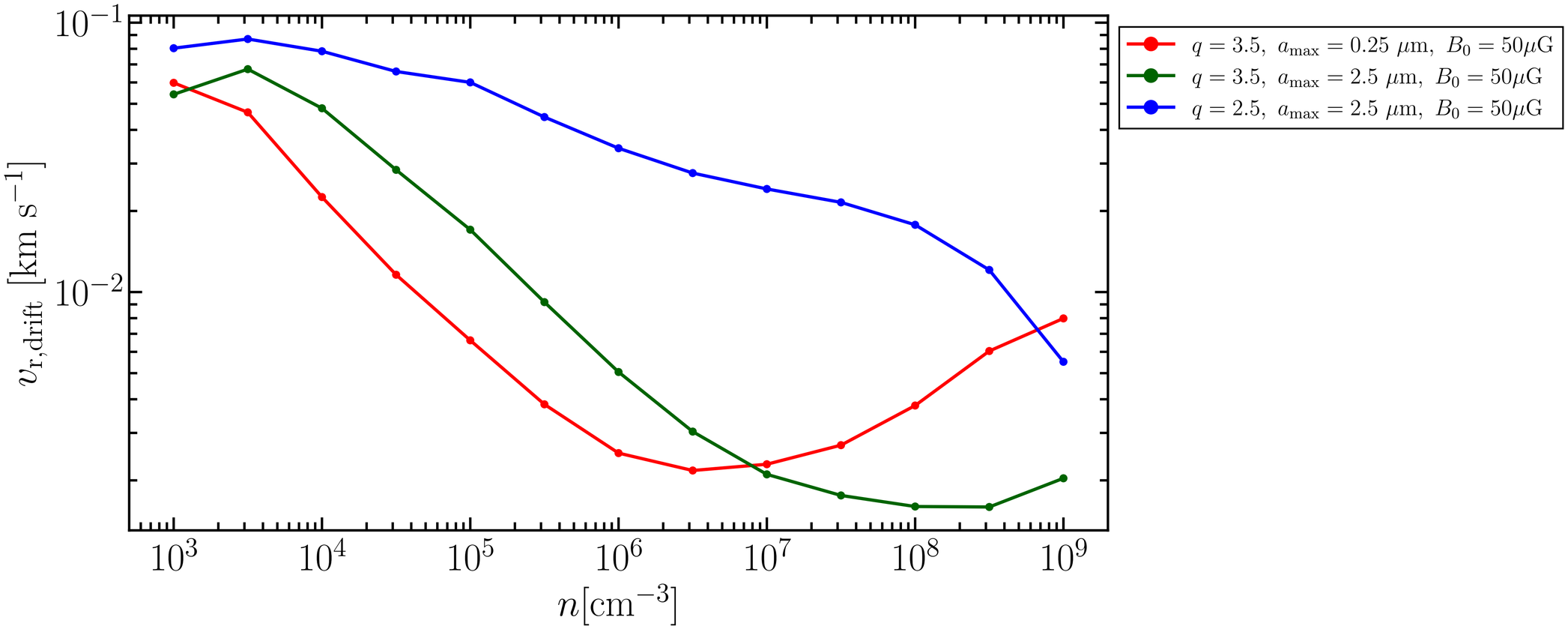

Drift velocity becomes smaller in high density region.
If the dust growth is efficient, the drift velocity become large.

Drift velocity (with inclination)

Dependence of the drift velocity on the maximum dust size

$$\frac{dn_{\rm d}}{da_{\rm d}} = A a_{\rm d}^{-q} \left(a_{\rm min} < a_{\rm d} < a_{\rm max} \right)$$

$\theta_{\rm inc} = 60^\circ,\ \phi_{\rm inc} = 0^\circ$

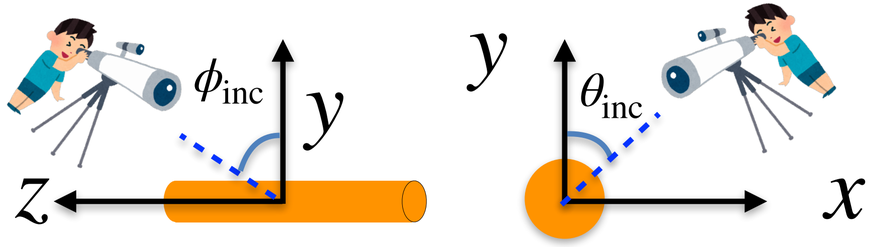

$a_{\rm min} = 5$ nm, $a_{\rm max} = 0.25$ μm, $q = 3.5$

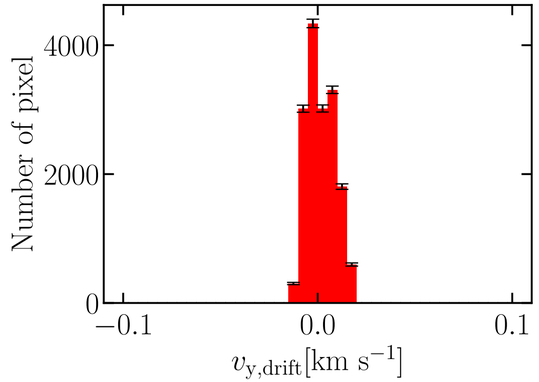

$a_{\rm min} = 5$ nm, $a_{\rm max} = 2.5$ μm, $q = 3.5$

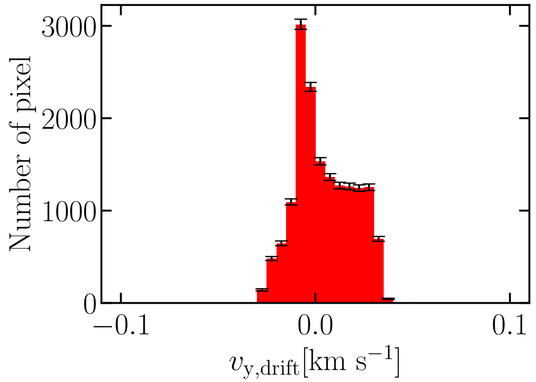

$a_{\rm min} = 5$ nm, $a_{\rm max} = 0.25$ μm, $q = 2.5$

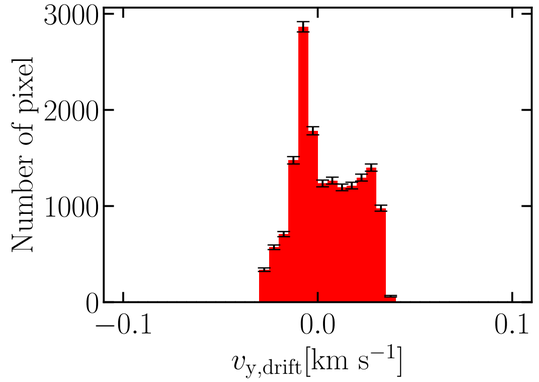

$a_{\rm min} = 5$ nm, $a_{\rm max} = 2.5$ μm, $q = 2.5$

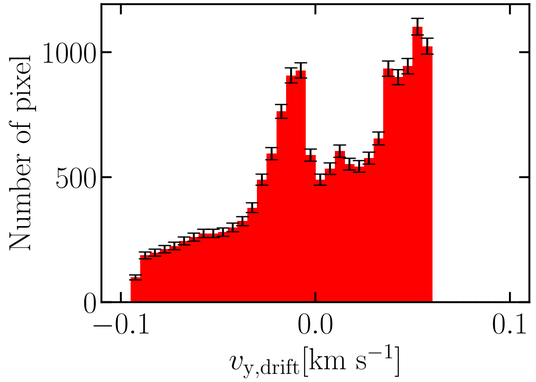

Drift velocity

Dependence of the drift velocity on the maximum dust size

$$\frac{dn_{\rm d}}{da_{\rm d}} = A a_{\rm d}^{-q} \left(a_{\rm min} < a_{\rm d} < a_{\rm max}\right)$$

$$B_0 = 20\ \mu{\rm G}$$

$$a_{\rm min} = 5\ {\rm nm}, a_{\rm max} = 0.25\ \mu{\rm m},\ q = 3.5$$

$$a_{\rm min} = 5\ {\rm nm}, a_{\rm max} = 2.5\ \mu{\rm m},\ q = 3.5$$

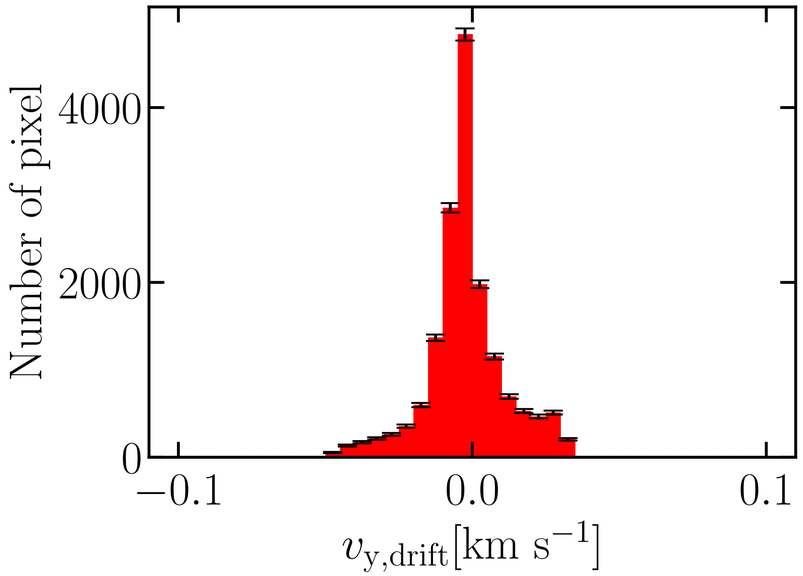

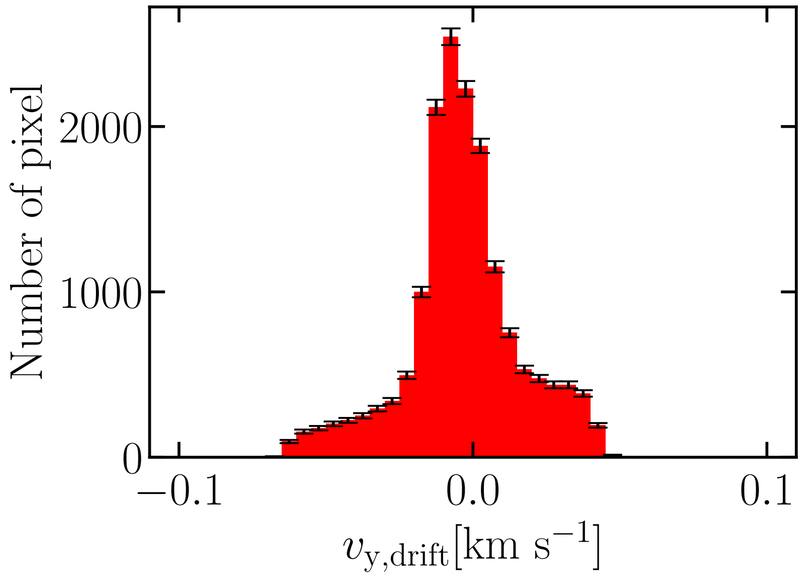

B-field

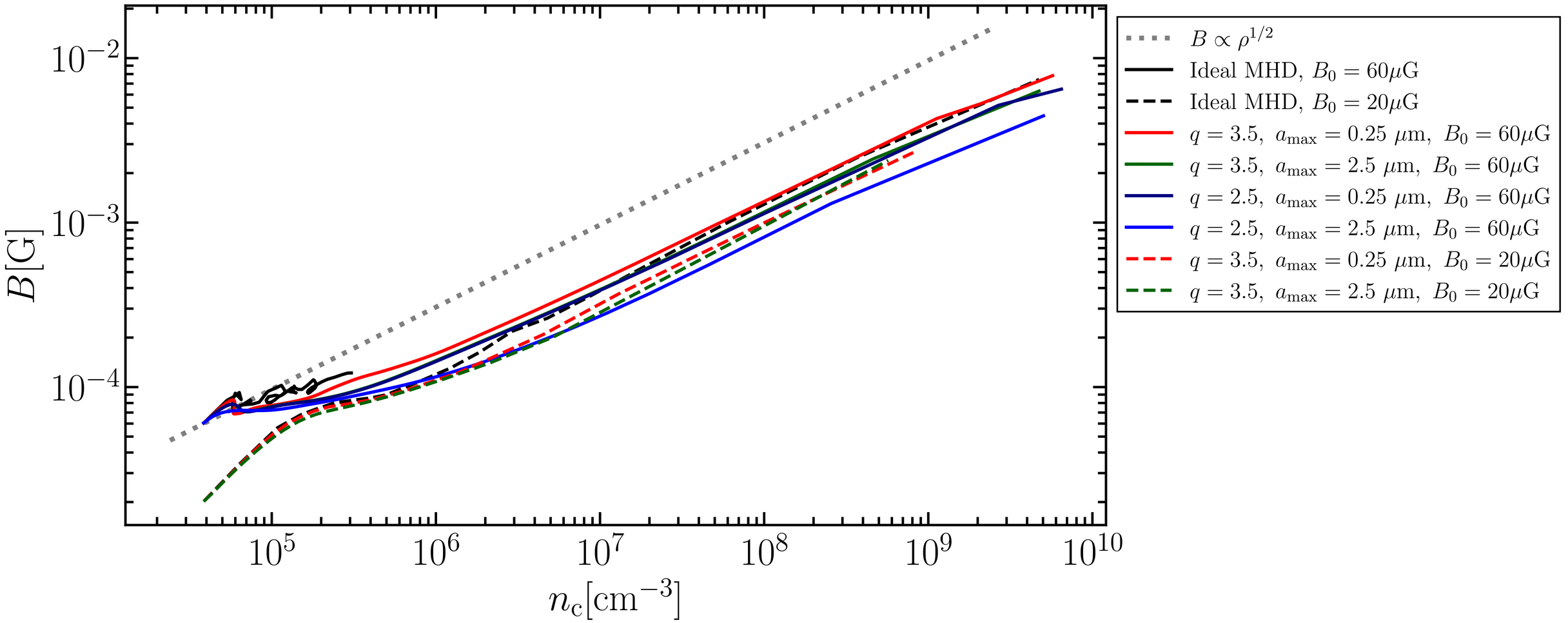
$B \propto \rho^{1/2}$
Ideal MHD, $B_0 = 60\mu$G
Ideal MHD, $B_0 = 20\mu$G
$q = 3.5,\ a_{\rm max} = 0.25\ \mu$m, $B_0 = 60\mu$G
$q = 3.5,\ a_{\rm max} = 2.5\ \mu$m, $B_0 = 60\mu$G
$q = 2.5,\ a_{\rm max} = 0.25\ \mu$m, $B_0 = 60\mu$G
$q = 2.5,\ a_{\rm max} = 2.5\ \mu$m, $B_0 = 60\mu$G
$q = 3.5,\ a_{\rm max} = 0.25\ \mu$m, $B_0 = 20\mu$G
$q = 3.5,\ a_{\rm max} = 2.5\ \mu$m, $B_0 = 20\mu$G
B[G]
10^{-2}
10^{-3}
10^{-4}
10^{5}
10^{6}
10^{7}
10^{8}
10^{9}
10^{10}
$n_{\rm c}$[cm^{-3}]

Internal Structure

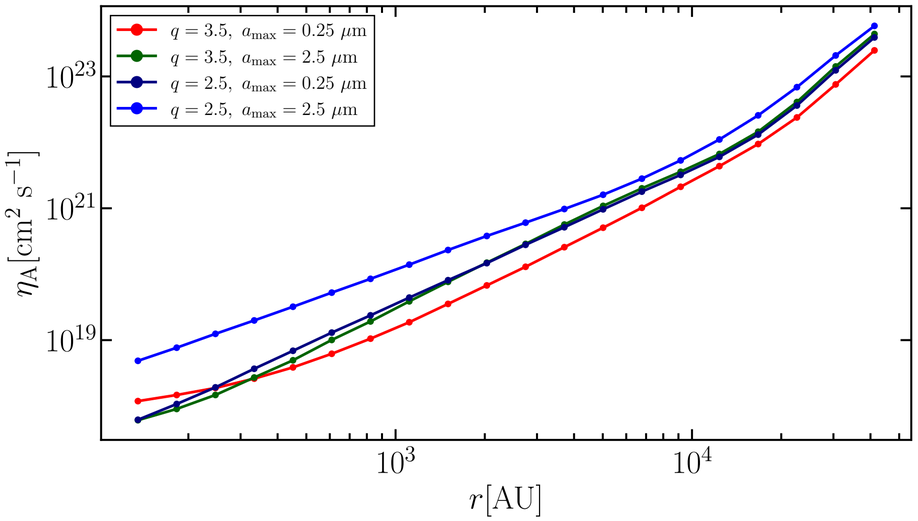

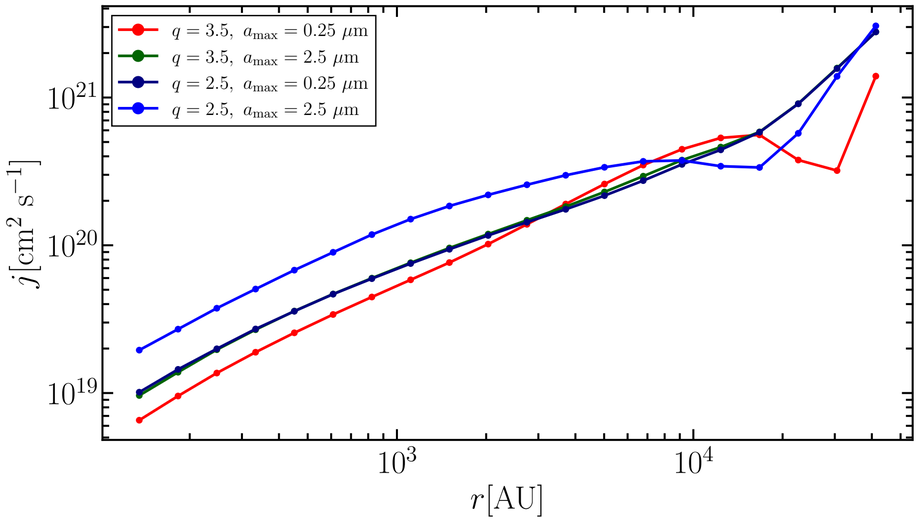

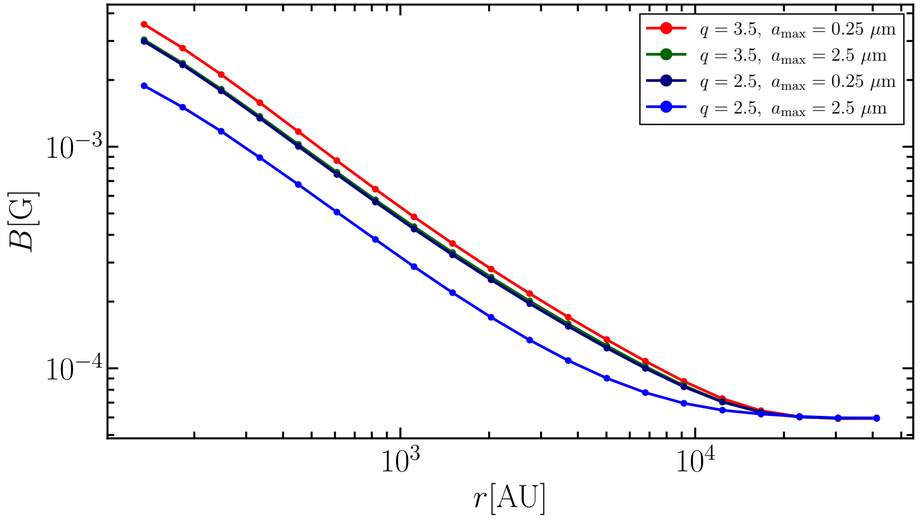

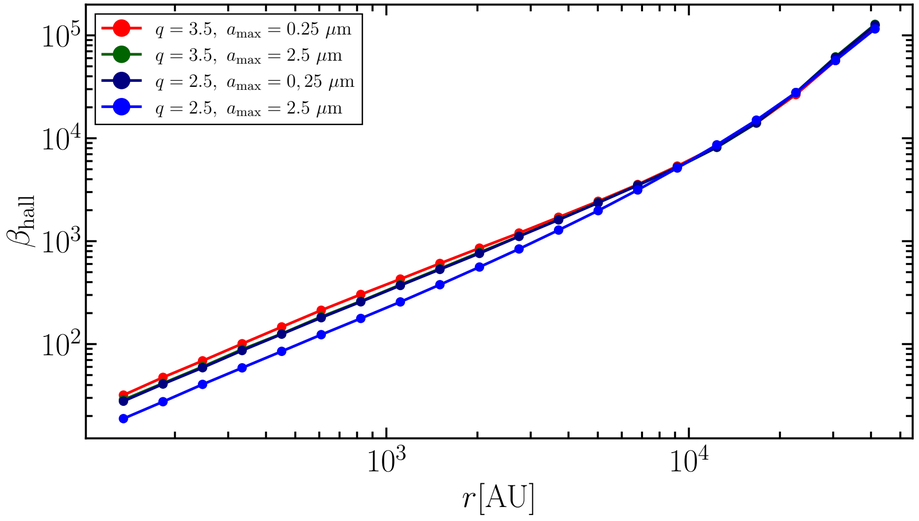

Column density vs Drift velocity

With inclination

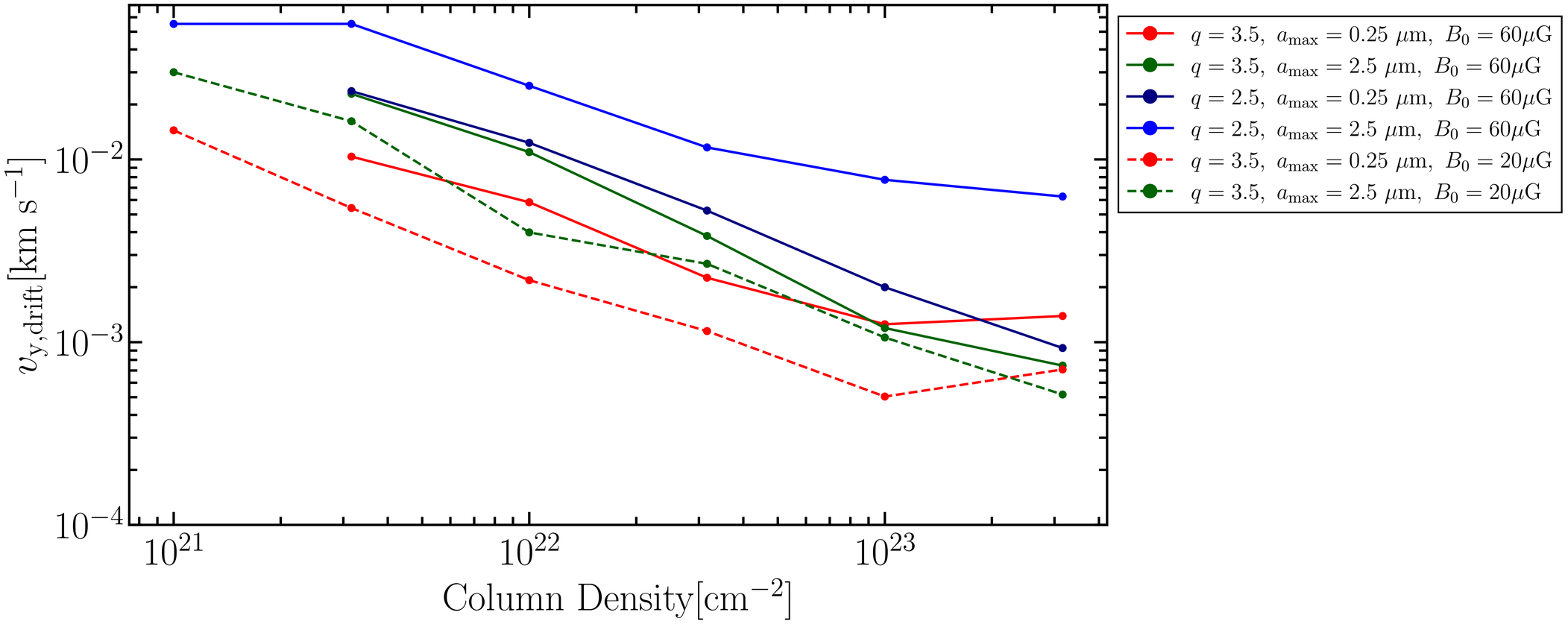

Magnetic Braking in Later Phase

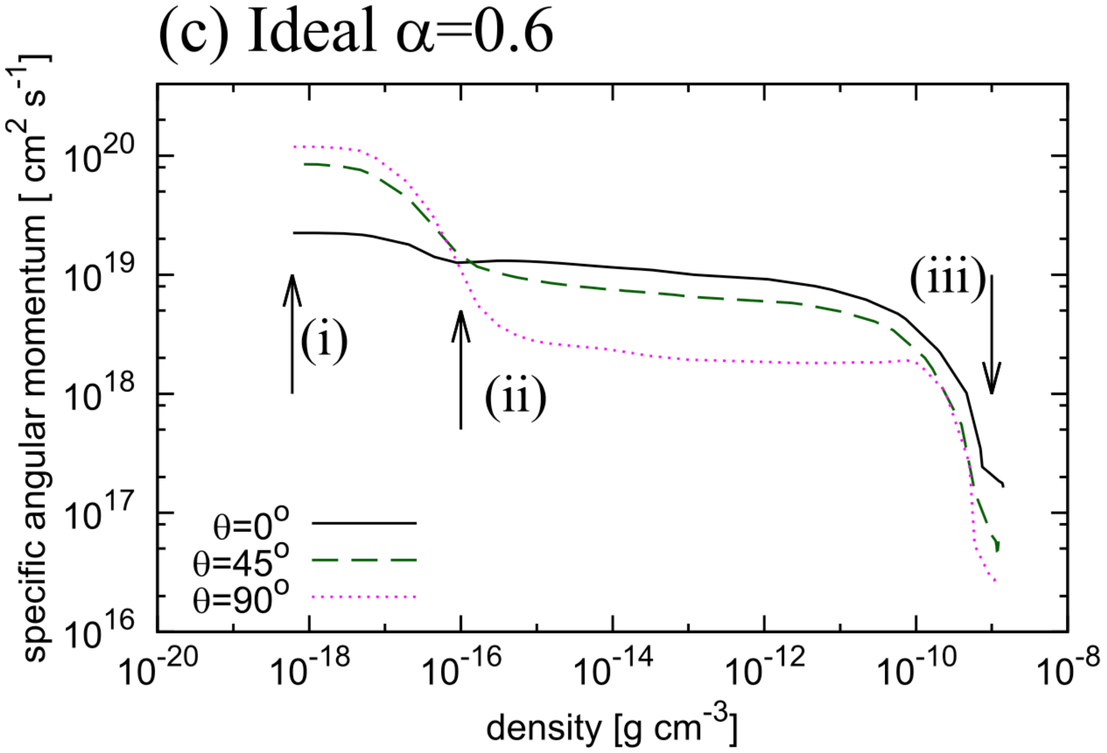

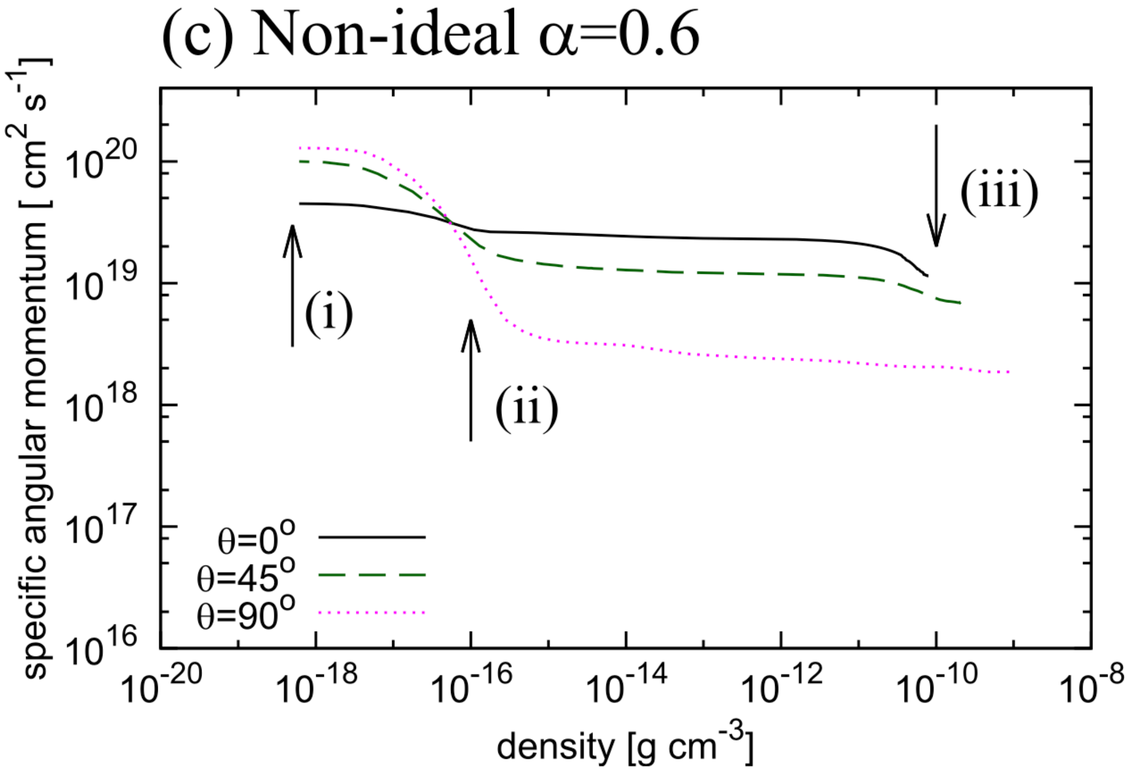

Tsukamoto et al. (2018)

If the non-ideal MHD effect is taken into account, the magnetic braking is suppressed in later evolutionary phase.

Rotation vs Infall

$B_0 = 50\mu\mathrm{G}$ $\quad \frac{dn_\mathrm{d}}{da_\mathrm{d}} = A a_\mathrm{d}^{-q} \left(a_\mathrm{min} < a_\mathrm{d} < a_\mathrm{max}\right)$

Ideal MHD

$a_\mathrm{min} = 5\ \mathrm{nm}, a_\mathrm{max} = 0.25\ \mu\mathrm{m},\ q = 3.5$

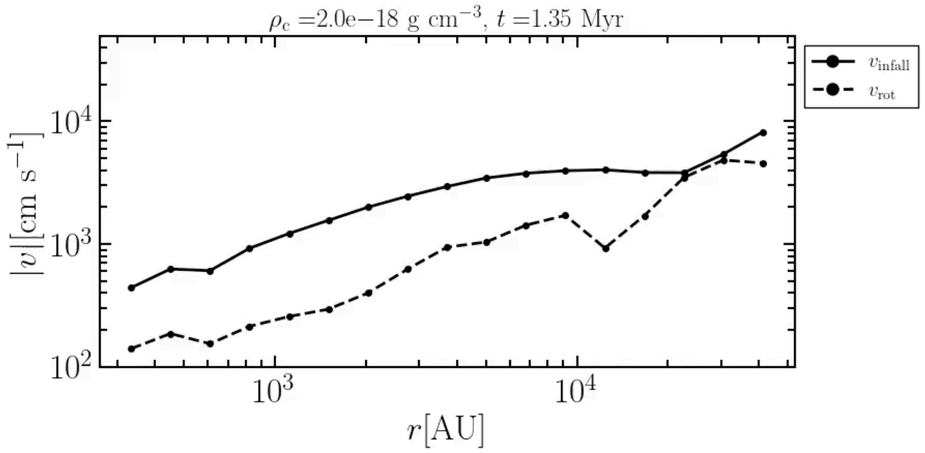

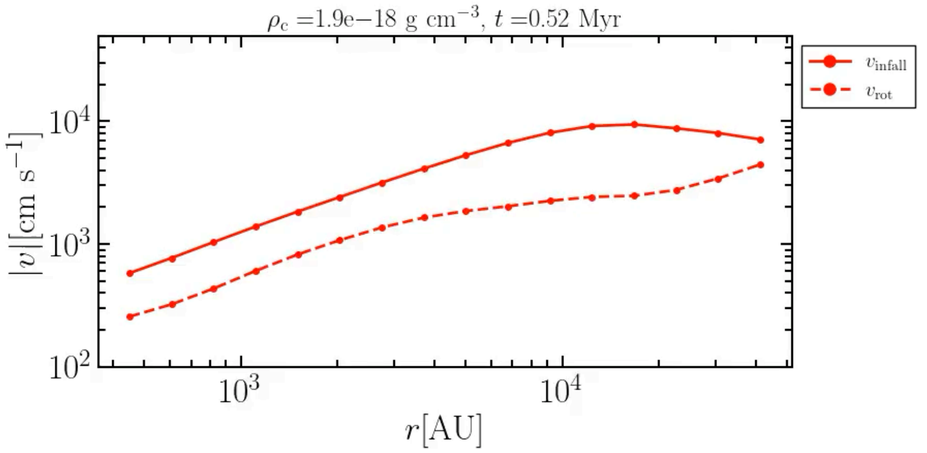

$a_\mathrm{min} = 5\ \mathrm{nm}, a_\mathrm{max} = 2.5\ \mu\mathrm{m},\ q = 2.5$

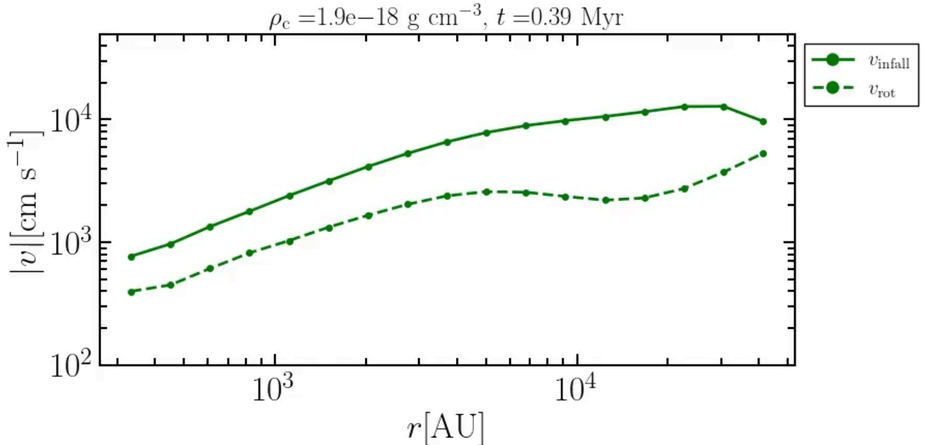

$a_\mathrm{min} = 5\ \mathrm{nm}, a_\mathrm{max} = 2.5\ \mu\mathrm{m},\ q = 3.5$

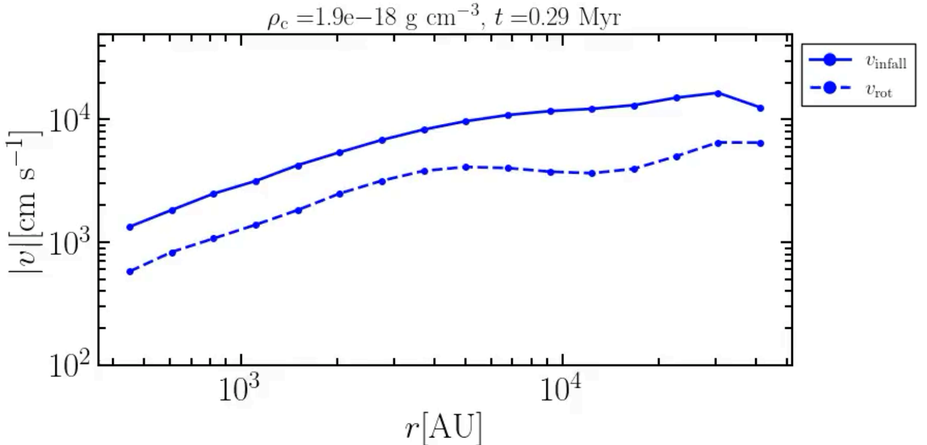

Velocity Dispersion

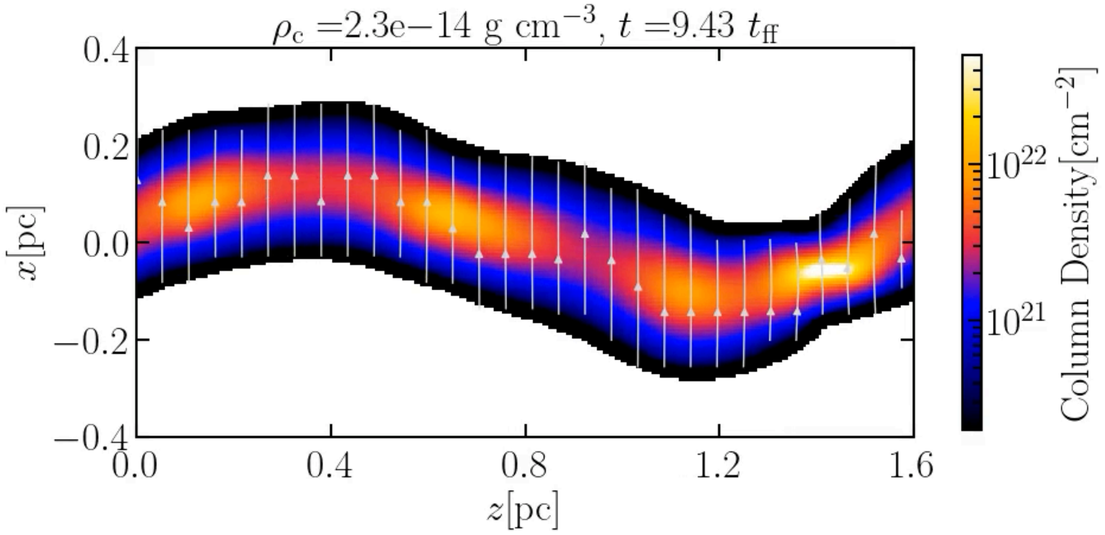

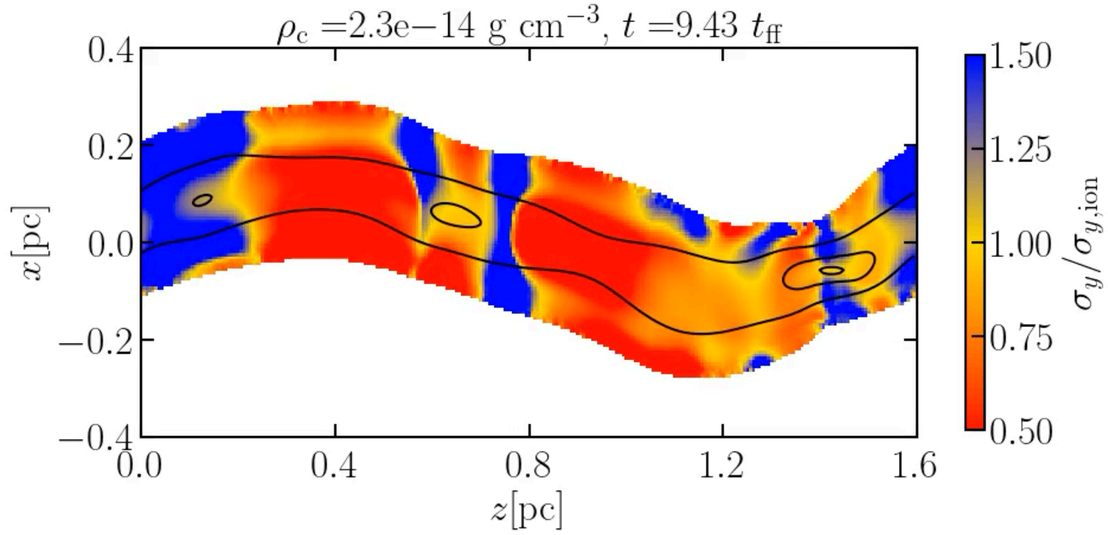

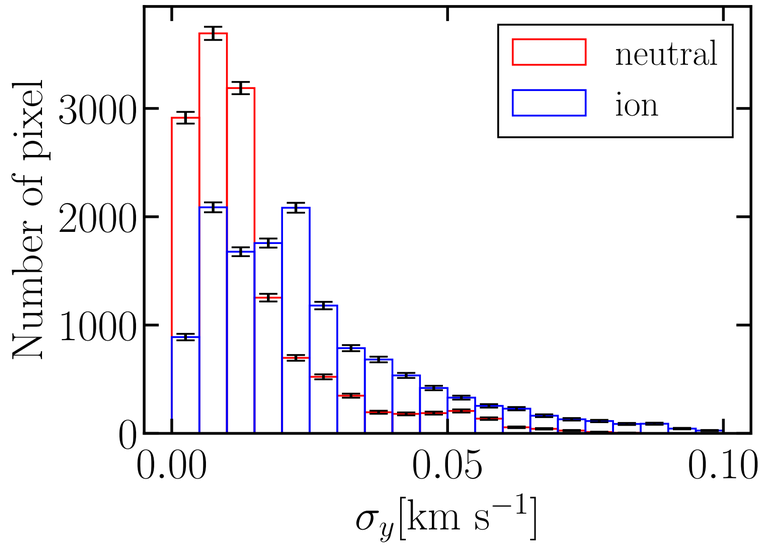

Velocity Dispersion

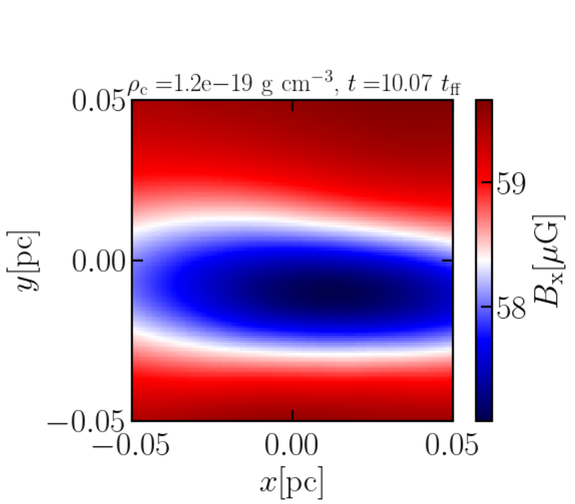

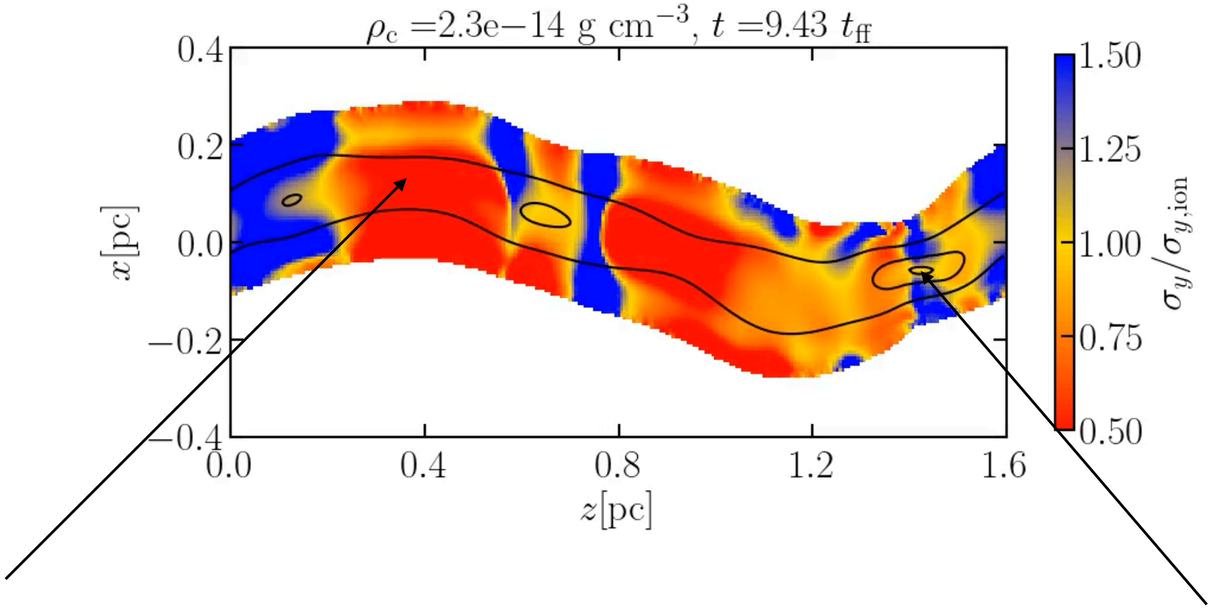

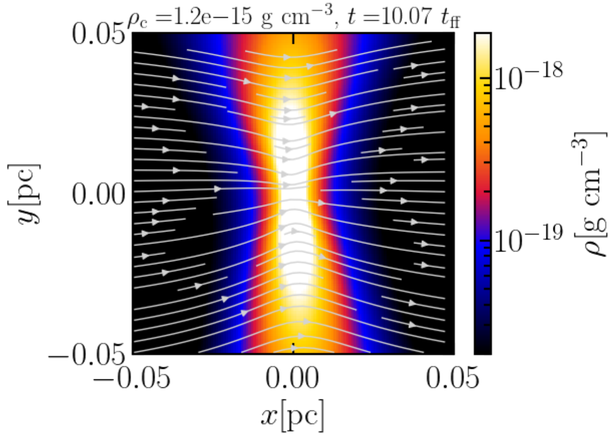

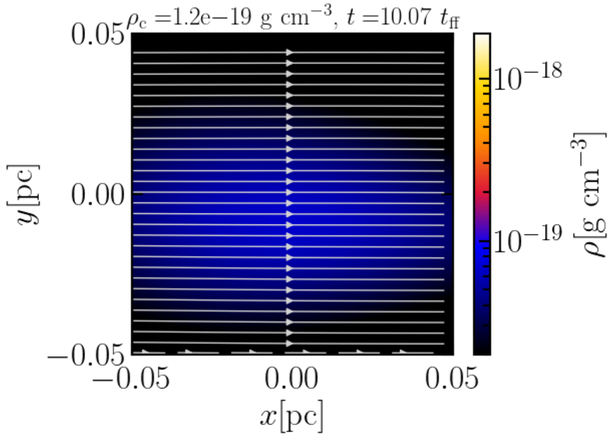

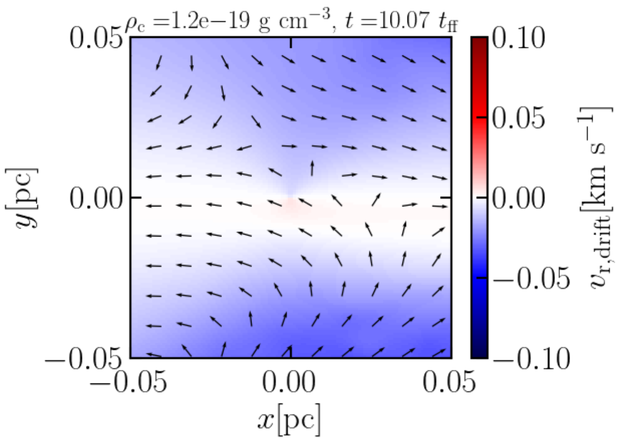

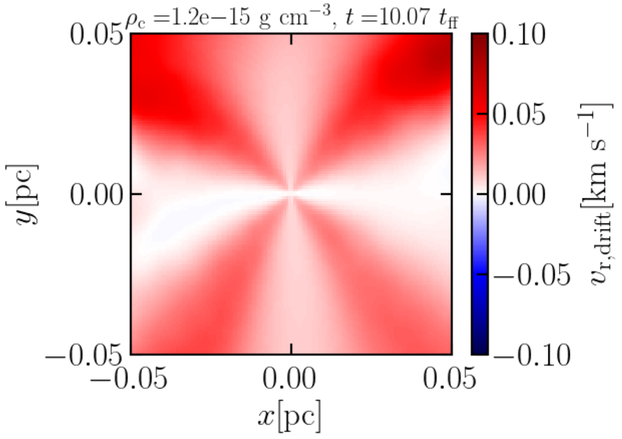

Evolution of AM

Core mass: $1\ \mathrm{M}_{\odot}$

$$\frac{dn_{\mathrm{d}}}{da_{\mathrm{d}}} = A a_{\mathrm{d}}^{-q} \left(a_{\mathrm{min}} < a_{\mathrm{d}} < a_{\mathrm{max}}\right)$$

Evolution of the specific angular momentum

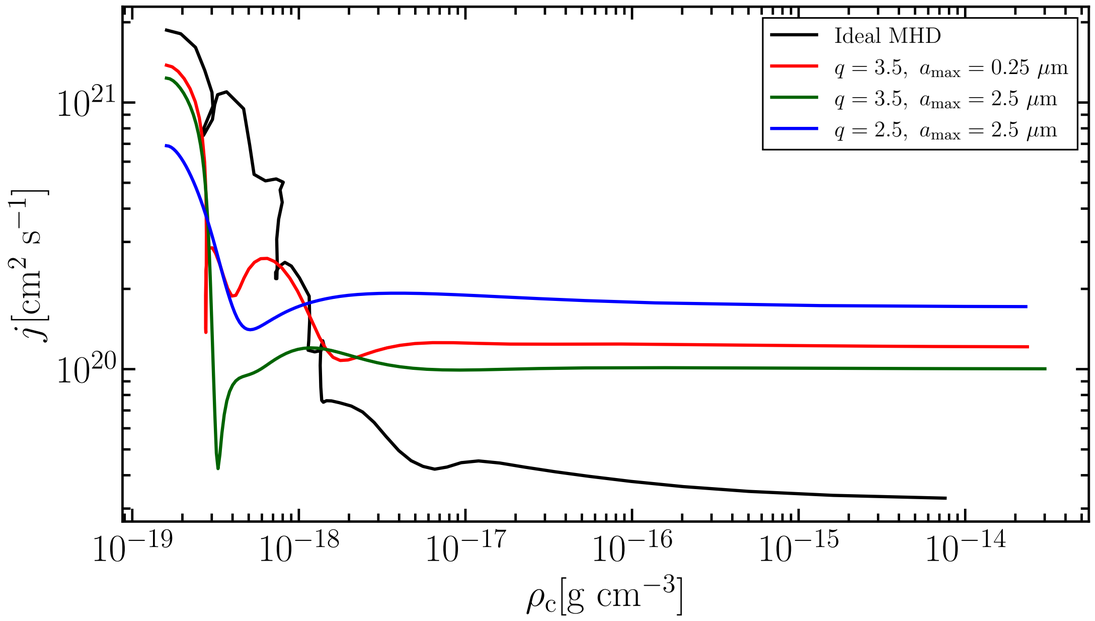

Evolution of the angle between the rotation and B-field

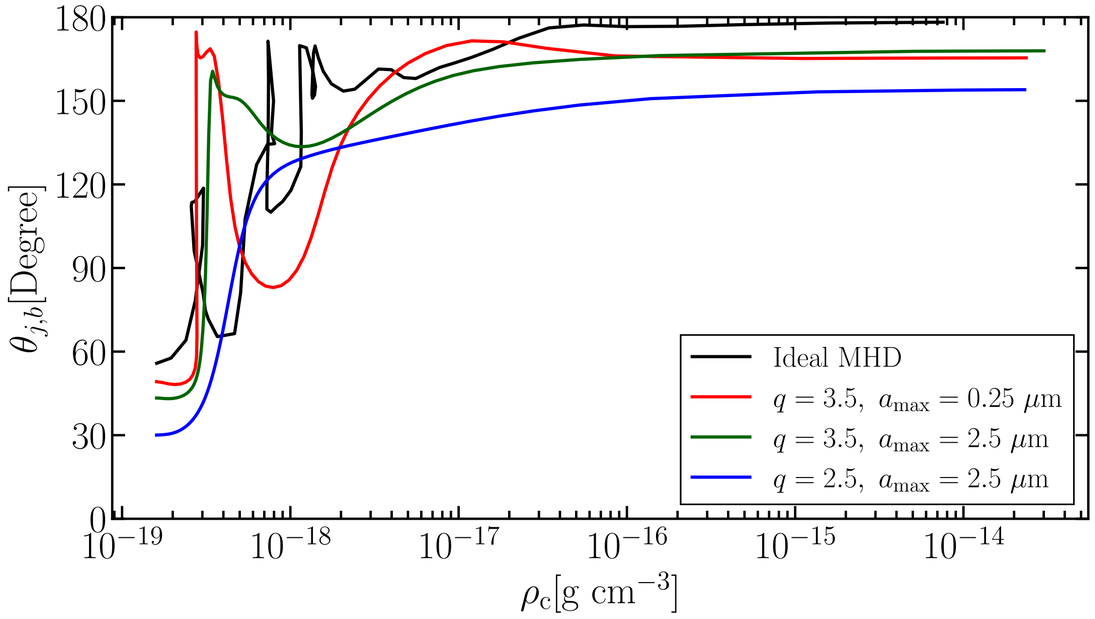

In the ideal MHD case, the AM decrease with oscillation, the rotation direction is aligned with magnetic field direction.